

1. Report No. FHWA-OR-RD-98-08		2. Government Accession No.		3. Recipient's Catalog No.	
4. Title and Subtitle Strengthening Bridges Using Composite Materials				5. Report Date March 1998	
				6. Performing Organization Code	
7. Author(s) Damian Kachlakev, PhD Oregon State University Civil Construction and Environmental Engineering Department Corvallis, OR 97330				8. Performing Organization Report No.	
9. Performing Organization Name and Address Oregon Department of Transportation Research Unit 2950 State Street Salem, Oregon 97310				10. Work Unit No. (TRAIS)	
				11. Contract or Grant No.	
12. Sponsoring Agency Name and Address Oregon Department of Transportation Federal Highway Administration Research Unit Washington DC 20560 2950 State Street and Salem, Oregon 97310				13. Type of Report and Period Covered Synthesis	
				14. Sponsoring Agency Code	
15. Supplementary Notes					
16. Abstract The objective of this research project is to outline methodologies for using Fiber Reinforced Polymer (FRP) composites to strengthen and rehabilitate reinforced concrete bridge elements. Infrastructure deterioration and bridge strengthening techniques using FRP materials are discussed as background. Properties and classifications of different reinforcing fibers and resin matrices are provided, along with the mechanical properties of the FRP composites. Basic concepts and design principles for composite FRP materials are introduced, and topics such as manufacturing processes, anisotropic elasticity, strength of anisotropic materials, and micro-mechanics are presented. Techniques and concepts for strengthening concrete beams with FRP composites are discussed, as are flexural and shear strengthening design and construction methodologies. The worldwide research experience in the behavior of FRP strengthened beams under various conditions are summarized. External reinforcement of concrete columns using FRP materials is examined. Theoretical background, factors influencing the performance of FRP wrapped columns, and various case studies are presented. Design methodologies and examples supplement the case studies for both beams and columns. Most FRP material systems available on the market today are summarized and evaluated. Construction and durability requirements of the retrofitted systems are presented. Reliability assessment, condition evaluation methods, and factors influencing the strengthening quality are included. The various steps of the construction process, such as selection of a composite strengthening system, concrete surface preparation, and bond between FRP and concrete are summarized. Quality control, environmental durability of FRP composites, and cost effectiveness are presented.					
17. Key Words BRIDGE, COMPOSITE, FIBER, FRP, POLYMER, REINFORCEMENT, STRENGTHENING				18. Distribution Statement	
19. Security Classif. (of this report) Unclassified		20. Security Classif. (of this page) Unclassified		21. No. of Pages 182	22. Price

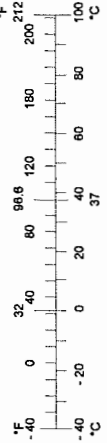
SI* (MODERN METRIC) CONVERSION FACTORS

APPROXIMATE CONVERSIONS TO SI UNITS

APPROXIMATE CONVERSIONS FROM SI UNITS

Symbol	When You Know	Multiply By	To Find	Symbol
LENGTH				
in	inches	25.4	millimeters	mm
ft	feet	0.305	meters	m
yd	yards	0.914	meters	m
mi	miles	1.61	kilometers	km
AREA				
in ²	square inches	645.2	millimeters squared	mm ²
ft ²	square feet	0.093	meters squared	m ²
yd ²	square yards	0.836	meters squared	m ²
ac	acres	0.405	hectares	ha
mi ²	square miles	2.59	kilometers	km ²
VOLUME				
fl oz	fluid ounces	29.57	milliliters	mL
gal	gallons	3.785	liters	L
ft ³	cubic feet	0.028	meters cubed	m ³
yd ³	cubic yards	0.765	meters cubed	m ³
NOTE: Volumes greater than 1000 L shall be shown in m ³ .				
MASS				
oz	ounces	28.35	grams	g
lb	pounds	0.454	kilograms	kg
T	short tons (2000 lb)	0.907	megagrams	Mg
TEMPERATURE (exact)				
°F	Fahrenheit temperature	5(F-32)/9	Celsius temperature	°C

Symbol	When You Know	Multiply By	To Find	Symbol
LENGTH				
mm	millimeters	0.039	inches	in
m	meters	3.28	feet	ft
m	meters	1.09	yards	yd
km	kilometers	0.621	miles	mi
AREA				
mm ²	millimeters squared	0.0016	square inches	in ²
m ²	meters squared	10.764	square feet	ft ²
ha	hectares	2.47	acres	ac
km ²	kilometers squared	0.386	square miles	mi ²
VOLUME				
mL	milliliters	0.034	fluid ounces	fl oz
L	liters	0.264	gallons	gal
m ³	meters cubed	35.315	cubic feet	ft ³
m ³	meters cubed	1.308	cubic yards	yd ³
MASS				
g	grams	0.035	ounces	oz
kg	kilograms	2.205	pounds	lb
Mg	megagrams	1.102	short tons (2000 lb)	T
TEMPERATURE (exact)				
°C	Celsius temperature	1.8 + 32	Fahrenheit	°F



* SI is the symbol for the International System of Measurement

ACKNOWLEDGEMENTS

The author wishes to express his appreciation to Marty Laylor, Project Manager, and Galen McGill, Manager, both of the Research Unit of the Oregon Department of Transportation, for their valuable suggestions and many contributions to this project. The author also gratefully acknowledges the rest of the technical advisory committee for their direction and review of this work.

DISCLAIMER

This document is disseminated under the sponsorship of the Oregon Department of Transportation and the United States Department of Transportation in the interest of information exchange. The State of Oregon and the United States Government assume no liability of its contents or use thereof.

The contents of this report reflect the views of the authors, who are responsible for the facts and accuracy of the data presented herein. The contents do not necessarily reflect the official policies of the Oregon Department of Transportation or the United States Department of Transportation.

The State of Oregon and the United States Government do not endorse products of manufacturers. Trademarks or manufacturers' names appear herein only because they are considered essential to the object of this document.

This report does not constitute a standard, specification, or regulation.

STRENGTHENING BRIDGES USING COMPOSITE MATERIALS

TABLE OF CONTENTS

STANDARD TERMINOLOGY RELATED TO COMPOSITE MATERIALS	ix
1.0 INTRODUCTION	1
1.1 BACKGROUND.....	1
1.2 SCOPE AND OBJECTIVES	4
2.0 CONSTITUENT MATERIALS FOR COMPOSITES	5
2.1 DEFINITION OF FRP COMPOSITE MATERIALS FOR STRUCTURAL APPLICATIONS	5
2.2 PROPERTIES OF CONSTITUENT MATERIALS.....	6
2.2.1 <i>Classification and Properties of Reinforcing Fibers</i>	6
2.2.2 <i>Classification and Properties of Resin Matrices</i>	9
2.3 MECHANICAL PROPERTIES OF FIBER REINFORCED POLYMER COMPOSITES	10
2.4 MATERIALS AND MANUFACTURING PROCESS SELECTION	13
3.0 DESIGN PRINCIPLES FOR COMPOSITE MATERIALS	15
3.1 DESIGN PHILOSOPHY.....	15
3.2 MECHANICS OF COMPOSITE MATERIALS.....	16
3.3 DESIGN PRINCIPLES.....	19
3.4 MICRO-MECHANICAL PREDICTION OF ELASTIC CONSTANTS	22
3.5 TEST METHODS FOR DETERMINATION OF MECHANICAL PROPERTIES OF FRP REINFORCEMENT.....	26
4.0 EXTERNAL REINFORCEMENT OF CONCRETE BEAMS USING FRP COMPOSITE MATERIALS.....	29
4.1 STRENGTHENING TECHNIQUES WITH CONVENTIONAL MATERIALS.....	29
4.2 STRENGTHENING TECHNIQUES WITH COMPOSITE MATERIALS.....	29
4.2.1 <i>Background</i>	29
4.2.2 <i>Some Early Evaluations</i>	30
4.3 DESIGN MODELS AND APPLICATION TECHNIQUES	34
4.3.1 <i>“Lack of Ductility” Problem Associated with FRP Strengthening</i>	34
4.3.2 <i>Flexural Strengthening – Case Studies</i>	35
4.3.3 <i>Shear Strengthening</i>	40
4.3.4 <i>External Prestressing</i>	42
4.3.5 <i>Strengthening of Reinforced Concrete Beams with FRP Sheets</i>	45
4.3.6 <i>Reinforced Concrete Decks/Slabs Strengthened with FRP Materials</i>	45
4.3.7 <i>Design Methodology</i>	46
4.4 FATIGUE AND CREEP BEHAVIOR OF CONCRETE BEAMS WITH EXTERNALLY BONDED FRP SHEETS	48
4.5 LOW TEMPERATURE RESPONSE OF RC BEAMS STRENGTHENED WITH FRP SHEETS.....	49
4.6 ANALYSIS OF THE FAILURE MECHANISM OF RC BEAMS STRENGTHENED WITH FRP PLATES	51
4.7 OTHER TECHNIQUES FOR STRENGTHENING CONCRETE BEAMS USING FRP MATERIALS.....	59
4.8 FIELD APPLICATIONS	59
4.8.1 <i>Canada</i>	59
4.8.2 <i>United States</i>	60
4.8.3 <i>Japan</i>	61
4.8.4 <i>Europe</i>	62
4.9 SUMMARY	63
4.10 DESIGN EXAMPLES.....	65
4.10.1 <i>Flexural Design – Calculation of FRP Strengthened Beam Bending Resistance</i>	65
4.10.2 <i>Shear Strength Enhancement of RC Beams Using FRP Laminates</i>	75
4.10.3 <i>List of Variables</i>	79

5.0	EXTERNAL REINFORCEMENT OF CONCRETE COLUMNS USING FRP COMPOSITE MATERIALS	81
5.1	INTRODUCTION.....	81
5.2	COLUMNAR CONFINEMENT OF CONCRETE WITH ADVANCED COMPOSITE MATERIALS.....	82
5.3	STRENGTHENING OF CONCRETE COLUMNS WITH EXTERNALLY APPLIED FRP – CASE STUDIES.....	84
5.3.1	<i>California Department of Transportation (CALTRANS)</i>	84
5.3.2	<i>University of California, San Diego (UCSD)</i>	85
5.3.3	<i>University of Arizona, Tucson</i>	88
5.3.4	<i>University of South Florida and Florida DOT</i>	90
5.3.5	<i>Japan</i>	91
5.4	THEORETICAL BACKGROUND AND ANALYSIS OF FRP WRAP-STRENGTHENED CONCRETE COLUMNS.....	92
5.5	FACTORS INFLUENCING THE PERFORMANCE OF FRP-STRENGTHENED COLUMNS.....	96
5.6	FREEZE-THAW RESPONSE OF FRP WRAPPED COLUMNS.....	98
5.7	SYSTEMS FOR FRP STRENGTHENING OF BRIDGE COLUMNS.....	99
5.8	SUMMARY	103
5.9	DESIGN EXAMPLES.....	103
5.9.1	<i>Shear Strengthening</i>	104
5.9.2	<i>Flexural Hinge Confinement for Circular Columns</i>	110
5.9.3	<i>Flexural Hinge Confinement for Rectangular Columns</i>	112
5.9.4	<i>Lap Splice Clamping</i>	114
5.9.5	<i>Numerical Design Examples</i>	116
5.9.6	<i>List of Variables</i>	121
6.0	CONSTRUCTION CONSIDERATIONS AND DURABILITY OF THE RETROFITTED SYSTEMS	123
6.1	RELIABILITY ASSESSMENT AND CONDITION EVALUATION OF EXISTING BRIDGE STRUCTURES.....	123
6.1.1	<i>Background</i>	123
6.1.2	<i>Reliability of FRP Materials</i>	125
6.1.3	<i>Reliability of FRP-Strengthened Concrete Members—Case Studies</i>	125
6.2	SELECTION OF COMPOSITE SYSTEM	126
6.3	CONCRETE SURFACE PREPARATION AND COMPOSITE SYSTEM INSTALLATION REQUIREMENTS.....	127
6.3.1	<i>Background</i>	127
6.3.2	<i>Surface Preparation Technological Operations</i>	128
6.3.3	<i>Additional Factors Influencing the Quality of Strengthening</i>	130
6.4	BOND BETWEEN FRP LAMINATES AND CONCRETE	131
6.5	MICROBIAL DEGRADATION OF FRP COMPOSITES.....	133
6.6	SHIPPING, STORAGE, HANDLING AND FIRE PROTECTION.....	137
6.6.1	<i>Shipping, Storage and Handling</i>	137
6.6.2	<i>Fire Protection</i>	137
6.7	QUALITY CONTROL AND QUALITY ASSURANCE	138
6.8	COST EFFECTIVENESS	139
7.0	CONCLUSIONS AND RECOMMENDATIONS	143
8.0	REFERENCES	151

LIST OF FIGURES

Figure 2.1: Performance Map of Fibers Used in Structural Composite Materials	7
Figure 2.2: Stress-Strain Curves of Typical Reinforcing Fibers	8
Figure 2.3: Performance Map of Structural Composites	11
Figure 3.1: Structural Design Approach for Composites	17
Figure 3.2: Mechanical Response of Various Types of Materials Subjected to Normal and Pure Shear Loading	18
Figure 3.3: Flow Chart for Determination of Transformed Elastic Constants of Fiber-Reinforced Composite Material Under Off-Axis Loading	22
Figure 3.4: Young's Modulus and Shear Modulus of Glass/Epoxy as a Function of Fiber Orientation	25
Figure 3.5: Poisson's Ratio and Shear Coupling Coefficient of Glass/Epoxy as a Function of Fiber Orientation	25
Figure 3.6: Tensile + Shear and Compression + Shear Concrete-Adhesive Specimens	27
Figure 4.1: Load-Deflection Curve of Regular and CFRP-Strengthened Beam	31
Figure 4.2: Crack Width in a Beam with and without External FRP Laminates	31
Figure 4.3: Layout of CFRP-Strips Strengthening with Sika Carbodur System	32
Figure 4.4: Strengthening Schemes of Concrete Beams	39
Figure 4.5: Repair Schemes	41
Figure 4.6: Procedure for Applying Prestressed FRP Sheet	43
Figure 4.7: Beam Flexural Behavior at Near Ultimate Load	46
Figure 4.8: Stress-Strain Distribution at Failure	52
Figure 4.9: Influence of the FRP Reinforcement on the Failure Mechanism	52
Figure 4.10: Different Failure Modes in RC Beams Strengthened with FRP Plate	53
Figure 4.11: Stress-Strain Distribution of Hybrid Beam	55
Figure 4.12: Percentage Increase in Moment Capacity	55
Figure 4.13: Different Methods for Strengthening RC Beams with FRP Plate	57
Figure 4.14: Plate Bonding by Polymerization in Situ Method and External Set Up	58
Figure 4.15: Measured Stress Reduction Due to GFRP Lamination	63
Figure 4.16: Rectangular Beam Cross-Section: Calculation of the Ultimate Moment of Resistance	66
Figure 4.17: Beam Cross Section, Numerical Example	69
Figure 4.18: Beam Cross Section, Serviceability and Deflections	73
Figure 5.1: Stress vs. Axial Strain	82
Figure 5.2: Stress vs. Transverse Strain	83
Figure 5.3: Failure Stress vs. Reinforcement Ratio	84
Figure 5.4: Comparison of Load Displacement Envelopes for Steel and Carbon Jackets	86
Figure 5.5: Load vs. Displacement Response of Columns Before and After Repair	90
Figure 5.6: Stress-Strain Curve of Unreinforced Concrete Cylinder with Hoop Wrap	92
Figure 5.7: Predicted Axial Compressive Stress of Concrete Cylinders with Composite Wraps	96
Figure 5.8: Increase in Load Carrying Capacity as a Function of Wrap Orientation	98
Figure 5.9: Various Steps of Repair Operation	102
Figure 5.10: Concrete Shear Capacity	106
Figure 5.11: Effective Column Dimensions	108
Figure 5.12: Axial Load Shear Component	109
Figure 5.13: Flexural Plastic Hinge Design for Rectangular Columns	113
Figure 5.14: Lap Splice Clamping	114
Figure 5.15: Summary of FRP Jacket Lay-Outs	120
Figure 6.1: Performance Prediction Curves	124
Figure 6.2: Interface Shear Stress vs. Shear Strain	127
Figure 6.3: Variables Influencing the Bond Between FRP Laminates and Concrete	131
Figure 6.4: Failure at the Concrete-FRP Plate Interface.	132
Figure 6.5: Fiberglass Damage by Bacteria Attack	135
Figure 6.6: Microbial Growth on Composites after 30 Days of Incubation	136

LIST OF TABLES

Table 2.1: Degree of Anisotropy of FRP Composites	5
Table 2.2: Typical Properties of Structural Fibers	8
Table 2.3: Advantages and Disadvantages of Reinforcing Fibers	9
Table 2.4: Standards for Determination of Epoxy Resin Properties	9
Table 2.5: Physical Properties of Some Thermosetting Resins Used in Structural Composites	10
Table 2.6: Structural Properties of FRP Reinforced Laminates	11
Table 2.7: Properties of Typical Unidirectional Composite Materials	12
Table 2.8: Elastic and Shear Moduli, and Poisson Ratio's for Conventional Metals and Composites	12
Table 2.9: Comparison of Axial and Flexural Efficiencies for Different Material Systems	13
Table 3.1: Independent Elastic Constants for Various Types of Materials	19
Table 3.1: Test Methods for FRP Material Systems Externally Bonded to Concrete	26
Table 4.1: Characteristics of Sika CarboDur Epoxy Adhesives	33
Table 4.2: Material Properties	35
Table 4.3: Results of Flexural Testing	36
Table 4.4: FRP Properties	36
Table 4.5: Behavior of Failure Modes	37
Table 4.6: Influence of the Plate Material	40
Table 4.7: Contribution to the Shear Capacity of Various Externally Applied Fabrics	42
Table 4.8: Technical Data of Prepreg CFRP Sheets	45
Table 4.9: Forca Tow Sheet FTS-C1-20	46
Table 4.10: Test Results	58
Table 4.11: Results from RC Beams Strengthened with Sprayed FRP Composite	59
Table 4.12: Construction Cost (Canadian Dollars) Using CFRP Sheets	60
Table 4.13: Transformed Moments of Inertia Calculations	74
Table 5.1: Shear-Flexural Strengthening Effects of GFRP and CFRP	91
Table 5.2: Properties of Carbon Wraps Depending on the Fiber Orientation	97
Table 5.3: Comparison of Hypothetical FRP Jacket Thicknesses	115
Table 6.1: EMPA Adhesive Properties	130
Table 6.2: Effect of Water Absorption on Mechanical Properties of Vinyl Ester Composites	134
Table 7.1: Comparison of FRP Application Techniques	147

STANDARD TERMINOLOGY RELATED TO COMPOSITE MATERIALS

Anisotropic Material – A material having properties that vary with direction or depend on the orientation of reference axes. Generally these material do not have planes of material property symmetry.

Fiber – A material characterized geometrically by its high length-to-diameter ratio.

Fiber Reinforced Polymers (FRP) – Composite materials that consist of high strength fibers bound together with an inert plastic resin.

Filler – In manufacturing carbon or glass product technology, particles comprising the base aggregate in an unbaked green-mix formulation. Generally a finely ground mineral that has been intimately mixed into a resin or resin component for the purpose controlling the rheology or extending the resin.

Hardness – The property of a material that resists deformation, particularly permanent deformation or indentation.

Heterogeneous Material – Also called **inhomogeneous**, a material having properties that vary from point to point or depend on location.

Homogeneous – A material having properties that are independent of location.

Hybrid Composite – Composite laminate containing lamina of two or more different types of materials.

Hybrid Structural Behavior – The response of hybrid structure, i.e., FRP-strengthened concrete.

Impregnation – Partial filling of the open pore structure with another material.

Isotropic Material – A material having the same properties in all directions which are independent of the orientation of the reference axes.

Lamina – Also called **ply**, is a plane (or curved) layer of fibers or woven fabric in a matrix. In the case of unidirectional fibers, it is referred to as **unidirectional lamina**.

Laminate – A sequence of two or more unidirectional laminae or plies bonded together at various orientations.

Lamination – The bonding or impregnating of superposed layers with resin and compressing under heat.

Lay-up – Installation of lamina to form a laminate; configuration of the laminate indicating its ply composition.

Macro-mechanics – A study of the composite material behavior wherein the material is presumed homogeneous and the effects of the constituent materials are detected only as average properties.

Micro-mechanics – A study of the composite behavior by examining the behavior and interaction of the constituent materials on a microscopic level.

Molded – Formed in a die by the application of external pressure.

Orthotropic Material – An orthogonally anisotropic material, i.e., having at least three mutually perpendicular planes of material property symmetry.

Phase – Constituent. Each constituent of a composite material, i.e. the fibers and the resin, is a phase. One phase, called reinforcement, is usually discontinuous and stronger, and the weaker phase is called a matrix.

Prepreg FRP – Pre-made materials which are cold laminated in place, by using a resin-fibers-resin lay-up technique to build up an appropriate thickness for the completed composite.

Pultruded Composite Plates – Plates, manufactured by pultrusion (as contrasted to extrusion) which are post-epoxy-bonded to the concrete structure.

Pultrusion – Manufacturing process for fiber-reinforced composites by pulling resin-impregnated fiber through a die.

Specially Orthotropic Material – Orthotropic material with axes of symmetry aligned with the material symmetry, i.e., “x “ axis coincides with fiber direction.

Specific Modulus – Elastic modulus of the material divided by its density.

Specific Strength – Strength of the material divided by its density.

Structural Composite – A material system consisting of two or more phases on a macroscopic level, whose mechanical properties and performance are designed to be superior to those of the constituent materials acting independently.

Working Direction – The direction of fiber or the direction of applied force used in forming a solid body; which defines its physical properties and orientation at installation.

1.0 INTRODUCTION

1.1 BACKGROUND

In the present age, civil engineers are frequently faced with the problem of strengthening an existing structure to assure or to increase its structural safety. Reasons for such actions include changes in the use of structures as well as increased traffic loads on bridges. Due to ever increasing damage caused by environmental effects, corrosion of steel and deterioration of concrete reduce structural safety and lead to inconvenience for the users.

The aging of infrastructures is a great safety and economic concern throughout the world today. The European Community directed that all highway bridges in the United Kingdom must either be capable of carrying 40-ton vehicles by 1999 or have a weight restriction order placed on them. This directive led to a major bridge assessment program, resulting in the need to address deficiencies in over 10,000 of the 60,000 reinforced concrete bridges in the UK. Similar problems are observed all over the world.

The backbone of America's commerce and industry consists of constructed facilities including highways, bridges, airports, and transit systems. Most of the constructed facilities are deteriorating at a rate faster than we can renovate them. Recent studies indicate that over three trillion dollars, or \$200 billion dollars per year (*Faza et al, 1994*), will be needed during the next fifteen years to bring these facilities to adequate operating levels (*McConnell, 1993*).

Many bridges across the United States are deteriorating due to problems associated with reinforced concrete. Factors contributing to this infrastructure deterioration include the effects of environment (i.e. harsh climate), de-icing fluids, seismic activity, and increase in both quantity and weight of traffic loads on structures. For example, 40 percent of the nation's 575,000 bridges are structurally deficient or structurally obsolete, and 25 percent are over 50 years old (*Marshall and Busel, 1996*). Many of these bridges were designed for lower traffic volumes and lighter loads than are common today. This makes them under-designed for current or projected traffic needs. Therefore, rehabilitation to original specifications will not bring these bridges up to the current standards. Strengthening must be considered.

The infrastructure in Oregon needs significant attention. Approximately 75 percent of Oregon's bridges are over 50 years old. These bridges were designed for H-15 traffic loads and do not meet the requirements for the current H-25 load standard. Based on their theoretical capacity, many of Oregon's bridges are classified as under-designed.

In addition to increased or changing traffic demands, common bridge deficiencies include deck deterioration due to wear, freeze/thaw cycles, corrosion of structural steel members, corrosion of reinforcement in concrete structures, response problems under extreme wind or earthquake loads; and aging materials.

With the majority of the U.S. bridge inventory built in the 1950s and 1960s, many bridges are at an age where environmental deterioration, wear, and level of service dictate rehabilitation and upgrading (*Seible et al, 1995*). Repair, strengthening, and/or retrofitting technologies are still at a stage where most applications are based on experience and trial and error, rather than on a sound scientific basis. In order to upgrade the bridge inventory to 21st century service levels, the large volume of rehabilitation work requires the development of new technologies based on new materials and new processes.

Restoring the structural integrity and enhancing the strength and stiffness capabilities of aging structures is a major challenge. The selection of proper methods to retrofit a structure is a complex task. Until recently, external post-tensioning and epoxy-bonded steel plates were the two alternative techniques used to retrofit structurally deficient structures.

External post-tensioning has been successfully used to increase strength of girders in existing bridges or buildings (*Klaiber et al, 1982; Saadatmanesh et al, 1989*). However, this method has several practical difficulties such as providing anchorage for the post-tensioning strands, maintaining the lateral stability of the girders during post-tensioning, and protecting the exposed strands against corrosion (*Saadatmanesh and Ehsani, 1996*). Additionally, post-tensioning requires considerable force to stress the concrete effectively, and may significantly reduce overhead clearance (*Dusseck, 1980*).

Epoxy-bonded steel plates have been used successfully in Europe, Japan, Australia, and South Africa for 25 years to increase the load-carrying capacity of existing reinforced concrete bridges (*Dusseck, 1980; Chan and Tan, 1996; Yong et al, 1996*). This strengthening technique has been found economical and efficient to apply. However, its application in the United States has been extremely rare (*Saadatmanesh et al, 1996*).

The use of Fiber Reinforced Polymer (FRP) composites for rehabilitation and strengthening of civil engineering structures is very promising. FRP composites consist of high strength fibers bound together with an inert plastic resin. Epoxy resins curing at room temperature or specially developed resin systems are usually selected for this. The epoxy resins used for structural bonding of steel plates to concrete are suitable for the bonding of FRP plates as well (*Steiner, 1996*).

FRP composites, primarily developed and used in the defense and aerospace industries, offer unique advantages in many applications where conventional materials cannot provide satisfactory service. Lightweight and natural corrosion resistance are among their main advantages over steel and metal alloys. Their high tensile strength is an excellent complement to concrete properties. Their impermeability and their ability to adhere to old concrete make FRP composites systems that outclass high-performance concrete (*Demers et al, 1996*). Other advantages of FRP over steel include ease of surface preparation at installation, enhanced structural characteristics, and improved durability. When compared to conventional materials, the high strength-to-weight ratio, minor disruption of traffic during repair, and minimal maintenance requirements help make FRP composites an excellent candidate for rehabilitation and strengthening of reinforced concrete structures.

FRP composites are being explored worldwide as a promising material for new structures and rehabilitation/retrofit of aging facilities. In Germany and Switzerland, replacement of steel plates with FRP plates is viewed as a major improvement in externally bonded repair (*Meier and Kaiser, 1991*). In the United States, Saadatmanesh and Ehsani (*1991, 1996*), Ritchie (*1991*), and Triantafillou and Plevris (*1992*) studied the behavior of reinforced concrete beams with externally bonded glass and carbon FRP. Fyfe (*1992*) first proposed a method for retrofitting bridge columns with glass FRP jackets. His work was followed by others (*Priestley et al, 1992*) and was supported by California Department of Transportation (Caltrans) in an effort to develop a method to enhance flexural and shear performance in critical regions of bridge columns during seismic retrofit. Of all countries, Japan has seen the largest research and development effort and the largest number of field applications using externally bonded FRP composites (*Nanni, 1995*). The Japanese work is different from American and European approaches in that it makes use of thin FRP sheets rather than FRP plates.

Two approaches for the provision and application of FRP materials have been developed internationally. One is to employ pre-impregnation (prepreg) materials, which are cold laminated in place, by using a resin-fibers-resin lay-up technique to build up an appropriate thickness of the completed composite reinforcement. The second is to use “pultruded” composite plates, which are post-epoxy-bonded to the concrete structure. Both forms of material can be applied to either unstressed or prestressed concrete elements to take advantage of the high strength offered by FRP materials. The prepreg has the advantage of ensuring better “wetting” of the individual fibers, but has a disadvantage in terms of shelf life and curing because it requires a heating source and precautions for environmental protection.

FRP composites have the potential for tremendous impact on the construction industry internationally. Recent earthquakes in Southern California demonstrated the need for civil engineering structures with enhanced seismic protection. Applications of composite material systems to repair and/or upgrade structures may save billions of dollars, as well as many human lives.

While the advantages and limitations of conventional materials are well established, the advanced composite science and industry must clearly answer questions such as: What is a composite?; How much will it cost?; How long will it last?; and many more. Properly designed and manufactured composite material systems offer superior structural performance while being compatible with existing construction industry practices. Consensus standards and design guidelines are needed so that composite materials can enter the construction market on a large scale in the near future (*McConnell, 1995*). Most importantly, selection and application of FRP materials for repair of structures should be used where the benefits of composites can be best realized.

Although strengthening of existing structures and construction of new facilities with FRP composites is a growing trend worldwide, many engineers are not aware that a significant body of knowledge exists. The existing knowledge can allow engineers to design retrofits and build new structures with composite materials based on sound engineering principles.

1.2 SCOPE AND OBJECTIVES

The objectives of this research project are to outline the methodologies that are needed for using FRP composites to strengthen and rehabilitate reinforced concrete bridge elements. This is achieved by examining the strengthening techniques and material properties of the available glass, carbon and aramid FRP composites. The most promising and cost effective composite systems and modeling techniques are recommended. Further consideration and potential use of composites for strengthening bridges in Oregon is recommended.

2.0 CONSTITUENT MATERIALS FOR COMPOSITES

2.1 DEFINITION OF FRP COMPOSITE MATERIALS FOR STRUCTURAL APPLICATIONS

A structural FRP composite is a material system that consists of two or more constituent materials or “phases”, whose mechanical properties and performance are superior to those of the constituent materials acting independently. One of the phases is typically discontinuous, stiffer, and stronger and is called reinforcement or “fiber”. The less stiff and weaker phase is continuous and is called matrix or “polymer”. Sometimes, because of chemical interactions or other effects, an additional phase, called interphase, exists between the reinforcement and the matrix.

The constituent materials of the composite are typically homogeneous and isotropic, i.e.; their properties are not a function of position or orientation. On the other hand, FRP composites are typically heterogeneous and anisotropic, and their properties depend on position, orientation and reinforcement volume (*Kachlakev, 1997*). On a macro-mechanical scale, their anisotropic behavior can be an advantage.

The average material behavior can be predicted and controlled by the properties of the constituents. However, the anisotropic analysis is complex and results often depend on the chosen computational procedure (*Daniel and Ishai, 1994*). The degree of anisotropy of the most widely used composite materials is shown in Table 2.1, where E_1 , E_2 are the elastic moduli in longitudinal and transverse direction, respectively, G_{12} is the shear modulus, and F_1 , F_{2t} are the tensile strength values in the longitudinal and transverse direction, respectively.

Table 2.1: Degree of Anisotropy of FRP Composites

FRP Composite	E_1/E_2	E_1/G_{12}	F_1/F_{2t}
Steel	1.00	2.58	1.00
Vinyl Ester Epoxy	1.00	0.94	1.00
S-glass/Epoxy	2.44	5.06	28
E-glass/Epoxy	4.42	8.76	17.7
Carbon/Epoxy	13.64	19.1	41.4
UHM/Epoxy	40	70	90
Kevlar/Epoxy	15.3	27.8	260

(*Daniel and Ishai, 1994*)

Steel and epoxy, which are isotropic materials, are presented for comparative purposes. Note that the steel has the same elastic modulus in longitudinal and transverse direction, e.g. $E_1 = E_2$. The other materials are anisotropic. For example, the longitudinal elastic modulus of E-glass/epoxy composite is 4.42 times greater than its transverse elastic modulus.

When viewed on a micro-mechanical scale, composites have the advantage of high stiffness and strength. For example, ordinary plane glass fractures at stresses of only few thousand pounds per square inch, while glass fibers, in commercially available forms, have strengths 100 times that of plane glass. The paradox of a fiber having different properties from the bulk form is due to the more perfect structure of the fiber. The fibers usually have a low fracture toughness, which, in the FRP composite, is compensated for by the ductility of the matrix. The stress transfer capability of the matrix enables development of multi-site failure mechanisms, which results in the high strength of the composite.

2.2 PROPERTIES OF CONSTITUENT MATERIALS

Among the main reasons for using composites are: improved strength, stiffness, corrosion and wear resistance, fatigue life, reduced weight and improved thermal behavior of the resulting structure. One of the most important features of the composites is their “tailorable” behavior. Properly designed, they allow control of the properties of the material according to specific needs.

Properties of a composite material depend on the properties of the constituents, geometry, and distribution of the phases. One of the most important parameters is the volume (or weight) fraction of the reinforcement. The distribution of the reinforcement determines the homogeneity of the material system. The more non-uniform is the reinforcement, the more heterogeneous is the composite material and the higher is the probability of failure in the weakest area. The geometry and orientation of the reinforcement affect the anisotropy of the system.

The phases of the composite materials have different roles that depend on the type of material and application for the composite. In the case of low performance composites, the reinforcement, usually in form of short fibers, provides some stiffening but only local strengthening. The matrix is the main load-bearing constituent governing the mechanical properties and performance of the composite. In case of high performance structural composites, the reinforcement usually consists of continuous fibers, which determine the stiffness and strength of the composite system in the direction of fibers. In such cases, the matrix phase provides protection of the fibers and transfers local stresses from one fiber to another.

2.2.1 Classification and Properties of Reinforcing Fibers

A fiber is characterized geometrically by its high length-to-diameter ratio. A large variety of fibers are available for reinforcement. The desirable characteristics of most reinforcing fibers are high strength, high stiffness, and low density. Each type of fiber has its own advantages and disadvantages, depending upon their manufacturer and specific properties.

The most common types of fibers used in advanced composites for structural applications are glass, carbon, and aramid. The fibers can be chopped, woven or braided and occupy 50 to 70 percent of the composites volume.

Figure 2.1 shows the relationship between specific modulus and specific strength of some of the most common fibers. The specific strength and specific modulus of a material are defined as the ratios of the ultimate strength to material's density and elastic modulus to material's density, respectively.

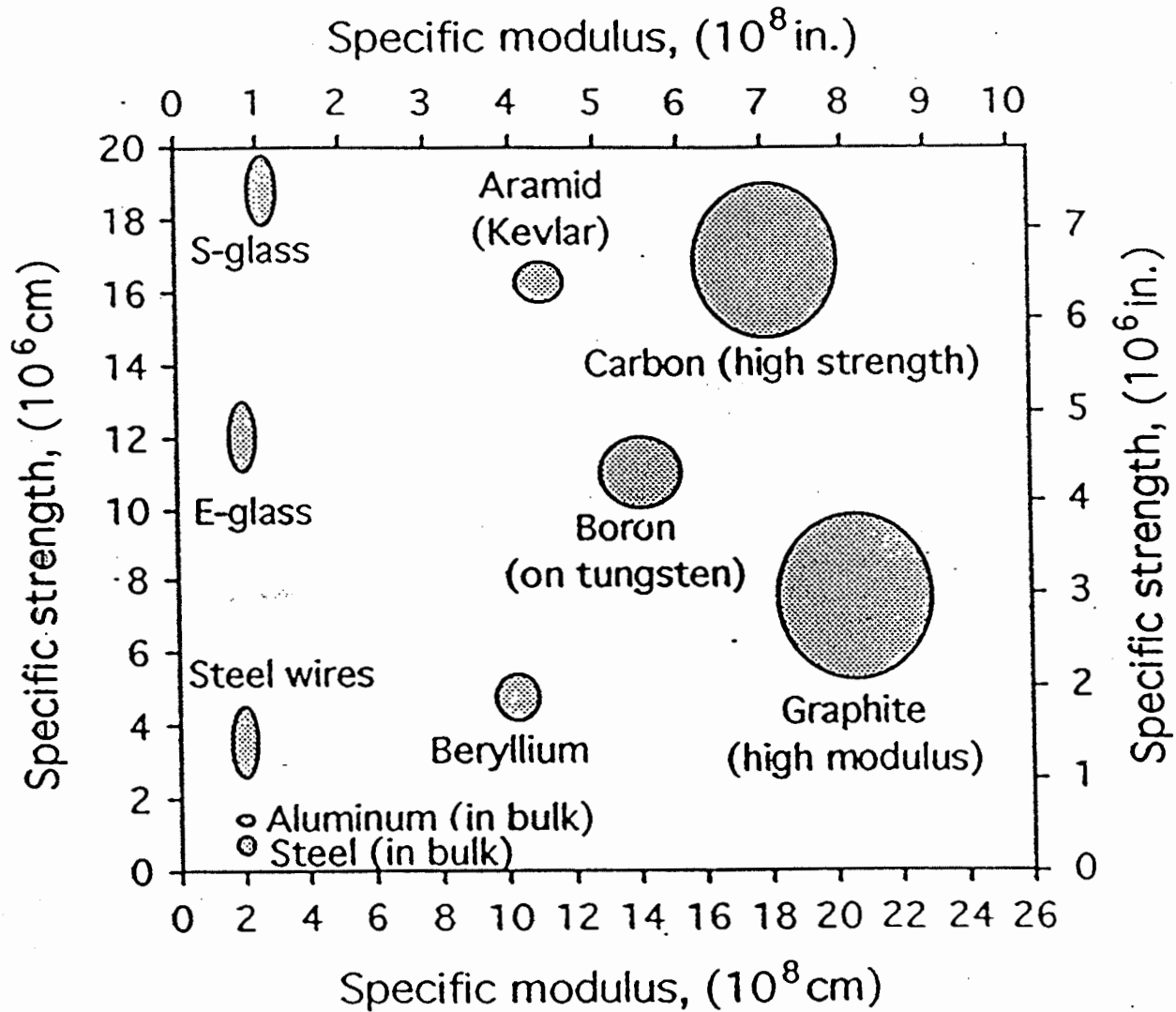


Figure 2.1: Performance Map of Fibers Used in Structural Composite Materials
(Daniel and Ishai, 1994)

Glass fibers are commonly used in structural composites because of their high tensile strength and low cost. They are limited for high performance applications due to their relatively low stiffness, and chemical degradation when exposed to severe hydrothermal conditions (Daniel and Ishai, 1994). Glass fibers have good characteristics for civil engineering applications. However, if not properly coated with resin, their durability in high alkaline environment is unacceptable. E-glass and S-glass are the two types of fibers most widely used in civil engineering. S-glass fibers possess strength and elastic modulus superior to E-glass, mainly due to better quality control during manufacturing.

The aramid fibers are aromatic polyamides. Aramid fibers exhibit excellent fatigue and creep behavior. However, their chemical or mechanical bond with resin may be problematic. Kevlar 29 and Kevlar 49 are the two most commonly used aramid fibers for structural applications. Aramid (or Kevlar) fibers have higher stiffness and lower density than S glass fibers, but they are limited by their very low compressive strength in the composites and high moisture absorption (Daniel and Ishai, 1994).

The graphite or carbon fibers are produced from three types of polymer precursors, polyacrylonitrile (PAN) fibers, rayon fibers, and pitch (Tang, 1997). Although there are many carbon fibers available on the market, they are divided into three categories, high strength (HS), high modulus (HM), and ultra-high modulus UHM). In the case of UHM carbon fibers, the increase in stiffness is achieved at the expense of strength. Their fatigue and creep resistance is excellent. Table 2.2 shows typical properties of the most widely used fibers for structural composites.

Table 2.2: Typical Properties of Structural Fibers

Fiber Type	Density (g/cm ³)	Elastic Modulus (GPa)	Tensile Strength (GPa)	Elongation (%)
E-Glass	2.54	72.5	1.72-3.45	2.5
S-Glass	2.49	87	2.53-4.48	2.9
Kevlar 29	1.45	85	2.27-3.80	2.8
Kevlar 49	1.45	117	2.27-3.80	1.8
Carbon (HS)	1.80	227	2.80-5.10	1.1
Carbon (HM)	1.80-1.86	370	1.80	0.5
Carbon (UHM)	1.86-2.10	350-520	1.00-1.75	0.2

Most fibers behave linearly up to failure. Figure 2.2 shows the stress-strain behavior of some of the most popular fibers.

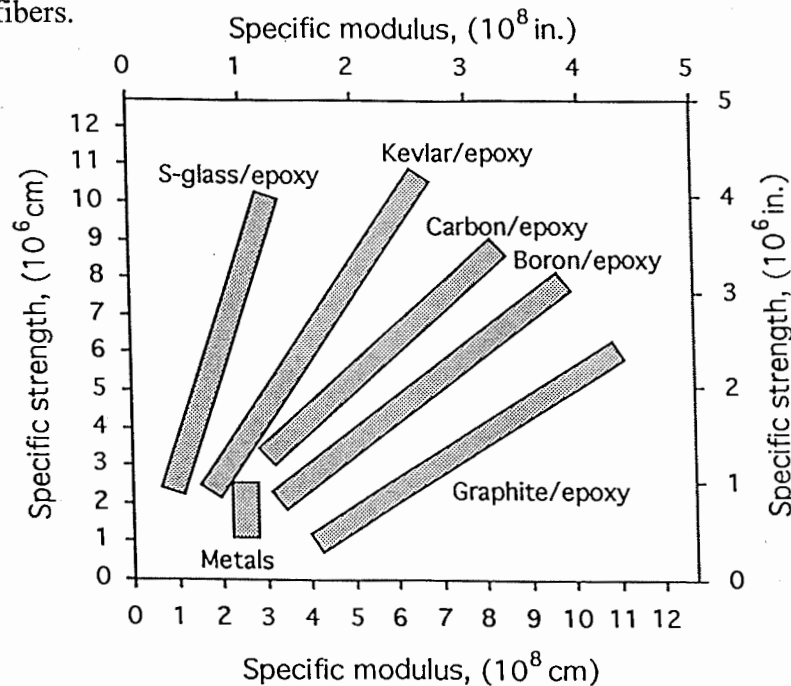


Figure 2.2: Stress-Strain Curves of Typical Reinforcing Fibers
(Daniel and Ishai, 1994)

The advantages and disadvantages of different types of reinforcing fibers are summarized in Table 2.3.

Table 2.3: Advantages and Disadvantages of Reinforcing Fibers

Fiber Type	Advantages	Disadvantages
E-glass, S-glass	High strength, low cost	Low stiffness, short fatigue life, temperature sensitivity
Aramid (Kevlar)	High tensile strength, low density	Low compressive strength, high moisture absorption
HS Carbon	High strength, high stiffness	High cost
UHM Carbon	Very high stiffness	Low strength, high cost

2.2.2 Classification and Properties of Resin Matrices

Epoxy resins are used widely in structural applications. Their attractive features for composite applications include adequate strength, chemical resistance, dimensional stability, low shrinkage compared to unsaturated polyesters, good adhesion to a variety of reinforcing fibers, and low material cost (*Billmeyer, 1984*).

The resin matrix protects the reinforcing fibers, which are typically rigid and brittle. More importantly, it distributes an applied load and acts as a stress-transfer element, so that when an individual fiber fails, the composite system does not lose its load carrying capability. Durability, shear, compressive and transverse strength are also provided by the resin matrix. To fulfill these functions, fiber-matrix interface adhesion is of great importance. The physical properties of the matrix that are critical for the performance of the overall composite are its tensile, compressive and shear strength, elastic modulus, toughness, yield and ultimate elongation, as well as its thermal and moisture resistance. Table 2.4 summarizes some of the test methods used for determination of resin properties.

Table 2.4: Standards for Determination of Epoxy Resin Properties

Mechanical Property	Test Method
Shore Hardness	ASTM D-2583-87
Heat Distortion Temperature	ASTM D-641-96
Tensile Strength	ASTM D-638-89
Tensile Modulus	ASTM D-638-89
Tensile Elongation	ASTM D-638-89
Flexural Strength	ASTM D-790-86
Flexural Modulus	ASTM D-790-86
Viscosity, Krebs Units	ASTM D 2393-86 and ASTM D 445-96
Weight per Gallon	ASTM D 3892-77
Epoxy Content	ASTM D 1652-88
Water Absorption	ASTM D 570-81
Pot Life	ASTM D 2566-86
Specifications of Epoxy Resins	ASTM D 1763-88
Fire Resistance	ASTM D 635-88

The most commonly used resin matrices in composites are polymeric. Polymers are long molecules that essentially consist of repeating structural units. Polymers for resin matrices can be divided into two groups: thermosets and thermoplastics. Typical thermoset matrices are

epoxies, polyesters, and polyamides. Thermoplastics are represented by polysulfone and poly-ether-ketone. Thermosets develop their properties as the result of exothermic reactions and are used for quick-curing systems, while thermoplastics develop their properties on solidification by cooling, and are more compatible with hot forming and injection molding fabrication methods.

Thermoset resins are typically associated with expensive multi-step manufacturing processes. They often exhibit low toughness, high moisture sensitivity, short shelf life, and may require complex repair methods. However, they are generally harder and less flexible than thermoplastics. They are usually solvent resistant and do not melt when heated. They cannot be easily shaped after polymerization, and therefore are polymerized into the final shape in the mold rather than in lay-up work. The thermosets are preferred for structural applications. Table 2.5 summarizes some of the physical properties of the thermosetting resins. Specifications of thermosetting polyesters can be found in ASTM D 1201-81 (1987).

Table 2.5: Physical Properties of Some Thermosetting Resins Used in Structural Composites

Resin Type	Density (kg/m ³)	Tensile Strength (MPa)	Elongation (%)	Elastic Modulus (GPa)	Long Term Use Temp. (°C)
Polyester	1.2	50-65	2-3	3.0	120
Vinyl Ester	1.15	70-80	4-6	3.5	140
Epoxy	1.1-1.4	50-90	2-8	3.0	120-200
Phenolic	1.2	40-50	1-2	3.0	120-150

(Moukwa, 1996)

Thermoplastic resins offer single step processing, good toughness, almost no moisture absorption, simple repair methods, and multiple reforming processes. However, they do exhibit sudden changes in properties when heated. Thus, they are not suitable for civil engineering applications.

2.3 MECHANICAL PROPERTIES OF FIBER REINFORCED POLYMER COMPOSITES

Composite materials have many characteristics that are different from those of conventional engineering materials. Some characteristics are merely modifications of conventional materials, while others require new analytical and experimental procedures. Most common engineering materials are assumed to be homogeneous and isotropic. In contrast, composite materials are often both heterogeneous and anisotropic to such a degree that the differences cannot be ignored.

Some material properties, such as density, are described by a single value for both isotropic and anisotropic materials. Properties such as stiffness, strength, Poisson's ratio, moisture, thermal expansion, and electrical conductivity are associated with direction and are treated as anisotropic. The largest differences typically occur between properties in longitudinal and transverse directions.

The performance of composites is typically rated on the basis of specific strength and specific modulus as defined in Section 2.2.1. A representation of the performance of typical structural composites is shown in Figure 2.3.

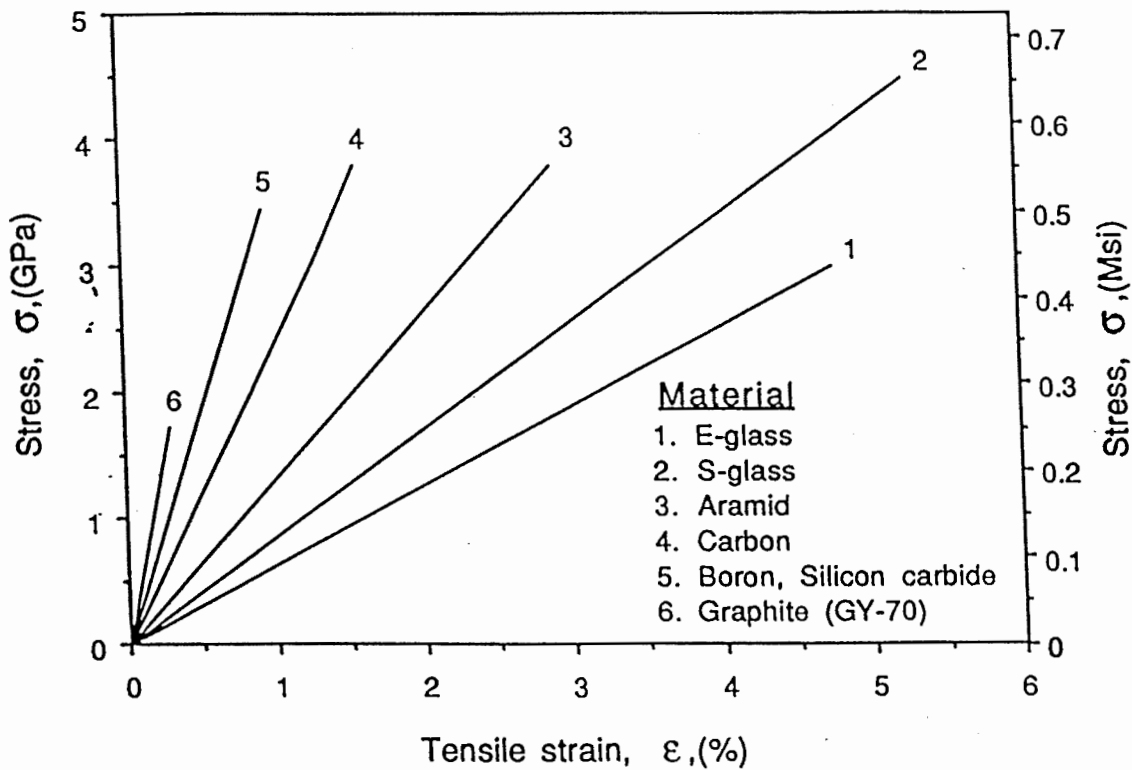


Figure 2.3: Performance Map of Structural Composites
(Daniel and Ishai, 1994)

The variation shown corresponds to the variation between quasi-isotropic and unidirectional laminates. As can be seen, most composites have higher specific modulus and specific strength than metals. The specific gravity of FRP composite reinforcement is one-fourth to one-seventh to that of steel reinforcement with equivalent diameter. The ratio of strength to mass density is 10 to 15 times greater than that of steel.

The structural properties of fiber reinforced laminates can be determined in accordance to the following standards:

Table 2.6: Structural Properties of FRP Reinforced Laminates

Structural Property	Test Method
Tensile Strength	ASTM D-638
Tensile Modulus	ASTM D-638
Flexural Strength	ASTM D-790
Flexural Modulus	ASTM D-790

Mechanical properties of some of the most widely used unidirectional composite materials are shown in Table 2.7.

Table 2.7: Properties of Typical Unidirectional Composite Materials

Property	E-Glass/Epoxy	S-Glass/Epoxy	Aramid/Epoxy	Carbon/Epoxy
Fiber Volume	0.55	0.50	0.60	0.63
Density, g/cm ³	2.10	2.00	1.38	1.58
Longitudinal Modulus, GPa	39	43	87	142
Transverse Modulus, GPa	8.6	8.9	5.5	10.3
Shear Modulus, GPa	3.8	4.5	2.2	7.2
Poisson's Ratio	0.28	0.27	0.34	0.27
Long. Tensile Strength, MPa	1080	1280	1280	2280
Compressive Strength, MPa	620	690	335	1440
Thermal Expansion Coeff., 10 ⁶ /°C	7.0	5.0	-2.0	-0.9
Moisture Expansion	0	0	0	0.001

(Jones, 1975; Daniel and Ishai, 1994)

Table 2.7 defines the stiffness, compressive and tensile strengths for the principal material directions. Thus, the degree of anisotropy of the composite material can be determined, similarly to that shown in Table 2.1. Therefore, the mechanical properties in the principal material directions can be combined in order to define the stiffness and strength parameters at an arbitrary orientation of the composite.

Shear strength and shear modulus are of particular importance for composites designed to work in a direction different than that of the principal material direction. With certain combinations of fiber-orientation, the corresponding elastic and shear moduli will define a material having superior properties than that of the constituent materials and improved performance of the reinforced structure.

Table 2.8 shows the elastic (E_i) and shear (G_i) moduli of some conventional metals and composites used for structural applications.

Table 2.8: Elastic and Shear Moduli, and Poisson Ratio's for Conventional Metals and Composites

Material	E_1	E_2	G_{12}	G_{13}	G_{23}
Aluminum	10.40	10.40	3.38	3.38	3.38
Copper	17.00	17.00	6.39	6.39	6.39
Steel	29.00	29.00	11.24	11.24	11.24
Carbon/Epoxy (AS/3501)	20.00	1.30	1.03	1.03	0.90
Carbon/Epoxy (T300/934)	19.00	1.50	1.00	0.90	0.90
Glass/Epoxy	7.80	2.60	1.25	1.25	0.50

(Daniel and Ishai, 1994)

Note: Values of the moduli are in msi = 1 million psi; 1 psi = 6.895 kN/m²

Usually, fatigue behavior of FRP composites is very good. Carbon and aramid fiber reinforcement have a fatigue characteristics as much as three times higher than steel (Kretsis, 1987). These FRP reinforcements do not fatigue when stressed to less than 1/2 of their ultimate strength. The fatigue strength of glass FRP reinforcement has not been researched in detail. Although the glass usually creeps under a sustained load, it can be designed to perform satisfactorily (Tang, 1997).

The two main failure modes for FRP composites are fiber-dominated failure and matrix-dominated failure. Laminates with sufficient 0° degree layer, i.e. fibers oriented in load direction, will exhibit the fiber-dominated failure mode. This type of failure is essentially independent of the rate and frequency of loading. On the other hand, matrix-dominated failure mode is a rate/frequency dependent phenomenon due to the viscous matrix behavior (*Kujawski and Ellyin, 1995*). The viscous-dependent matrix behavior plays an essential role in fatigue performance of FRP composites.

2.4 MATERIALS AND MANUFACTURING PROCESS SELECTION

Materials have to be chosen based on their properties and costs. Based on economics, glass FRP is the preferred reinforcing material for reinforced concrete, while carbon would only be used in critical areas.

Manufacturing processes, such as pultrusion, yield products in the \$2 to \$3 per pound range, with raw materials cost being as high as 80 percent of the overall cost (*Seible et al, 1995*). Other methods of fiber placement can cost hundreds of dollars per pound, with material cost as low as 10 to 30 percent.

Additional considerations concerning the design purpose of the structural elements must be taken into account for any load carrying structural element. Shape factor is often forgotten. Shape factor is a dimensionless parameter characterizing the efficiency of a specific shape to carry a given load. It is clear that under tension the best performance is seen when the axial loading capacity at the lowest self-weight is realized. This is obtained by maximizing E/ρ , where E is the Young's modulus and ρ is the density (*Seible et al, 1995*). Similarly, in flexure, the highest factor of $E^{1/2}/\rho$ indicates the best material for flexural shapes. Table 2.9 gives the results for a number of material systems based on these two measures and shows the mechanical advantages that can be derived for advanced composite structural elements and systems.

Table 2.9: Comparison of Axial and Flexural Efficiencies for Different Material Systems

Materials System	E, GPa	ρ , g/cm ³	AXIAL EFFICIENCY		FLEXURAL EFFICIENCY	
			E/ρ	Ranking	$E^{1/2}/\rho$	Ranking
HS Carbon/Epoxy	181	1.6	113.1	1	8.4	1
Carbon – PEEK	134	1.6	83.8	2	7.2	2
Kevlar/Epoxy	76	1.46	52.1	3	6.0	3
Mild Steel	200	7.8	25.6	4	1.8	5
E-Glass/Epoxy	38.6	1.8	21.4	5	3.5	4

(*Seible et al, 1995*)

3.0 DESIGN PRINCIPLES FOR COMPOSITE MATERIALS

3.1 DESIGN PHILOSOPHY

The advantages of advanced composite materials, including the potential to tailor their behavior according to specific needs, has led to increased research in civil infrastructure-related applications. The successful implementation of composites in all applications requires an understanding that design cannot follow the paradigms of metals or other conventional materials. The materials, configurations, and processes involved in designing with composites have intricate connections and interrelations. For example, reinforcement of cylindrical structural elements can be done with a number of techniques, but the final choice will be based on the columns basic shape, structural strengthening requirements and available materials.

Designing with advanced composite materials requires the engineer to make a number of decisions. Advanced composite design is not only the design of an element or structure, but starts with the selection of materials that will give the laminae properties allowing the composite to perform correctly. This design process involves topics such as anisotropic elasticity, strength of anisotropic materials, micro-mechanics, and manufacturing processes.

Specialists will likely limit their attention to one or two specialty areas such as constituent materials and design, micro-mechanics, or macro-mechanics. Although the design of composite materials and composite structures requires a background in advanced mechanics of materials, three-dimensional stress-strain relations, plate theory, and anisotropic elasticity, the actual implementation of composites for structural strengthening is much simpler. However, background in structural design and analysis is essential for successful designs of reinforced concrete structures incorporating composite materials.

The objective of this chapter is to introduce basic concepts related to composite materials. The information presented here cannot be regarded as guide for designing composites, but is rather to make the physical significance of the concepts understandable.

3.2 MECHANICS OF COMPOSITE MATERIALS

The design and analysis of composites, as opposed to conventional materials, are not supplemented with available design charts and guidelines to help the structural engineer. Although dependent upon the characteristics of the constituent materials, FRP composites can be tailored and designed to meet almost any desired specifications.

Unlike conventional materials, which have two elastic constants and two strength values, typical composites possess a large number of descriptive material parameters. The number of degrees of freedom associated with the number of descriptive parameters enables material optimization, but at the same time makes the analysis much more complex. In contrast, the optimization of conventional materials is typically limited to three degrees of freedom, usually the geometric parameters (*Kachlakev, 1997*).

Composite materials are evaluated from two perspectives; micro-mechanical and macro-mechanical. Micro-mechanics examines the interaction of the constituent materials on a microscopic level. Macro-mechanics is the study of the composite material behavior when the material is presumed homogeneous and the effects of the constituent materials are treated as average properties of the composite (*Jones, 1975*). For basic structural analysis, the materials are typically treated macro-mechanically. However, in order to study some of the effects of anisotropy, micro-mechanical analysis is often required. A schematic diagram of the various levels of analysis is shown in Figure 3.1.

The anisotropy of composites leads to mechanical behavior quite different from that of conventional materials. Isotropic materials subjected to a stress in one direction exhibit extension in the direction of the applied stress and contraction in the perpendicular direction. Shear stresses cause only shear deformations. For anisotropic materials, application of stress in one direction leads not only to extensions and contractions, but also produces shear deformations. Conversely, applied shear stress causes extension and contraction in addition to the shear deformation. This complex relationship between loading and deformation is referred to as “coupling” between the loading and deformation modes (see Figure 3.2).

Orthotropic materials are special subset of anisotropic materials. The distinguishing characteristics are related to the directionality of the material properties with the property being different for each axis. For example, when loaded in the “on-axis” direction (principal material direction), which coincides with the direction of fibers, extension in the direction of the applied load and contraction in the direction perpendicular to the load occurs. However, due to different properties in the two directions, the contraction may result in a deformation that is more or less than that of a similarly loaded isotropic material even though the isotropic material has the same elastic modulus as the composite in the direction of loading.

Additionally, in orthotropic materials the magnitude of the shear deformations is independent of the Young’s modulus and Poisson’s ratios. Thus, the shear modulus of an orthotropic material does not depend on other elastic constants.

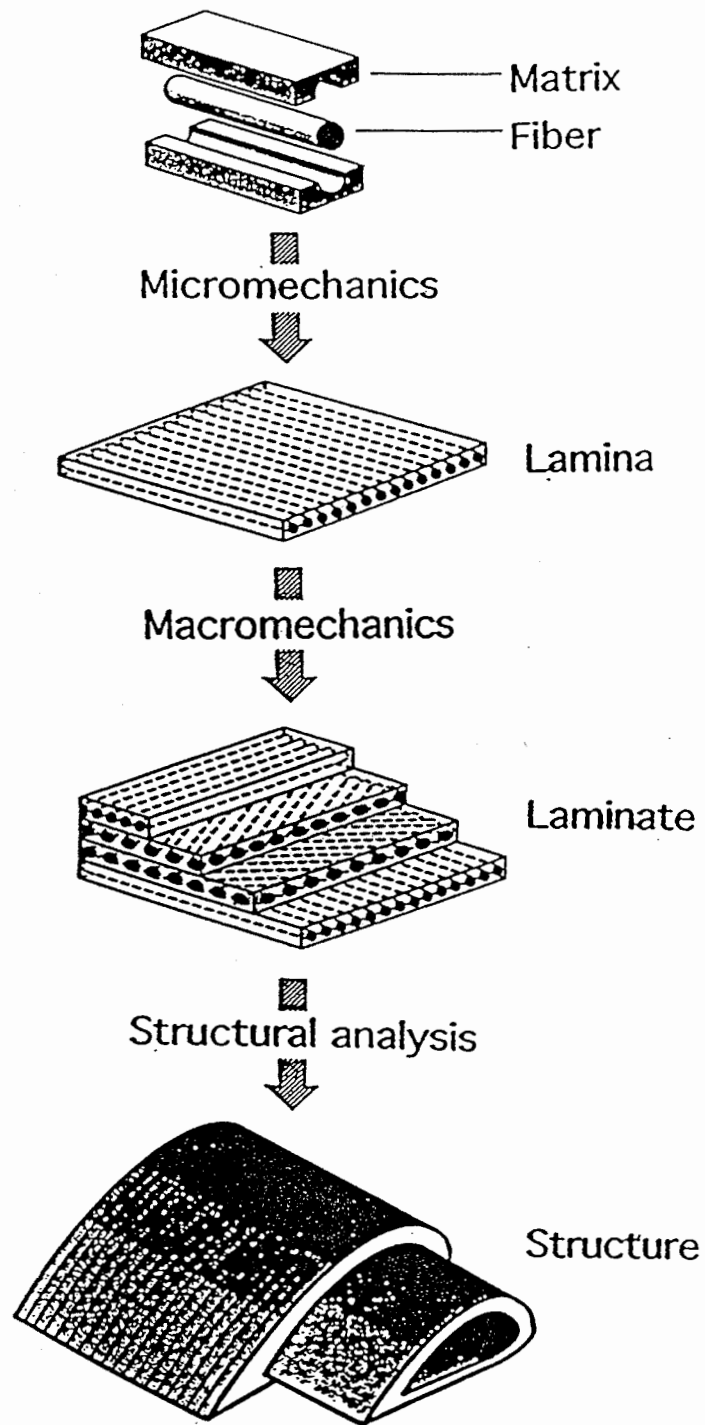


Figure 3.1: Structural Design Approach for Composites
(Daniel and Ishai, 1994)

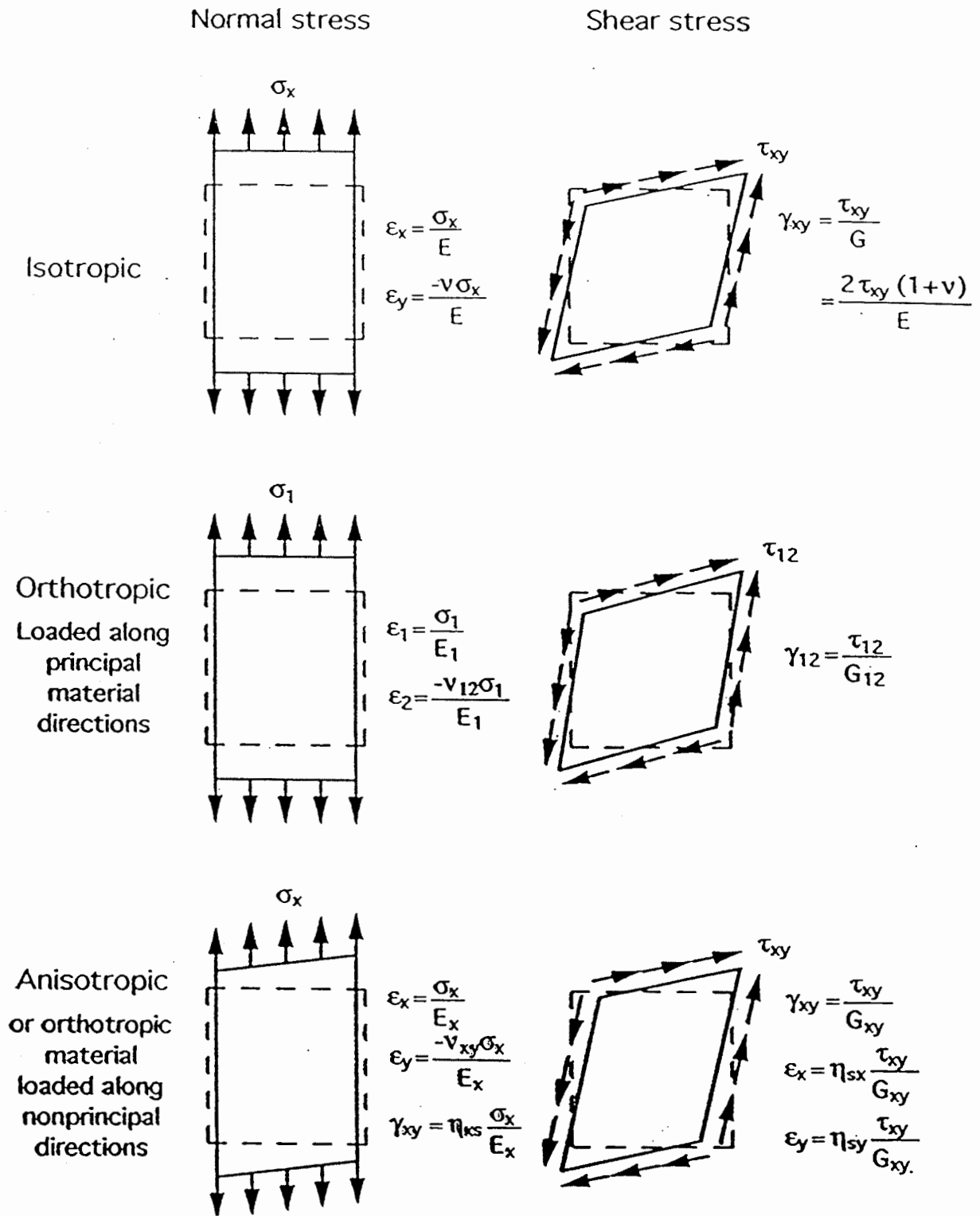


Figure 3.2: Mechanical Response of Various Types of Materials Subjected to Normal and Pure Shear Loading
(Daniel and Ishai, 1994)

3.3 DESIGN PRINCIPLES

In the most general form of Hook's law, the state of stress at a point is represented by nine stress components σ_{ij} acting on the sides of an elementary cube with sides parallel to the xyz axes. Similarly, the state of deformations is represented by nine-strain components ε_{ij} . The stress and strain components, representing the behavior of an anisotropic material, are:

$$\sigma_{ij} = C_{ijkl} \varepsilon_{kl} \quad |_{i,j,k,l=1,2,3} \quad (3-1)$$

$$\varepsilon_{ij} = S_{ijkl} \sigma_{kl} \quad |_{i,j,k,l=1,2,3} \quad (3-2)$$

where:

- σ – stress tensor
- ε – strain tensor
- C – stiffness matrix component
- S – compliance matrix component

Note that:

$$\sigma_{kl} = S_{ijkl}^{-1} \varepsilon_{ij} \quad |_{i,j,k,l=1,2,3} \quad (3-3)$$

In Appendix A it is shown that there are 81 elastic constants needed to characterize an anisotropic composite material. However, since $\sigma_{ij} = \sigma_{ji}$ and $\varepsilon_{ij} = \varepsilon_{ji}$, the number of independent elastic constants is reduced to 36.

In the case of a specially orthotropic material (with three mutually perpendicular planes of material symmetry), the number of independent elastic constants is reduced to 9, as various stiffness and compliance coefficients are interrelated. Most of the composite materials for structural applications are analyzed assuming these conditions. Table 3.1 gives the number of independent constants for the various types of materials.

Table 3.1: Independent Elastic Constants for Various Types of Materials

Material	Independent Elastic Constants
General anisotropic material	81
Anisotropic material with symmetric stress and strain tensors	36
With elastic energy considerations	21
Specially orthotropic materials	9
Assuming transverse isotropy	5
Isotropic Materials	2

(Daniel and Ishai, 1994)

The stiffness and compliance components (C_{ijkl} and S_{ijkl}) have more physical than engineering meaning. The relationships between these mathematical constants and the engineering constants, i.e. elastic moduli and Poisson's ratios, for a two dimensional stress state are as follows (*Jones, 1975*):

$$\begin{aligned} S_{11} &= \frac{1}{E_1} & S_{12} &= \frac{-\nu_{12}}{E_1} = \frac{-\nu_{21}}{E_2} \\ S_{22} &= \frac{1}{E_2} & S_{66} &= \frac{1}{G_{12}} \end{aligned} \quad (3-4a)$$

$$\begin{aligned} C_{11} &= \frac{E_1}{1-\nu_{12}\nu_{21}} & C_{12} &= \frac{E_2\nu_{12}}{1-\nu_{12}\nu_{21}} \\ C_{22} &= \frac{E_2}{1-\nu_{12}\nu_{21}} & C_{66} &= G_{12} \end{aligned} \quad (3-4b)$$

where:

E_1, E_2 – Young's moduli parallel and perpendicular to the fiber orientation
 ν_{ij} – Poisson's ratio for strain in direction j when stressed in direction i
 G_{12} – shear modulus

Further details regarding relationships between mathematical and engineering constants for a specially orthotropic materials subjected to tensile loading in the longitudinal and transverse direction are provided in Appendix A (Equations A-20 to A-23).

In order to design a composite material, the values of the independent constants are needed. The experimental determinations of the elastic constants and consequently the strength of a material are based on uniaxial stress states. However, the actual stress states of these materials are at least biaxial if not triaxial. Some of the biaxial strength theories are the maximum stress theory, maximum strain theory, the Tsai-Hill theory, and the Tsai-Wu theory. According to these theories the material, although orthotropic, must be assumed homogeneous (*Jones, 1975*). Thus, some of the observed microscopic failure mechanisms cannot be accounted for.

Under off-axis loading, the stress imposed on the material must be transferred in the principal material directions. According to the maximum stress theory, the stresses in the principal material directions are obtained by (*Tsai, 1968*):

$$\sigma_1 = \sigma_x \cos^2 \theta \quad \sigma_2 = \sigma_x \sin^2 \theta \quad \tau_{12} = \sigma_x \sin \theta \cos \theta \quad (3-5)$$

where:

θ – is the angle between the applied load and the fiber orientation
 σ_x – is the stress in the direction of the applied load
 $\sigma_1, \sigma_2, \tau_{12}$ – stresses in the principal material directions

In the maximum stress theory, the stresses in principle material directions ($\sigma_1, \sigma_2, \tau_{12}$) must be less than the respective ultimate stresses (X_t, Y_t, S), otherwise fracture will occur.

$$\sigma_1 < X_t, \quad \sigma_2 < Y_t, \quad \tau_{12} < S \quad (3-6)$$

By inversion of Equation 3.5 and substitution of Equation 3.6, the maximum allowed uniaxial stress, σ_x is the smallest of:

$$\sigma_x < \frac{X_t}{\cos^2 \theta}, \quad \sigma_x < \frac{Y_t}{\sin^2 \theta}, \quad \sigma_x < \frac{S}{\sin \theta \cos \theta} \quad (3-7)$$

The maximum strain theory is similar to the maximum stress theory in that the strains are limited rather than stresses. Specifically, the material will fail if one or more of the following inequalities is not satisfied:

$$\varepsilon_1 < X_{\varepsilon} = \frac{X_t}{E_1}, \quad \varepsilon_2 < Y_{\varepsilon} = \frac{Y_t}{E_2}, \quad \gamma_{12} < S_{\varepsilon} = \frac{S}{G_{12}} \quad (3-8)$$

where:

- X_{ε} – maximum normal strains in the x direction
- Y_{ε} – maximum normal strains in the y direction
- S_{ε} – shear strain;
- X_t – maximum normal stresses in the x direction
- Y_t – maximum normal stresses in the y direction
- S – shear stress

The stress-strain relations are:

$$\varepsilon_1 = \frac{\sigma_1 - \nu_{12}\sigma_2}{E_1}, \quad \varepsilon_2 = \frac{\sigma_2 - \nu_{21}\sigma_1}{E_2}, \quad \gamma_{12} = \frac{\tau_{12}}{G_{12}} \quad (3-9)$$

Upon substitution of Equation 3-5 in Equation 3-9 and accounting for the failure inequalities shown in Equation 3-8, the maximum strain criterion can be expressed as:

$$\begin{aligned} \sigma_x &< \frac{X_t}{\cos^2 \theta - \nu_{12} \sin^2 \theta} \\ \sigma_x &< \frac{Y_t}{\sin^2 \theta - \nu_{21} \cos^2 \theta} \\ \sigma_x &< \frac{S}{\sin \theta \cos \theta} \end{aligned} \quad (3-10)$$

A flow chart for calculation of the elastic engineering constants in the general case of off-axis loading is illustrated in Figure 3.3.

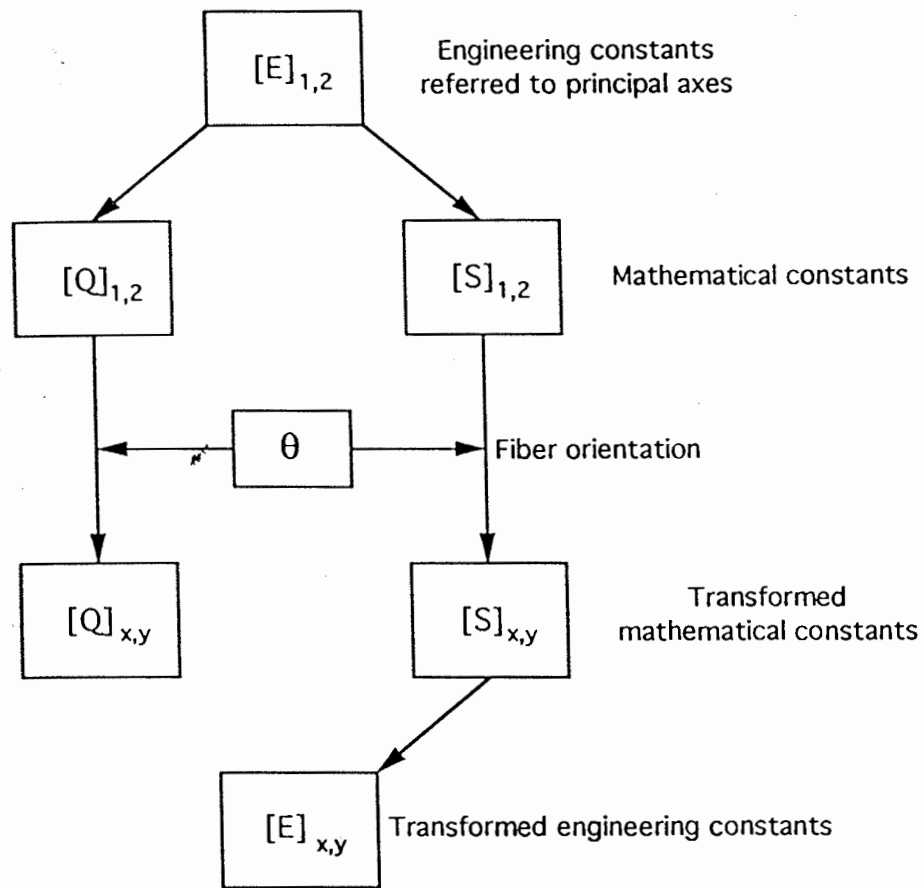


Figure 3.3: Flow Chart for Determination of Transformed Elastic Constants of Fiber-Reinforced Composite Material Under Off-Axis Loading (Daniel and Ishai, 1994)

The constants E_1 , E_2 , ν_{12} , and G_{12} are obtained by “characterization” tests. Then, the relations in Equation 3-4a and 3-4b are used to obtain the reduced principal compliance and stiffness, S_{ij} and C_{ij} . Transformed stiffness and compliance S_{xy} and C_{xy} are calculated for the off-axis fiber orientation. Finally, the transformed engineering constants E_x and E_y are calculated with the equations in Appendix A.

3.4 MICRO-MECHANICAL PREDICTION OF ELASTIC CONSTANTS

Elastic constants of composites can be estimated by using the micro-mechanical approach. The parameters that determine the strength of composite are shape, size, orientation and concentration of the fibers, the matrix, and the bond between the fibers and matrix. A variety of methods have been used to predict the properties of constituent materials, namely: mechanics of materials, numerical, semi-empirical and experimental approaches (Hashin, 1983).

The mechanics of materials approach is based on simplifying assumptions of either uniform strain or uniform stress in the constituents. This approach adequately predicts the longitudinal modulus and Poisson's ratio, since these properties are not sensitive to fiber shape and distribution (*Hashin, 1983*). On the other hand, this approach underestimates the transverse and shear moduli. Since the other approaches are very time consuming and/or give unrealistic results, the mechanics of materials is the most widely used method. Two variations of this method are the parallel and series models.

The parallel model is recommended when the properties in the longitudinal direction are dominated by the fibers. The stiffness and strength are predicted using the rule of mixtures (Equations 3-11, 3-12, and 3-13). Assumptions made in the parallel model satisfy "isostrain" conditions, i.e., the strains in the reinforcement and matrix are equal, Equation 3-11. Also, ideal bond between them is assumed. Equations 3-12 and 3-13 can be used to estimate the longitudinal modulus of the composite lamina:

$$\varepsilon_c = \varepsilon_f = \varepsilon_m \quad (3-11)$$

$$\frac{\sigma_c}{\varepsilon_c} = \frac{\sigma_f V_f}{\varepsilon_f} + \frac{\sigma_m (1 - V_f)}{\varepsilon_m} \quad (3-12)$$

$$E_c = V_f E_f + \frac{E_m}{1 - V_f} \quad (3-13)$$

where:

- E_c – moduli of elasticity of the composite
- E_r – moduli of elasticity of the reinforcement
- E_m – moduli of elasticity of the matrix phase
- V_f – volume fractions of fibers
- V_m – volume fractions of fibers and matrix, respectively.
- $\varepsilon_c, \varepsilon_f, \varepsilon_m$ – strains in the composite, fibers and matrix
- $\sigma_c, \sigma_f, \sigma_m$ – stresses in the composite, fibers and matrix

The series model is the case when loading is normal to the fiber direction. The state of stress in the matrix surrounding the fibers is complex and is affected by interaction with neighboring fibers. The transverse modulus of fiber-reinforced composites is a matrix-dominated property and it is sensitive to local stresses. The series model assumes that $\sigma_c = \sigma_r = \sigma_m$, i.e. stresses resulting from a certain load in the composite system, reinforcement, and matrix phases are equal. Thus, the series model is also called "isostress" model (Equations 3-14, 3-15, and 3-16).

When the stress is applied in the direction perpendicular to both the matrix and the fibers, their loaded areas are also equal, i.e. $A_c = A_r = A_m$. Unlike the parallel model, the strains in the matrix and fibers are different. Equation 3-16 models the transverse modulus of elasticity of the composite system.

The series model is given by:

$$\varepsilon_c = \varepsilon_f V_f + \varepsilon_m V_m \quad (3-14)$$

$$\frac{\sigma_c}{E_c} = \frac{\sigma_f}{E_f} V_f + \frac{\sigma_m}{E_m} V_m \quad (3-15)$$

$$\frac{1}{E_c} = \sum \frac{V_i}{E_i} \quad (3-16)$$

Both the parallel and series models represent the limiting conditions of loading and fiber orientation. The actual properties vary between these extremes.

Elastic properties of composites also vary with fiber orientation. Typically, the elastic modulus of glass/epoxy composite decreases monotonically from a maximum at $\theta = 0^\circ$ to its minimum at $\theta = 45^\circ$, and increases again to a local maximum at $\theta = 90^\circ$. The shear modulus exhibits maximum at $\theta = 45^\circ$ and reaches its minimum at $\theta = 0^\circ$ and 90° . Poisson's ratio has minimums at $\theta = 0^\circ$ and $\theta = 90^\circ$, and peaks at approximately $\theta = 45^\circ$. Figures 3.4 and 3.5 show the elastic constants for a typical glass/epoxy composite as a function of the fiber orientation (*Daniel and Ishai, 1994*).

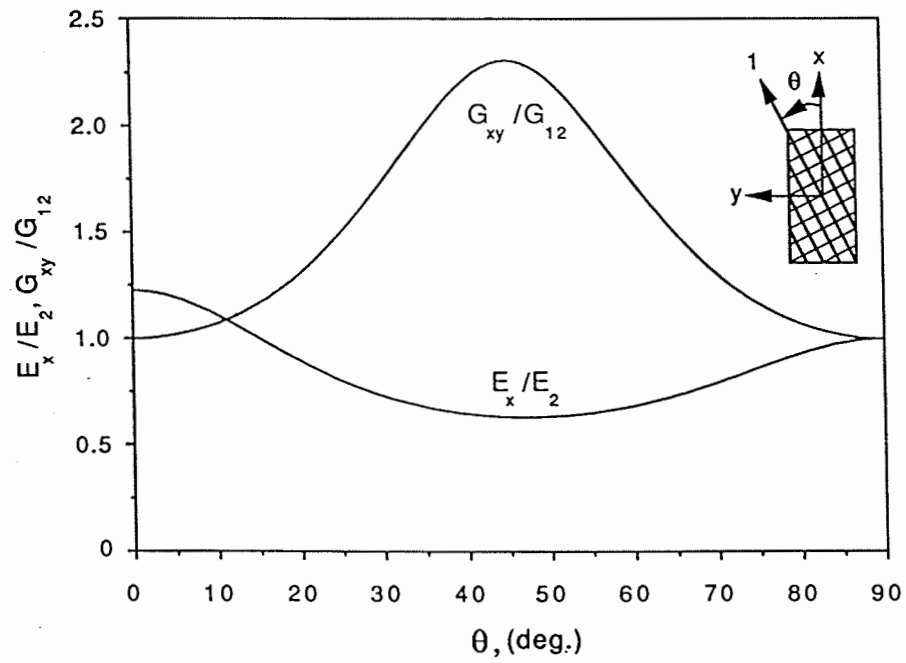


Figure 3.4: Young's Modulus and Shear Modulus of Glass/Epoxy as a Function of Fiber Orientation
(Daniel and Ishai, 1994)

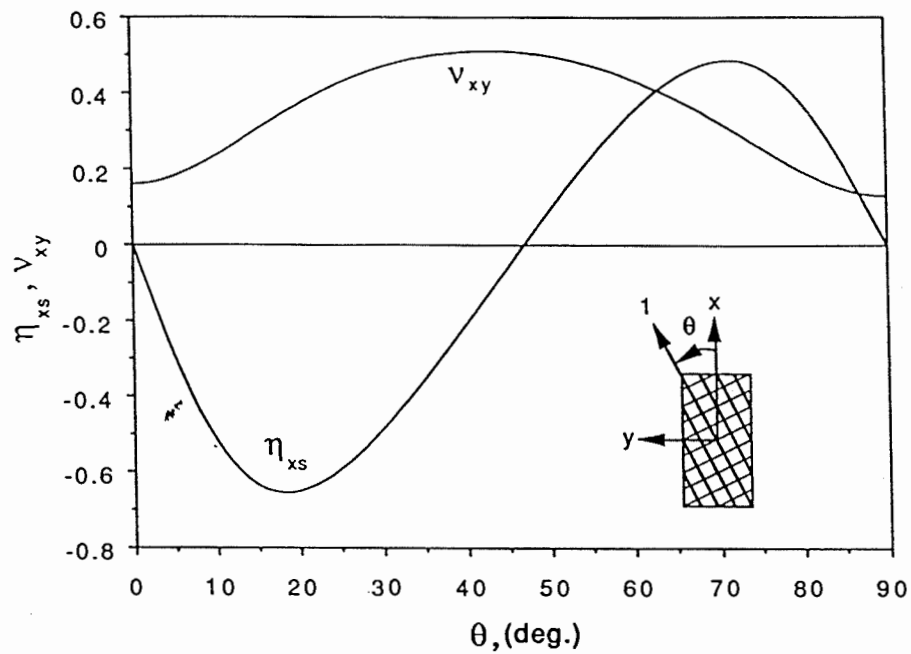


Figure 3.5: Poisson's Ratio and Shear Coupling Coefficient of Glass/Epoxy as a Function of Fiber Orientation
(Daniel and Ishai, 1994)

3.5 TEST METHODS FOR DETERMINATION OF MECHANICAL PROPERTIES OF FRP REINFORCEMENT

Currently ASTM is developing test methods for FRP materials. However, at this time there is no standard suite of ASTM test methods for quantifying structural performance and mechanical properties of FRP composites bonded to concrete. Certain ASTM standards are applicable to FRP materials. Thus, FRP composites may be tested in accordance with these methods as long as all exceptions to the method are listed in the test report.

Design and analysis of structures with composite materials requires reliable experimental data. A significant amount of reliable experimental data on the mechanical properties of the composite laminae and adhesives can be determined by using some or all of the tests listed in Table 3.1 (*ACI 440-F, 1997*).

Table 3.1: Test Methods for FRP Material Systems Externally Bonded to Concrete

Property	Test Method
Tensile Strength, Strain, and Modulus of FRP Sheets	ASTM D 3039 or SACMA SRM 4-99
Fatigue Strength of FRP Sheets	N/A
Coefficient of Thermal Expansion of FRP Sheets	ASTM C 531 or E 851
Sheet to Sheet Adhesive Shear	ASTM C 531
Sheet to Concrete Adhesive Shear	ASTM C 531
Sheet to Concrete Adhesive Tension	ASTM C 531
Tensile Strength, Strain, and Modulus of FRP Shells	N/A
Fatigue Strength of FRP Shells	N/A
Coefficient of Thermal Expansion of FRP Shells	N/A
Shell to Concrete Adhesive Shear	N/A
Shell to Concrete Adhesive Tension	N/A
Shell to Shell Adhesive Shear	N/A
Stress Rupture of FRP Shells	N/A

In order to complement the suite of tests listed above some researchers have developed their own test procedures. Two of them follow.

A single-lap shear test specimen was developed at the University of Delaware for evaluating composite material plates bonded to concrete (*Finch et al, 1995*). The test specimens consisted of 25 mm-wide FRP plates bonded to concrete blocks. The bond lengths varied from 50 mm to 200 mm. In the test setup, the concrete block is securely mounted to the bottom cross-head of a testing machine. The free end of the composite plate is clamped in a grip mounted on the top cross-head. A load is applied until the bond fails. From the load at failure, the shear bond strength can be determined. The test method can be used to evaluate the effects of surface preparation, type of adhesives, and concrete properties on average bond strength.

In order to study the interface characteristics between adhesive and concrete, Arduini et al (1997) carried out tension shear and compression tests. The shear tests were on prismatic and cubic concrete specimens. The test set-up is shown in Figure 3.6. After curing, the specimens were saw-cut at different angles, which varied from 20 to 70 degrees. The cut faces were rejoined with a layer of adhesive that was being evaluated. The bonded samples were taken to failure on a testing machine and the results were used to construct a Mohr-Coulomb failure envelope. From the envelope, the shear strength of the interface was found to be about 5 MPa (0.73 ksi).

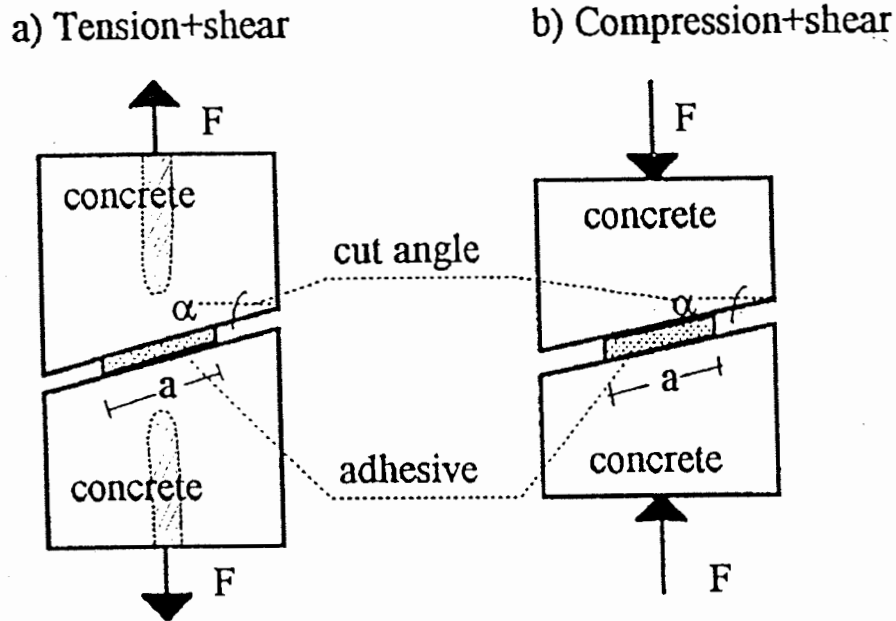


Figure 3.6: Tensile + Shear and Compression + Shear Concrete-Adhesive Specimens (Arduini et al, 1997)

4.0 EXTERNAL REINFORCEMENT OF CONCRETE BEAMS USING FRP COMPOSITE MATERIALS

4.1 STRENGTHENING TECHNIQUES WITH CONVENTIONAL MATERIALS

Numerous researchers have studied strengthening of existing concrete structures through the use of externally bonded steel plates to increase the load-carrying capacity of concrete bridge girders. Most report promising results. However, some researchers report that epoxy-bonded steel plates alone will not increase the ultimate strength, though the stiffness is enhanced marginally (*Chan and Tan, 1996*). Other researchers have reported that a shortcoming of this method is the possibility of corrosion at the epoxy-steel interface, which may affect the bond strength (*MacDonald and Calder, 1982*). Some studies showed that, at higher temperatures, the epoxy can fail to transfer the shearing stresses from the steel plate to the concrete, with resultant crack propagation through the epoxy joint (*Van Gemert and Bosch, 1985*).

Jones et al (*1982*) described the characteristics of under- and over-reinforced concrete beams with bonded steel plates. Five under-reinforced and three over-reinforced beams of the same dimensions were tested in four-point bending. The beams were strengthened with steel plates 1.5 mm to 10 mm thick. The study found that the composite action between the reinforced concrete beam and the glued steel plate was effective up to failure. The ultimate strength of both under- and over-reinforced beams increased significantly. The bending stiffness increased and the deflections decreased. The plates delayed the occurrence of the first crack, but had very little effect on crack spacing.

4.2 STRENGTHENING TECHNIQUES WITH COMPOSITE MATERIALS

4.2.1 Background

A survey conducted by the U.S. Army Corps of Engineers reported on composites repair technologies, upgrade and strengthening technologies, research, and demonstrations in the U.S., Western Europe and Japan. The survey revealed that in the U.S., the use of composite materials for structural retrofitting is still in the research and development stage (*Marshall and Busel, 1996*). In Europe and Japan, these materials are being used in practical applications (*Nanni, 1997; Meier et al, 1992*).

In an effort to overcome the structural disadvantages and construction difficulties of the steel plate technique, the Swiss Federal Laboratories for Testing and Research (EMPA) conducted an extensive project on "Post Reinforcement of Concrete Structures with Carbon Fiber-Reinforced Epoxies" (*Meier and Deuring, 1991*). Restoration of real structures followed the research (*Meier et al, 1992*).

Most projects conducted in Europe and Japan used carbon/epoxy sheet materials and laminates bonded to concrete. The most critical failure mode reported was bond failure accompanied by separation of the FRP laminate from the concrete substrate. Therefore, the bond strength of FRP to concrete was identified as a critical issue.

In order to promote faster development of the composite material systems in the U.S., the Construction Productivity Advancement Research Program (CPAR) was established in 1988. The program resulted in an agreement between the Corps of Engineering laboratories and private industry for cooperatively supporting composite research for structural applications.

Another study conducted by the Corps of Engineers found that civil works infrastructure is rapidly deteriorating and has long outlived its design life (*Marshall and Busel, 1996*). Economically viable solutions to extend the useful life of the existing structures and to protect against earthquake damage are needed.

The goals of the ODOT project are to identify candidate material systems, study performance at the laboratory level, establish materials and installation performance specifications, and develop design guidelines to be used for each type of viable strengthening system. Demonstration projects, field tests and long term durability assessment will be considered as part of the project.

4.2.2 Some Early Evaluations

An extension of the steel plating method, which negates the corrosion problem, is to bond high-strength composite FRP plates or sheets to the tension face of concrete beams. Several researchers have studied the benefits of bonding non-corrosive composite materials to concrete (*Ritchie et al, 1991; Meier et al, 1992; Finch et al, 1995; Saadatmanesh and Ehsani, 1996*). Some researchers have developed practical rehabilitation schemes for actual structures using graphite/epoxy plates (*Iyer et al, 1989; Rostasy et al, 1992*).

Figure 4.1 shows a typical load-deflection diagram of simple steel-reinforced concrete beam without any external reinforcement, and then compares it to a similar beam strengthened with a 0.3 mm thick carbon FRP (CFRP) laminate (*Meier, 1992*). The thin laminate nearly doubles the ultimate load carried by the beam. Furthermore, the deflection at ultimate load is only half of that of the unreinforced beam.

After the appearance of the first cracks in the concrete, the internal steel and external FRP carry the tensile stresses. As soon as the internal steel reaches its yield point, the FRP laminate continues to contribute to the additional increase of load. Finally, the laminate fails in a brittle manner, which results in a beam failure.

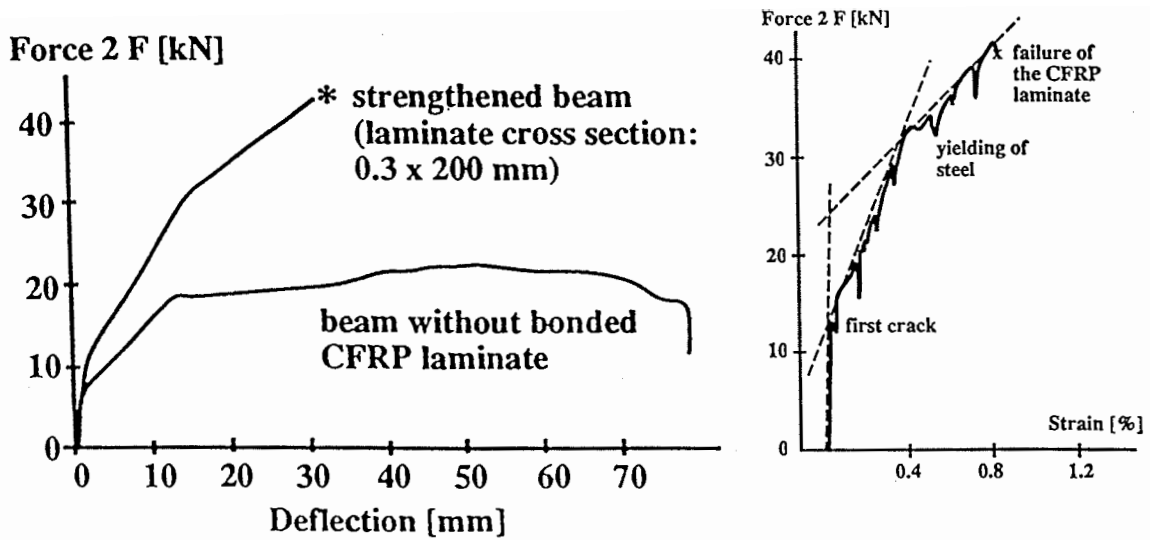


Figure 4.1: Load-Deflection Curve of Regular and CFRP-Strengthened Beam
(Meier and Kaiser, 1991, Las Vegas)

In order to demonstrate the effectiveness of FRP-strengthening, the Swiss Federal Laboratories conducted a study on strengthened and non-strengthened 200 mm x 150 mm x 2000 mm beams (Meier and Kaiser, 1991; Meier, 1992). Initially, a non-strengthened beam was loaded with a force of 9.5 kN, which resulted in a few bending cracks with total crack width of 3.85 mm. The unloaded beam was then strengthened with 0.75 mm x 200 mm CFRP laminate and reloaded with force of 15 kN. As the load increased, additional cracks were observed, but the total crack width was reduced to 2.58 mm. The influence of externally bonded FRP laminates on the development of bending cracks is shown in Figure 4.2. The FRP reinforced beam achieved a more even distribution of the cracks and a smaller total crack opening.

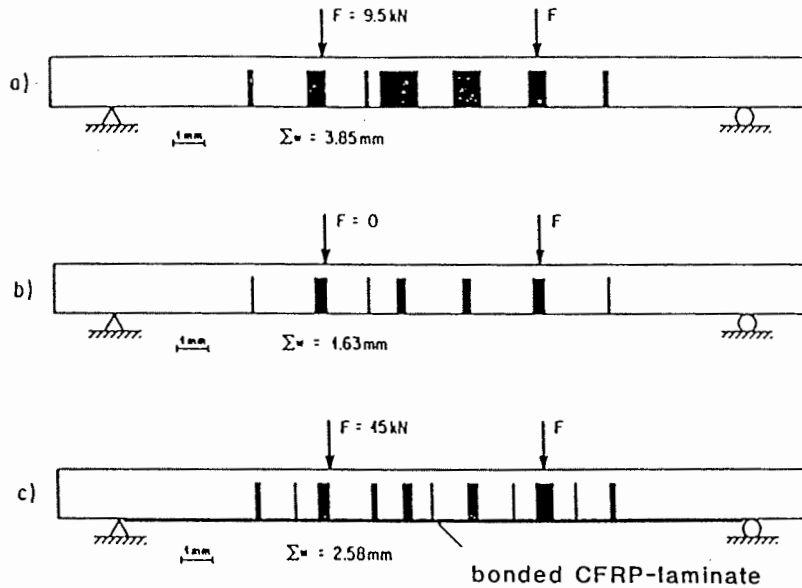


Figure 4.2: Crack Width in a Beam with and without External FRP Laminates
(Meier and Kaiser, 1991)

Sika AG of Zurich, Switzerland developed and tested a new CFRP strengthening system for concrete slabs, Sika CarboDur (Figure 4.3). The carbon FRP strips (1 mm to 2 mm thick and up to 500 m long) used with Sika CarboDur system are manufactured by pultrusion and have a tensile strength in the range of 3 kN/mm^2 in the direction of fibers. The system allows for strengthening of concrete slabs weakened by cut out openings that require crosswise-applied strips. The rigidity of the CFRP strips is such that they cannot be applied onto large concave surfaces. At strip crossings, adhesive 1.2 mm thick is applied. Carbon FRP strips are supplied on rolls up to 500 m long. Thus, an application that requires very long strips can be executed without lap joints. Two-component epoxy adhesives are used to bond the strips to the concrete. Good wetting of the concrete surface prior to plate bonding is essential. Particularly important is the smoothness of the adhesive layer in order to reduce the peak stresses. The adhesives requirements are listed in Table 4.1.

The system requires detailed surface preparation according to the principles described above. The bond strength between the CFRP and the concrete at the anchorage zones of the strips should have an average value of 2 N/mm^2 and no single value should be less than 1.5 N/mm^2 .

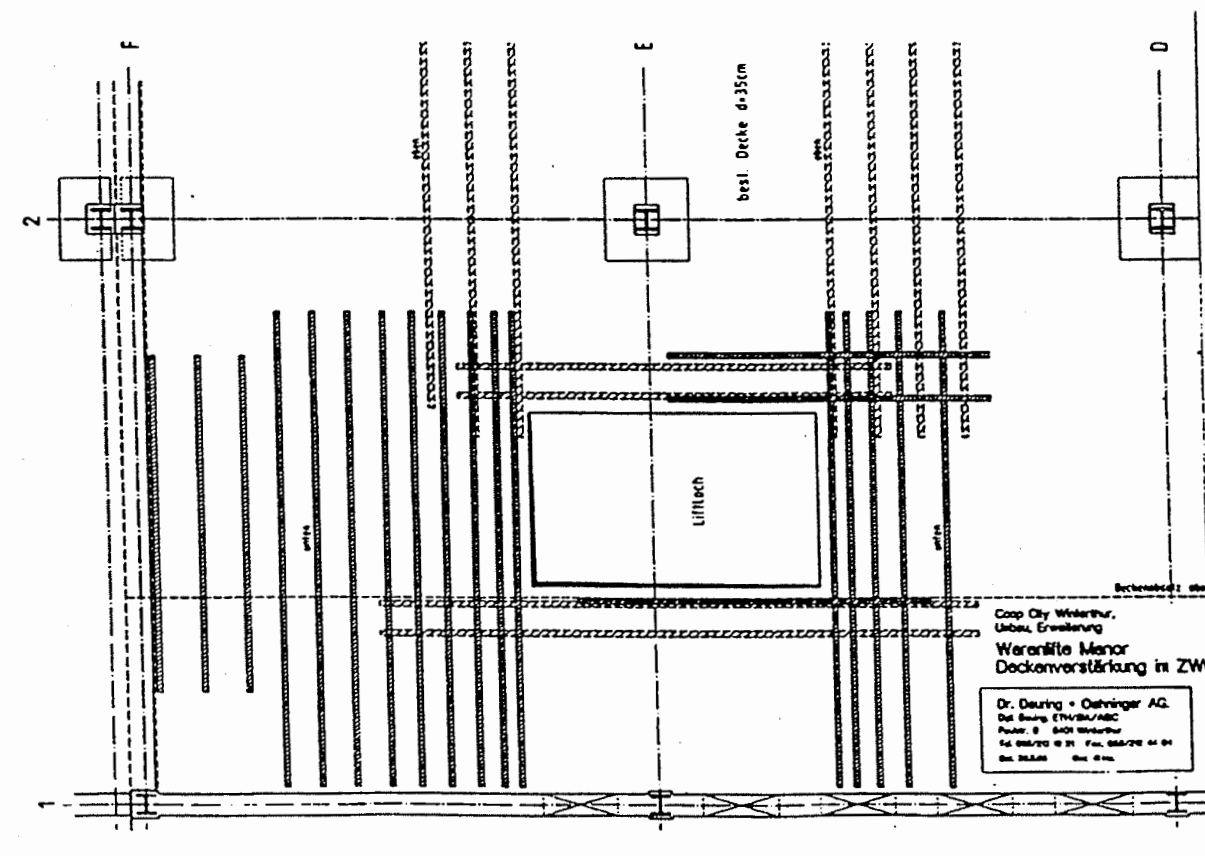


Figure 4.3: Layout of CFRP-Strips Strengthening with Sika CarboDur System
(Steiner, 1996)

Table 4.1: Characteristics of Sika CarboDur Epoxy Adhesives

Characteristics	Guide Values
Pot Life	40-80 min. at 20°C
Sag Flow	3-5 min. at 35°C
Squeezability	3000-4000 mm ² at 15°C
Compressive Strength	75-100 N/mm ²
Tensile Strength	20-30 N/mm ²
Shear Strength	15-20 N/mm ²
Elastic Modulus	8-16 kN/mm ²
Shrinkage	0.04-0.08%
Adhesion to Wet Surface	4 N/mm ²
Glass Transition Point	50-70°C

(Steiner, 1996)

The strengthening technique used by Sika AG can be summarized as follows. The CFRP strips to be used are placed on a table and checked for possible damage. The bonding surface of the strips has to be cleaned with solvent. As a next step, homogeneously mixed epoxy is applied to the prepared concrete surface with trowel and leveled by scraping. This assures complete filling of the rough surface and wets the concrete completely. Next, the cleaned and completely dried CFRP strip is coated with epoxy adhesive, then applied to the concrete surface and fixed by light pressure. The adhesive layer should be about 2 mm thick, minimum 1 mm and maximum 5 mm. The extraordinary stability of the adhesive, as well as the light weight of the strips allows work without any clamping or supporting devices. Then the CFRP is pressed onto the concrete by means of rubber roller, squeezing the fresh epoxy out on both sides. Parallel CFRP strips are applied with a gap of 5 mm in between. The squeezed adhesive is removed with a painter's knife and the CFRP surface is cleaned.

For quality control purposes, steel discs or pieces of FRP strips are bonded to the concrete and pulled off after hardening. At least two prisms (4 x 4 x 16 cm) of adhesive, taken from the last mix of the day or from each different batch, must later be tested in a laboratory. The bonded FRP strips should be examined for hollow spots by light tapping.

If desired for aesthetic reasons, the outer face of the FRP strips can be painted or covered with cement mortars after priming the strip with a suitable bonding agent.

4.3 DESIGN MODELS AND APPLICATION TECHNIQUES

4.3.1 “Lack of Ductility” Problem Associated with FRP Strengthening

The scope of engineering use of any material depends primarily on its stress-strain profile. FRP materials can offer strength and stiffness several times higher than those of conventional metals. The strength and stiffness of FRPs depends on the type and volume of fibers and resin, which can be tailored according to design requirements. But the unique aspect of the stress-strain diagram for FRPs, which make them very different from metals, is the absence of yield plateau. This means that FRPs fail in a sudden brittle manner. The use of advanced composite plates, in lieu of steel, depends on how effectively the designer can accommodate and exploit the material in conjunction with the existing structural element, without sacrificing any of its desirable properties. Compromising on ductility at failure is a major concern, which has to be carefully considered when designing for FRP-strengthening.

The ductility of a reinforced concrete beam is a measure of its energy absorption capacity. Ductility mainly depends upon the distinct yielding level. Typically, ductility is defined as a ratio of deflection or curvature at ultimate strength to that at yield. Ductility of a structural member, in a broad sense, is an indication of its ability to undergo large strains before failure. From the mechanics of materials perspective, good ductility is also an indicator of a relatively high strain-energy absorption capacity of the member. Energy absorption in concrete beams can be estimated by considering the area under load-deflection or moment-curvature diagrams (*Vijay and GangaRao, 1996*). Consideration of the serviceability-based energy level (*ACI 318-95*) with respect to the total energy in a moment-curvature plot provides a basis for addressing ductility and deformability in the design of FRP-strengthened concrete beams.

Interpretation of ductility of FRP strengthened concrete beams on the basis of conventional definitions may be misleading due to the linear stress-strain relation of FRP materials up to failure (*Vijay and GangaRao, 1996*). An acceptable definition of ductility for FRP strengthened concrete beams should consider factors such as: uniform elongation of FRP laminates as compared to localized yielding of steel; confinement effects; and uniform crack location and spacing.

The ultimate strain and elastic modulus of glass FRP varies from 10800 to 19500 microstrain and 10.3 to 37.2 GPa, respectively. For carbon FRP these parameters vary from 7800 to 16200 microstrain and 54.5 to 305 GPa, respectively. In this context, an appropriate expression of ductility should not be a function of the FRP's ultimate stress and strain values. One attempt in to address this issue is the relative comparison in terms of strain-energy absorption, i.e. the area under the load-deflection curve.

A comparative study (*Swamy et al, 1996*) indicates that at any load level, the higher the FRP plate fraction area, the lower is the energy absorption capacity of the strengthened concrete member. In all strengthened beams, the load carrying capacity is increased substantially but the energy absorption capacity is reduced drastically at the equivalent load level. This is more pronounced for CFRP compared to GFRP plates.

One very clear distinction between CFRP and GFRP plate strengthened beams is the presence of a noticeable plastic region on the stress-strain plot for the latter. In real sense this is a pseudo-plastic region, because the steel rebars are in plastic stage but the external GFRP is still elastic. This is not the case when CFRP plates are used. Because of their higher stiffness and strength, the contribution of the external plate to the total tensile force is higher, which keeps the neutral axis down and delays or totally prevents the plastic deformation of the steel rebars.

4.3.2 Flexural Strengthening – Case Studies

One technique for flexural strengthening of existing reinforced concrete bridge elements is to apply externally bonded reinforcement to the tension side of the elements. Cracking and the ultimate moment of resistance are two important factors in flexural strengthening of reinforced concrete. In concrete elements there exists an envelope of potential structural enhancements, which is governed by the amount and distribution of internal reinforcement as well as the properties and geometry of the concrete. In particular, the tensile and shear strength of the cover concrete will limit stress transfer into the external reinforcement.

A study conducted at Oxford Brookes University, UK, describes the influence of various parameters on the flexural behavior of beams strengthened with externally bonded FRP reinforcement (*Hutchinson and Rahimi, 1996*). These parameters include the concrete strength as well as the modulus and strength of FRP external reinforcement. Over thirty 2300 x 200 x 150 mm conventionally reinforced beams were fabricated and strengthened with epoxy-bonded unstressed CFRP and glass FRP (GFRP) laminates. Unidirectional pultruded Ciba Fibredux glass/epoxy and carbon/epoxy composite plates were used. The thickness of the cured laminate was between 0.4 and 1.8 mm. Representative properties of the materials are summarized in Table 4.2.

Table 4.2: Material Properties

Properties	Concrete	GFRP Composite	CFRP Composite	Epoxy Adhesive
Density, kg/m ³	2200	2200	1500	1500
Young's Modulus, GN.m ⁻²	25	36	127	7
Shear Strength, MNm ⁻²	6	–	80	23
Tensile Strength, MNm ⁻²	3	1074	1532	20
Compressive Strength, MNm ⁻²	55-69	–	–	70
Poisson's Ratio	0.2	0.3	0.3	0.3
Elongation at Break, %	0.15	3.1	1.21	0.7
Thermal Expansion, 10 ⁻⁶ C ⁻¹	10	8	-0.8	30

(*Hutchinson and Rahimi, 1996*)

The concrete beams were lightly sand blasted in order to remove the laitance and expose small and medium sized pieces of aggregate. A nylon peel layer was molded onto one surface of the composite during manufacture and was peeled off prior to bonding. Sikadur 31 PBA, a two-component cold-curing epoxy, was used. The unstressed composite plate was held against the concrete with a vacuum bag during curing to keep a uniform pressure over the bonded area. The resulting bond-line was about 2 mm thick. All of the beams with bonded external reinforcement performed significantly better than the controls. Test results are shown in Table 4.3. The GFRP provided significant ductility and reasonable strength. For the CFRP plates, the increased beam

enhancement was achieved at the expense of a loss of ductility with increasing thickness of CFRP.

Table 4.3: Results of Flexural Testing

FRP Reinforcement	FRP Cross Section, mm ²	Ultimate Deflection, mm	Ultimate Load, kN
None	0	53	26
Carbon	117	41	69
Carbon	60	38	54
Glass	270	33	60

(Hutchinson and Rahimi, 1996)

Five rectangular beams and one T-beam were tested at the University of Arizona, Tucson (Saadatmanesh and Ehsani, 1996). Each beam was 4880 x 455 x 205 mm and was supported over a clear span of 4.57 m. The study investigated the effect of the original reinforcement ratio and the effect of shear cracking and shear reinforcement on the strength of composite reinforced beams. A 1.5 mm thick layer epoxy was used to attach 152 mm wide, 4.26 m long, and 6 mm thick glass FRP plates to the bottom of the beams.

The GFRP plates were tested under uniaxial tension. They exhibited linear-elastic behavior up to failure, with an average modulus of elasticity of 37 GPa and an average ultimate strength of 400 MPa. The lap shear strength of the epoxy was 14 to 15 MPa, elongation at failure was 40 percent, and curing time was 4 hours at room temperature.

The load vs. deflection curves of the strengthened and control beams indicated that plating increased the yield and ultimate loads by about 15 percent and 65 percent, respectively. The gain in ultimate flexural strength was more significant in beams with lower steel reinforcement ratios.

University of Toronto, Ontario, conducted research on the performance of conventionally reinforced concrete beams strengthened with bonded CFRP and GFRP plates (Bonacci, 1996). The characteristics of the FRPs are given in Table 4.4. The failure modes are given in Table 4.5. Bond failure was the most common failure mechanism.

Table 4.4: FRP Properties

Property	Glass FRP	Carbon FRP
FRP Modulus, GPa	10-40	60-170
FRP Strength, MPa	200-750	700-1500

Two of the indices that can be used to compare strengthened beams to unstrengthened ones are strengthening ratio and deflection ratio. Strengthening ratio is defined as the strength of the beam with externally bonded FRPs divided by the strength of the control beam. Deflection ratio is defined as the centerline deflection at peak for the strengthened beam to that of the control beam. Strengthening ratios in this study varied from 1.0 (a bond failure with inadequate epoxy) to 4.3. Deflection ratios were from 0.1 to almost 1.0. Deflection ratio values near 1.0 were the result of having a small composite strengthened area or inadequate epoxy performance. Table 4.5 lists the strengthening ratios and failure modes. It appears that bond failure predominated in the high strengthening ratio cases. However, this cannot be generalized.

Table 4.5: Behavior of Failure Modes

	Failure Modes			
	Shear	Compression	Fracture	Bond
% of Specimens	8%	6%	22%	64%
Strengthening Ratio	1.38	1.55	2.01	4.35
Deflection Ratio	0.84	0.92	0.99	0.97
% of CFRP	0%	0%	33%	67%
% GFRP	18%	14%	11%	57%

Because of the brittle and complex nature of the failure modes, there is a need for safety factors when designing for strengthening with external FRP plates. Bonding failure depends on parameters that are not treated in analysis of conventional materials. Parameters such as epoxy thickness and mechanical response, preparation of the concrete surface before application of the epoxy, and sensitivity to faulting motions along existing cracks on the tension faces need to be considered. Also, there is concern that beams reinforced in this manner would have inadequate ductility. However, with proper design, externally strengthened beams can develop considerable deformation before failure. The design should assure flexurally balanced failures with shear and bond failure modes precluded. Shear, compression and bond failure result in a sudden failure mode, which is prohibited by the design codes.

Aramid/epoxy strengthened concrete slabs were tested at the University of Sherbrooke (*Demers et al, 1996*). The ultimate strength of the aramid/epoxy-reinforced slabs was three times that of the plain concrete slab. The failure occurred with sufficient warning since the center deflection was larger than the clear span divided by 60. The failure of these slabs occurred by punch, and the composite sheet remained glued on all sides of the slab. Although the effective amount of fibers in each direction was the same for all reinforced slabs, there were some differences in their load-deflection response due to different reinforcement configurations. The study found that the fiber orientation, i.e. 0° and 90° or $\pm 45^\circ$, has no significant effect on the overall behavior. However, this conclusion cannot be generalized.

Queen's University, Ontario collaborated with Royal Military College of Canada in an experimental testing program of large-scale prestressed concrete beams strengthened by unstressed and prestressed CFRP pre-preg sheets (*Wight et al, 1996*). Mitsubishi Chemical fabricated sheets with a fiber volume fraction of 65 percent, and a fiber tensile strength of 235 GPa. The sheets were 0.2 mm thick, 300 mm wide and had an effective tensile modulus of elasticity of 125 GPa. Sheets were precut and bonded to the beam surface with a two-part epoxy.

The unstressed plate strengthening used alternate layers of epoxy and FRP sheets until the desired thickness was achieved. The first sheet applied to the beam was the longest and each subsequent layer was shorter than the preceding one.

The prestressed plate strengthening system consisted of steel round bar anchors bonded to the sheets and steel anchor assemblies fixed to the beam. The bar at one end of the FRP was fixed and the other bar was movable. When the sheet was fully prestressed with a hydraulic jack the movable bar was attached to the beam. The application of the FRP sheet resulted in an increase in the cracking load and a delay in the yielding of the reinforcing steel. A forty percent increase in the ultimate load of the control beam was observed in the beams with non-prestressed CFRP

sheets, whereas a 45-50 percent increase in the ultimate load was noted in the beams strengthened with prestressed sheets. The addition of non-prestressed FRP sheets delayed the yielding of the steel until a load of 30 percent higher than the control beam was attained. When prestressed sheets were bonded to the concrete beams, yielding occurred at a load 50 percent higher than that in the control beam.

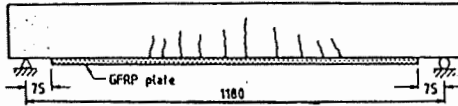
Sharif et al (1994) investigated the strengthening effects of FRP plates on damaged, pre-loaded reinforced concrete beams. The beams were preloaded to develop central deflection corresponding to approximately 85 percent of their ultimate capacity.

The damaged beams were repaired using four different schemes as shown in Figure 4.4.

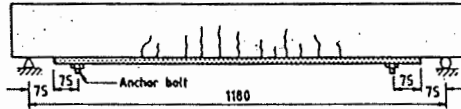
The results of the experiment suggested that shear and normal stresses in the FRP plates increase with increasing plate thickness, leading to premature failure by plate separation and concrete pull-out.

The steel anchor bolts prevented plate separation for the 3 mm plates and the beams failed due to diagonal tension cracks.

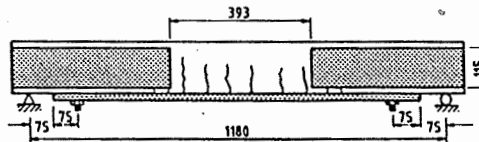
I-jacket plates provided the best strengthening system. This configuration eliminated plate separation and diagonal tension cracking, and developed the full flexural strength.



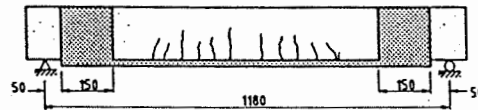
Various repair schemes for damaged beams: (a) Bonded fiberglass plate to beam soffit



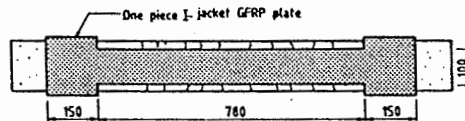
Various repair schemes for damaged beams: (b) Steel bolts anchoring bonded fiberglass plate



Various repair schemes for damaged beams: (c) Additional plates (wings bonded to beam sides)



I-jacket fiberglass plate strengthening damaged beam: (a) Side view



I-jacket fiberglass plate strengthening damaged beam: (b) Bottom view

Figure 4.4: Strengthening Schemes of Concrete Beams
(Sharif et al, 1994)

The study concluded that repaired concrete beams developed adequate flexural capacities to provide enough ductility despite of the brittleness of FRP plates. The procedures demonstrated the effectiveness of using externally applied FRP plates for strengthening damaged or upgrading of under-designed concrete beams.

A study conducted at the University of Sheffield investigated the differences between beams strengthened with GFRP plates and steel plates (Swamy et al, 1996). The study found that the beams strengthened with steel carried more ultimate load and were stiffer than GFRP-strengthened beams, but the deflections at ultimate load of the GFRP-plated beams was larger. The study compared the beams' ductility based on their strain-energy absorption capacity. Differences between the performance of the beams are summarized in Table 4.6.

It was observed that the FRP- plated beam developed horizontal cracks at the concrete-FRP interface prior to failure. This is very detrimental to the effective stress transfer from the concrete to the external plate. The reason for this type of failure is the inability of the epoxy-concrete interface to remain intact when the external GFRP is undergoing large strains (Swamy *et al*, 1996).

Table 4.6: Influence of the Plate Material

Beam Design	Plate Material	Ultimate Deflection mm	Ultimate Plate Strain μs	Ultimate Load kN
No Plate	None	32	–	200
Normal	Steel	30	4000	211
Normal	GFRP	33	6200	193
Special	GFRP	37	7000	232
Special	GFRP	49	10000	182

Contradictory results from specially designed GFRP plated beams indicated that bearing capacity can be increased considerably, while failure was more ductile than the un-plated beam. The results show that through special design considerations it is possible to increase the ductility at failure even when the bonded plate is a brittle material.

4.3.3 Shear Strengthening

A reinforced concrete beam must be designed to develop its full flexural strength to insure a ductile flexural failure mode under extreme loading. Hence, a beam must have a safety margin against other types of failure that are more dangerous and less predictable than flexural failure. Shear failure of reinforced concrete beam would have a catastrophic effect, should it occur. If a beam deficient in shear strength is overloaded, failure may occur suddenly without advanced warning of distress.

A study on strengthening reinforced concrete beams having deficient shear strength was conducted by Al-Sulaimani *et al* (1994). Beams with different design shear strengths were damaged to a predetermined level, corresponding to appearance of the first shear crack, and then repaired with fiberglass plates. Different shear repair schemes were used, including GFRP shear strips, shear wings, and U-jackets in the shear span of the beams. These techniques are shown in Figure 4.5.

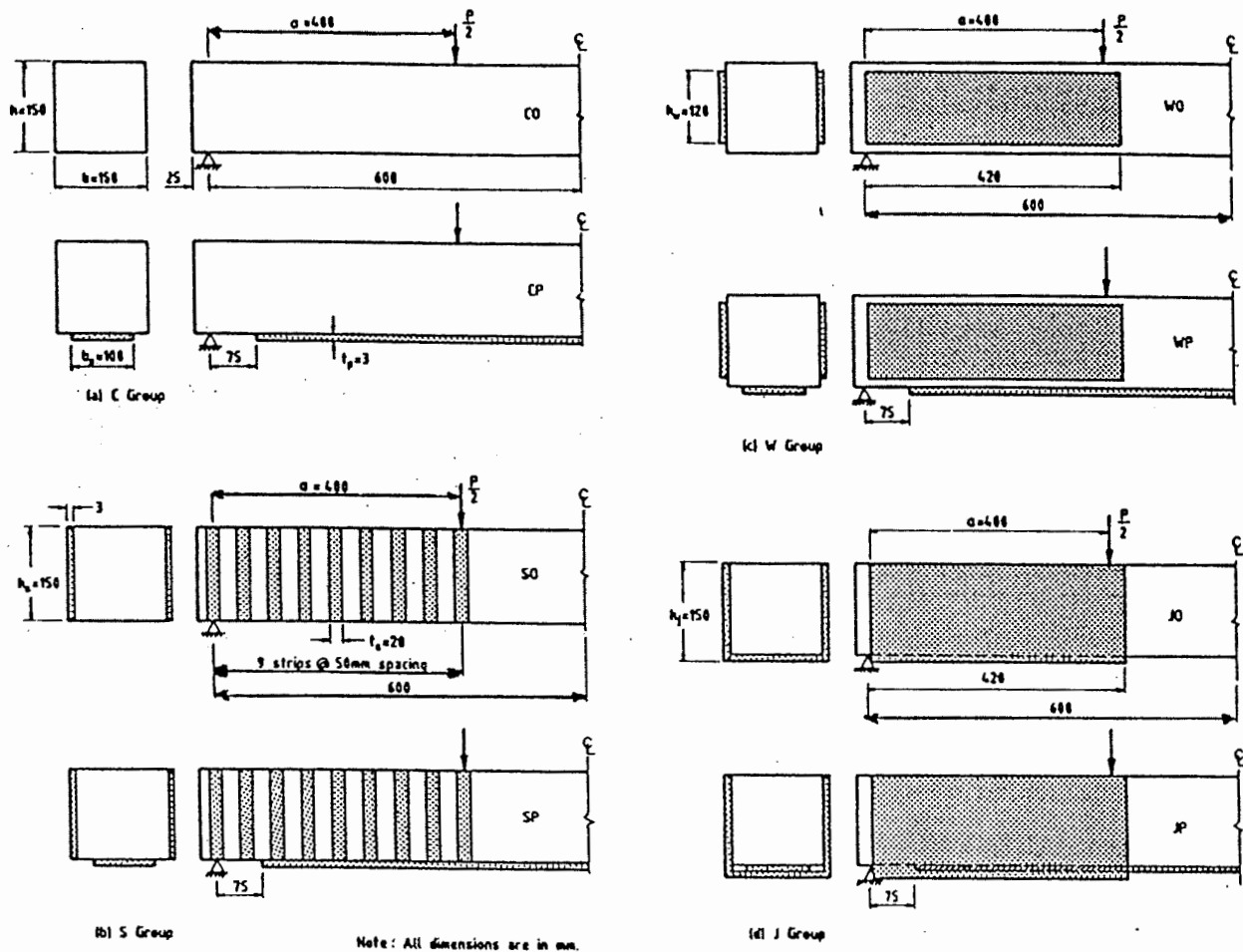


Figure 4.5: Repair Schemes
(Al-Sulaimani et al, 1994)

GFRP plates three millimeters thick were used in all schemes for external shear reinforcement. The GFRP material consisted of three layers of woven fiber-glass embedded in a polyester matrix and had an ultimate tensile strength of 200 MPa (29 ksi). Experimental data on strength, stiffness, deflection, and mode of failure were obtained, and comparison between the different shear schemes was made. The results showed that the increase in shear capacity was almost identical for strips and wings shear repair. They both increased shear capacity and restored degraded stiffness. However, the increase was not enough to cause the beams to fail in flexure. The failure of the strip and wing strengthening was by peeling.

The enhanced shear capacity provided by the U-jackets was sufficient to insure flexural failure in these beams. Thus, shear repair by jackets appears to be better than strips and wings schemes, since the continuity rendered by the geometry of the jacket minimizes the effects of stress concentrations present in the other two types of plates.

Shear reinforcing using CFRP sheets was studied in Japan (*Sato et al, 1996*). CFRP sheets were glued to the sides and bottom of concrete beams with and without stirrups. Addition of CFRP sheets increased the shear strength of the specimens from about 50 to over 100 percent. Delimitation of the CFRP along the shear cracks was the failure mode in the beams without stirrups.

Chajes et al (*1995*) tested twelve under-reinforced T-beams to study the effectiveness of using externally applied composite materials as a method of increasing a beam's shear capacity. Woven fabrics made of aramid, E-glass, and graphite were bonded to the web of the T-beams using a two-component epoxy. The beams were tested in flexure, and the performance of the strengthened beams was compared to control beams with no external reinforcement. All of the beams failed in shear. The reinforced beams had an increase in ultimate strength of 60 to 150 and excellent resistance to composite peeling. The results are shown in Table 4.7.

Table 4.7: Contribution to the Shear Capacity of Various Externally Applied Fabrics

Beam Treatment	Concrete Shear Capacity, kips	Fabric Shear Capacity, kips	Ultimate Shear Capacity, kips
Control	4.23	—	4.23
Aramid	4.23	3.50	7.73
E-Glass	4.23	3.72	7.95
0/90 Graphite	4.23	3.85	8.08
45/135 Graphite	4.23	5.30	9.53

(*Chajes et al, 1995*)

4.3.4 External Prestressing

In some cases it may be necessary to provide additional camber in the concrete beam. This way, the serviceability of the structure can be improved and the shearing off of the FRP sheets, due to shear failure of the concrete, can be avoided (*Meier et al, 1992*).

This type of prestressing is typically accomplished by cambering the girders with hydraulic jacks while in loose contact with an epoxy-coated composite plate. The jacks are removed when the epoxy has cured. This puts the composite plate in tension, preventing a complete elastic return of the girder.

This results in initial compression and tension stress in the girder, which oppose the stresses induced by gravity and external loads. The elimination of anchorage in this prestressing scheme precludes development of localized stresses in the anchorage zones.

Another technique for strengthening with prestressed sheets has been used by the Swiss Federal Laboratories (*Meier, 1991*) and is illustrated in Figure 4.6. The two far ends of the composite are cut when the adhesive has fully hardened and the sheet is then transformed into a pre-stressing element.

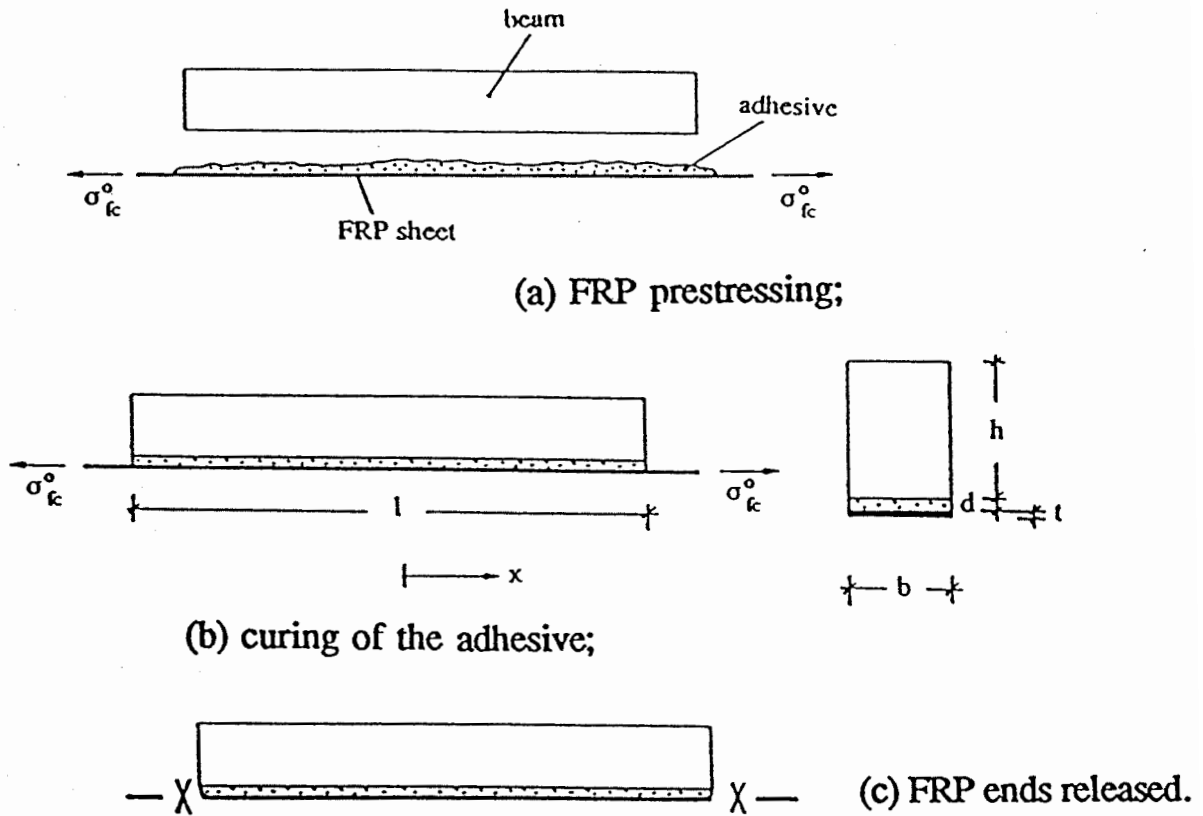


Figure 4.6: Procedure for Applying Prestressed FRP Sheet
(Triantafillou and Plevris, 1991)

When the pre-tensioning force is too high, failure of the system due to pre-tension release may occur at the two ends. This is caused by the development of high shear stresses in the concrete layer just above the FRP sheet. It can be avoided by limiting the prestress to approximately 50% of the ultimate. The study performed at EMPA, Switzerland (Meier *et al.*, 1992) suggests that without special end anchorage, FRP sheets shear off from the end zones immediately if prestressed over 5% of their failure strength. On the other hand, technically and economically rational prestress is typically achieved at rate of 50% of the ultimate. Therefore, the design and construction of the end regions requires careful attention. The initial pretension calculations can be found in Triantafillou and Plevris (1991).

Karam (1992) proposed a technique that increases the efficiency of the anchorage zones by increasing the FRP area at the high shear regions hyperbolically. The hyperbolic profile of the end anchorage zone can be obtained by either successive sheet lamination to increase the thickness or by flaring the ends of the sheet to increase its width. The lamination solution is the most practical and the profile can be approximated by a series of equal steps, depending on the thickness of the sheet used. Another option is to increase the width of the FRP laminate, bonding the added area either to the bottom of the beam or to its sides. This will result in a decrease in the shear stresses, thus increasing the capacity and safety of the assembly.

A test program conducted at University of Arizona at Tucson, involved strengthening of concrete beam with GFRP plates (*Saadatmanesh, 1994*). To simulate the loss of steel area due to corrosion, the test beam was significantly under-reinforced. External prestressing was applied to the beam by bonding the GFRP plate while the beam was held in a cambered position by jacking forces. The beam was initially loaded to approximately 110 kN and cyclically loaded until failure occurred between the FRP plate and concrete.

The resulting load-deflection curve showed that plating increased the yield and ultimate loads of the beam approximately 500 percent, and reduced the deflection approximately 250 percent. Additionally, GFRP plating reduced crack sizes and ductility in the beam at all load levels.

Before field application of this technique, further studies should be conducted to examine the creep behavior of the epoxy joint subjected to sustained cambering stresses. Also, effects of temperature and moisture on the epoxy joint should be examined.

The research conducted by Saadatmanesh et al (*1994*) was followed by analytical and parametric studies to evaluate the moments and curvatures for concrete girders externally prestressed with FRP plates (*Char et al, 1994*). The analytical study was based on the same assumptions made in the classical theories of reinforced concrete members subjected to flexure, namely linear strain distribution, no creep or shrinkage, no shear deformations, and complete composite action between the FRP plate and concrete beam. The subsequent experiments showed agreement between the calculated and measured loads and strains. The parametric study investigated the effects of the initial camber and type of the composite plate on the moment-curvature relationship. CFRP and GFRP plates with typical properties and design were considered. A comparison of the moment-curvature relationships before and after strengthening revealed an increase in the maximum moment by a factor of 2 to 3 for GFRP plates, and 3.5 to 4.5 for CFRP plates.

Traintafillou and Plevris (*1992*) conducted a comprehensive study of short-term flexural behavior of reinforced concrete beams strengthened with bonded pretensioned composite laminates. The principal findings were as follows:

- A pretensioned laminate of a given thickness and unstressed laminate with greater thickness can be equally efficient in enhancing a member's mechanical properties.
- FRP sheets can be prestressed only to a certain degree. If the sheets are stressed beyond that level and then released, cracks are observed in the epoxy layer and near the ends of FRP sheets.
- To avoid sudden collapse, it is essential that the members be designed to fail in the compression zone first, followed by tensile fracture of the laminate.

The foregoing information is important to the development of composite strengthening of reinforced concrete beams. However, because of the added complications of prestressing in the field it would have limited use in the transportation environment.

4.3.5 Strengthening of Reinforced Concrete Beams with FRP Sheets

While most of the European institutions use exclusively rigid carbon or glass plates to enhance the bending capacity of RC beams, the Federal Institute for Materials and Testing (BAM) in Berlin, Germany, applied flexible CFRP prepreg unidirectional sheets to upgrade bending and shear capacity (*Limberger and Vielhaber, 1996*).

In Japan and most recently in the United States, flexible CFRP sheets with thicknesses of 0.1 to 0.25 mm have been used in lieu of the 1 mm to 3 mm thick plates. The advantage of the flexible sheets is realized when curved structural elements require treatment. The disadvantage is that the cost of the rehabilitation is increased due to necessity of manually applying several plies. Typical properties of prepreg CFRP sheets are shown in Table 4.8.

Table 4.8: Technical Data of Prepreg CFRP Sheets

Type	Regular Modulus (RM)	High Modulus (HM)
Thickness, mm	0.097-0.167	0.095
Elastic Modulus, MPa	240000	650000
Tensile Strength, MPa	2500	2000
Ultimate Strain, %	0.1-0.14	0.3-0.4

(Mitsubishi Chemical Co., Japan)

It appears that the reduction of ductility typically associated with CFRP-plate beams can be avoided by using prepreg material with a combination of low modulus (LM) and high modulus (HM) fibers (*Limberger and Vielhaber, 1996*). While the ultimate load is determined by the LM carbon fibers, the HM fibers contribute to improved serviceability and reduced crack width.

4.3.6 Reinforced Concrete Decks/Slabs Strengthened with FRP Materials

Research conducted by the Naval Facilities Engineering Service Center (NFESC) studied the use of FRP sheet to upgrade the decks of existing reinforced concrete piers and wharves. Laboratory tests on simply supported under-reinforced slabs were conducted to determine the effects of upgrading on moment capacity, shear strength, deflection, ductility and failure mode (*Malvar, 1996*). The slabs were strengthened with one transverse and three longitudinal CFRP layers of Forca Tow Sheet (*Kliger, 1993*). This sheet has unidirectional carbon fibers and was selected for this project because of its ease of application. Properties of the Forca Tow CFRP Sheets are listed in Table 4.9. Both laboratory and field specimens showed a punching-shear failure mode. Laboratory specimens reinforced with one CFRP layer in each direction exhibited an ultimate load increase of up to 47 percent. CFRP reinforced slabs showed increased ductility compatible to that of the non-strengthened slabs.

Table 4.9: Forca Tow Sheet FTS-C1-20

Property	Value
Laminate Type	Unidirectional Carbon
Fiber Weight/Area	200 g/cm ²
Tensile Strength	385 kN/m of width
Tensile Modulus	25.4 MN/m of width
Ultimate Strain	1.5%

The laboratory conducted tests showed that the CFRP sheets increased the load carrying capacity by 31 percent. The load capacity increase for the field specimens averaged 20 percent. However, the ultimate deflection was reduced 42 and 27 percent for the one-way and two-way CFRP flexural reinforcement, respectively.

4.3.7 Design Methodology

This section explains the behavior and basic steps for designing reinforced concrete beams externally strengthened with FRP plates. Assuming a known value of concrete strain in the extreme compression fiber (top of the beam), the depth of the neutral axis can be obtained from the equilibrium of forces across the cross-section of the beam (Figure 4.7).

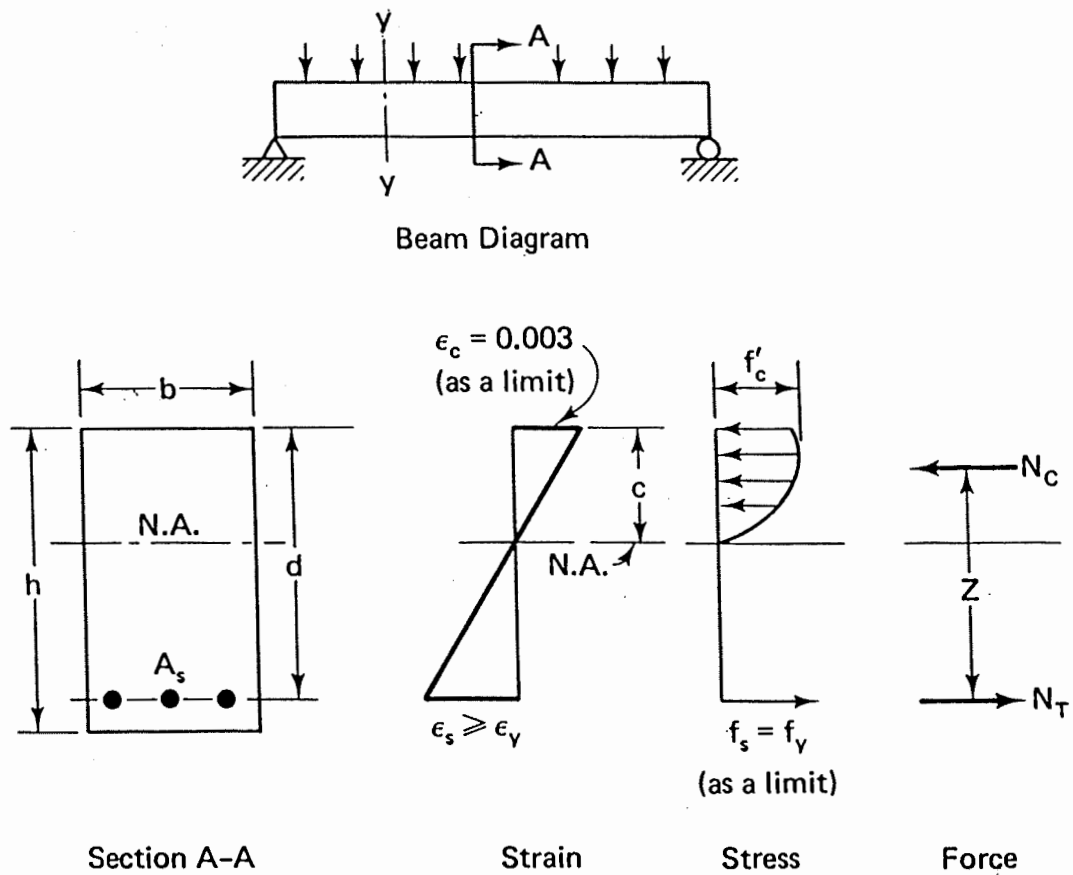


Figure 4.7: Beam Flexural Behavior at Near Ultimate Load

After the location of the neutral axis is determined, the strains in the concrete, the steel reinforcement bars, and the FRP plate can be calculated using the linear strain diagrams. It is assumed that the stress-strain curves for both steel and FRP material are idealized by Hognestad's parabola (*Park and Paulay, 1975*). The stress-strain relation for steel is assumed to be elastic-perfectly plastic, and a linear relationship is assumed for FRP plates with ultimate stresses and strain depending upon the material used in the plate. The stresses in concrete, FRP, and steel bars are obtained from their idealized diagrams. The internal forces are then calculated multiplying the stresses by their corresponding areas. The moment capacity of the strengthened beam can be found by summarizing the moments of all internal forces about the neutral axis. Finally, the curvature can be calculated by dividing the strain in the extreme compression fiber by the distance to the neutral axis.

Similar design assumptions were adopted by Char et al (*1994*) who developed a computer program for calculating stresses and deflections of FRP strengthened beams. The merit of the design methodology was demonstrated by a numerical example that illustrated how a typical reinforced concrete bridge, originally designed for H15 truck loading, can be upgraded to H20 truck loading by bonding composite plates to the tension flange of the girders. Initially, the stresses in the steel and concrete were below the maximum allowed values for H15 loading when the bridge was loaded with live H15 truck loads, but exceeded the H15 values when under H20 loads.

Four retrofitting techniques were considered: bonding with GFRP plates; cambering the girder with GFRP plates; bonding with CFRP plates; and cambering the girder with the CFRP plates.

AASHTO standard specifications and design requirements were taken into account. The stresses in the beams strengthened with GFRP and CFRP plate but no camber were slightly higher than the allowable stresses provided by AASHTO. The cambered beams exceeded the required capacity of H20 loading by 150 percent.

A simplified approach for determining the flexural strength increase due to lamination is based on comparing it with the effects of additional steel reinforcement. The equivalent steel thickness, which is based on the thickness of the fibers only, is used in this design (*Thomas et al, 1996*). Since the resin content and laminate thickness are not accurately controlled during strengthening, it would be difficult to obtain reliable strength and modulus values based on laminate composite area. Using the ACI or the AASHTO equations, the area of FRP laminate and the resulting moment capacity can be estimated. However, the merit of this approach is questionable and is not recommended for use by ODOT.

4.4 FATIGUE AND CREEP BEHAVIOR OF CONCRETE BEAMS WITH EXTERNALLY BONDED FRP SHEETS

At the present time, some of the important engineering properties of the FRP materials, such as strength and elastic modulus, are successfully predicted on the basis of simple mathematical models. Toughness, fatigue performance, and time-dependent behavior are much more difficult to forecast. Fiber-reinforced composites are heterogeneous and they exhibit complex behavior under cyclic loading. In a laminated composite, the state of stress and strain are multi-axial even under simple tensile loads. This is due to the inter-laminar shear and normal stresses between the layers. Moreover, fiber/matrix composite systems are often rate sensitive (*Ellyin and Kujawski, 1992*). Damage modes in composites generally do not combine to form a single dominant crack in a self-similar manner, as in the case of metals. In a laminate, a complex damage state is observed under cyclic loading. For example, in multidirectional laminate cracks in 90° plies usually occur first. Then an increase in density occurs, leading subsequently to delamination or transverse cracking in closely oriented plies. Final fracture occurs when 0° plies fail.

In contrast to metals, the fatigue strength of FRP materials decreases with increasing compressive stress. Another significant difference observed between metals and composite materials is their response to a notch (*Ellyin and Kujawski, 1992*). FRPs have high notch sensitivity to static or low cycle fatigue, and relatively low sensitivity to high cycle fatigue. These differences must be taken into account when the combined behavior of an FRP-concrete beam system is investigated.

A study conducted at West Virginia University investigated the effect of sustained load on concrete beams externally reinforced with CFRP. The research focused on the rate of increase in concrete creep strains due to sustained four-point loading. The reinforcing material was carbon Fiber Tow Sheets, type FTS-C1-20, manufactured by Tonen Corporation, Japan. The design thickness of a single ply was 0.11 mm, while the total thickness of the strengthening sheets varied from 0.6 to 1.0 mm. The Tow Sheet had a tensile strength of 382 N/mm, a tensile modulus of 23×10^4 N/mm, and ultimate strain at failure of 1.5% (*Ligday et al, 1996*). Two concrete beams, one unwrapped and one wrapped with Carbon Tow Sheet, were tested under sustained load (50% of the ultimate) for a duration of 50 days. The study found that the external wrap on the concrete beam significantly decreases the rate of creep strain. In this particular study, the creep reduction factor was calculated to be 0.3. However, these results should not be generalized.

The effect of repeated loading on the performance of concrete members strengthened by externally bonded advanced composites was studied by the Wright Laboratory Airbase Survivability Section, Wright Patterson Air Force Base, Ohio. CFRP external reinforcement laminates were attached to the specimens using a high-performance epoxy adhesive. The CFRP was three-ply and unidirectional, having a tensile strength and modulus of elasticity of 2270 MPa and 138 GPa, respectively. The specimens were tested under non-reversed fatigue loading, having loads ranging up to 90 percent of the maximum static load, applied at a rate of 20 Hz for two million cycles (*Muszynski and Sierakowski, 1996*).

Additionally, toughness was measured using Japanese standard JCI-SF4 that determines the total area under the load-deflection curve to the point where the maximum deflection occurs.

The study also evaluated the endurance limit of the specimens. Endurance limit is defined as the maximum fatigue flexural stress at which the concrete (plain or reinforced) can withstand two million cycles of fatigue loading, expressed as a percentage of the modulus of rupture of plain concrete (*Wu et al, 1989*). The endurance limit of CFRP reinforced beams was greater than 250 percent that of the control specimens.

The results of this study showed that the CFRP external reinforcement increased the load carrying capacity by a factor of 3 and the toughness of non-reinforced concrete beams by a factor of 40. Furthermore, the static flexural strength and toughness after fatigue loading were approximately the same as the non-fatigued control CFRP reinforced concrete samples.

The behavior of 4.7 x 0.2 x 0.15 m reinforced concrete beam subjected to fatigue loading was investigated at the Swiss Federal Laboratories (*Meier et al, 1992; Kaiser, 1989*). The steel reinforcement consisted of two 8 mm bars in the tension and compression zones. The beam was post-strengthened with hybrid (carbon/glass FRP) sheets that had tensile strength and elastic modulus of 960 MPa and 80 GPa, respectively. A sinusoidal fatigue loading was applied at a frequency of 4 Hz. The fatigue failure initiated after 480,000 cycles in the first steel rod, and after 560,000 cycles in the second one. In comparison, the FRP sheet failed after 805,000 cycles.

This experiment provides insight into the failure mechanism of hybrid (steel rods/FRP sheet) beam reinforcing system, and shows how much the FRP sheet can withstand after failure of the steel reinforcement.

A second fatigue test was conducted on a beam with a 6.0 m span under more realistic conditions. The goal was to verify that bonded FRP sheets can withstand very high humidity and temperature combined with fatigue loading (*Meier et al, 1992*). The beam was strengthened with CFRP sheets, thus increasing the static strength by 32 percent. After strengthening the beam was subjected to 10.7 million cycles of fatigue loading. Crack development was observed after 2 million cycles. Upon the completion of 10.7 million cycles, the test was continued in a climatically controlled room, at temperature of 40°C and 95 percent relative humidity. After 12 million cycles, the steel reinforcement failed, while the CFRP sheet did not present even the slightest problems. After 14.09 million cycles, cracking initiated and rapidly grew into the external FRP reinforcement which led to failure.

4.5 LOW TEMPERATURE RESPONSE OF RC BEAMS STRENGTHENED WITH FRP SHEETS

Low temperature testing is an important area of research because many mature technologies developed for warmer climates can fail when applied in cold regions. Although not typical for Oregon, a temperature range from -46°C to 38°C is not uncommon for the northern parts of the United States and Canada (*Baumert et al, 1996*). Experiments on tensile loading of unidirectional FRP at low temperatures (*Dutta, 1990*) have shown that the longitudinal tensile strength decreases. This contradicts the commonly accepted notion that at low temperatures, material strength increases.

Behavior of composites is primarily governed by the fiber properties. After the beginning of fiber failure, the additional tensile load that can be applied to the composite will depend upon how efficiently the high local stresses around the broken fibers are transferred to the neighboring fibers. The properties of the matrix and the interface govern this stress transfer mechanism. At low temperatures most of the polymers show increased yield stress (*Kreibich et al, 1979*). The reduced ability of the matrix to yield causes the load distribution across the fibers to be less uniform. Thus, at low temperatures, some fibers will share more load than others and will fail earlier, causing progressive failure to the other fibers. However, the actual load sharing process within the laminates is very complex and not fully understood (*Jones, 1975*).

Another concern is that the differences in the coefficient of thermal expansion between concrete and unidirectional laminate may cause significant adhesive shear stress in the end of the FRP plates. Researchers from Switzerland developed a model to predict the temperature change that would cause adhesive bond damage. To investigate the effect of freeze/thaw, six beams were subjected to 100 cycles of 20°C to -25°C before being tested to failure (*Baumert, 1996*). Half of the beams were cracked prior to application of the laminates. It was expected that water would enter the cracks and expand with subsequent freezing, resulting in peeling of the laminates. All frozen beams were brought to room temperature before testing. A comparison of the ultimate loads sustained by the frozen beams, with those of the control beams, showed no detrimental influence from the freeze/thaw cycles.

Baumert et al (1996) reported results of a plain concrete beams strengthened with CFRP tested at 21°C and -27°C. At both temperatures, the failure occurred by shear peeling off the CFRP sheets. For plain concrete beam tests, the addition of CFRP sheets appears to have a little effect on the magnitude of the first crack development. At low temperature, a significant increase in the first crack load was observed, without noticeable change in beam stiffness. It appears that the main reason for strength increase of FRP-strengthened unreinforced beams at low temperatures is the concrete strength increase.

4.6 ANALYSIS OF THE FAILURE MECHANISM OF RC BEAMS STRENGTHENED WITH FRP PLATES

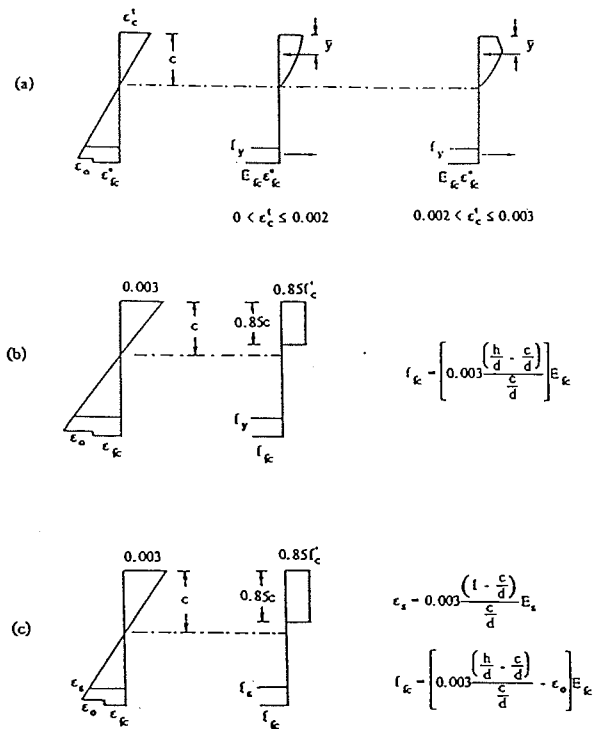
As a result of FRP repair, the mode of failure of a flexural member may change from ductile to brittle (*Arduini et al, 1997*). Brittle shear failure in concrete may substantially reduce the nominal expected flexural capacity based on standard design computations. Furthermore, changing the thickness of the FRP plate, the bonded length, or adding shear reinforcement significantly modifies the crack distribution pattern along the beam and changes the failure mechanism.

FRP-strengthened concrete beams can fail in several ways when loaded in bending. The following collapse mechanisms are the most widely recognized:

- steel yield-FRP rupture when the ultimate strain of the material is reached. If both, steel and FRP area fractions, are quite small, steel yielding may be followed by rupture of the composite sheet.
- steel yield-concrete crushing when the maximum compressive strength is reached. If the FRP area fraction is high and steel fraction area is small, failure is typically due to concrete crushing, while steel may yield or not, depending on its area fraction.
- shear failure of the concrete when the ultimate shear strength is reached. If both FRP and steel fractions are high, the concrete will reach its maximum capacity before the steel yields and before the composite sheet ruptures.
- debonding or local adhesive failure when the ultimate tensile strain of the adhesive is reached. The bond between the FRP and concrete may fail.

Stress-strain distribution of various failure modes is shown in Figure 4.8. Internal equilibrium and the ultimate bending moment calculations for the various failure modes are given in Triantafillou and Plevris, 1991.

Figure 4.9 illustrates how the failure mechanism depends on the quantity of the external FRP reinforcement.



Strain and stress distribution at a section when the flexural strength is reached: (a) steel-yield-FRP rupture; (b) steel yield-concrete crushing; and (c) compression failure.

Figure 4.8: Stress-Strain Distribution at Failure
(Triantafillou and Pvevris, 1991)

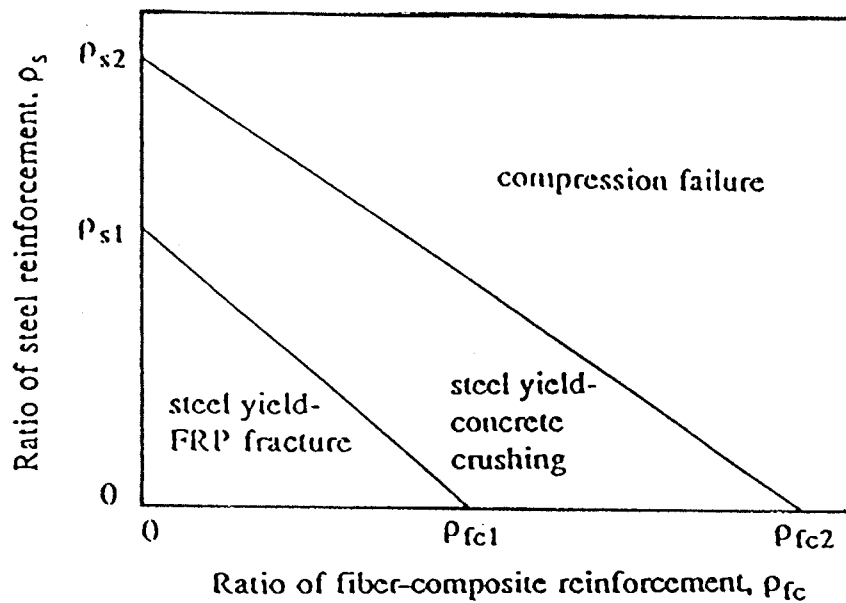


Figure 4.9: Influence of the FRP Reinforcement on the Failure Mechanism
(Triantafillou and Plevris, 1991)

Different failure modes of a beam strengthened with FRP plate are illustrated in Figure 4.10. The most typical type of failure is by rupture, i.e., either by a plate tensile failure or by concrete crushing in the compression zone. However, possibility of premature failure exists at the FRP-concrete interface due to separation of the plate. While the composite sheet is loaded on tension, the adhesive is loaded primarily in shear. The debonding occurs because of:

- Imperfections in the spreading of the adhesive;
- Flexural cracking of the concrete;
- Peeling-off of the composite when the beam face is not perfectly flat;
- Fatigue loads.

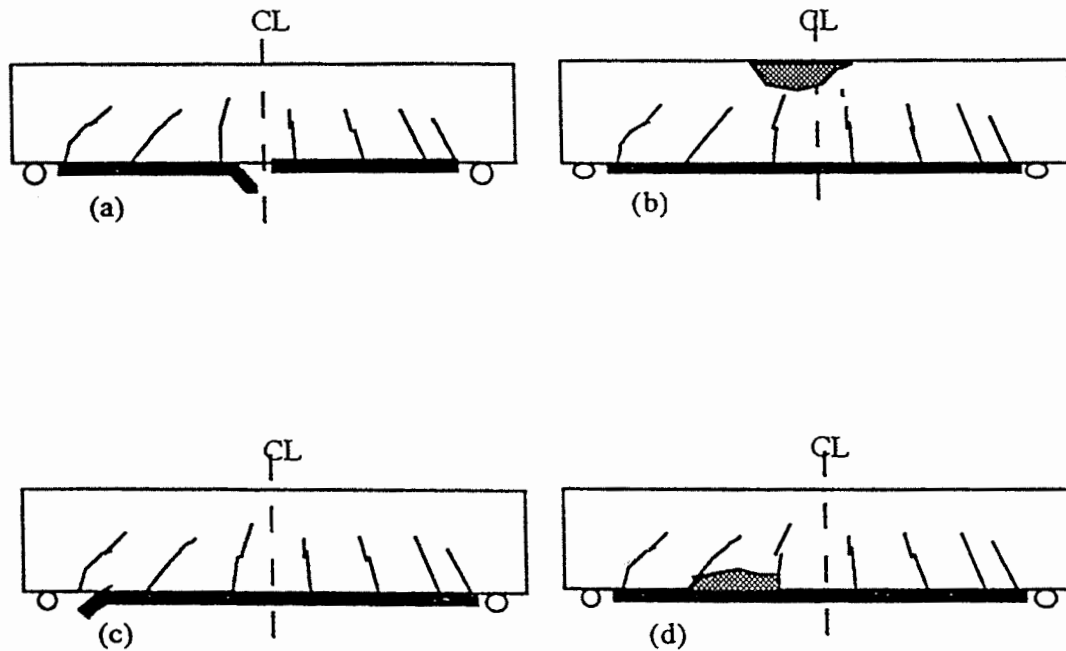


Figure 4.10: Different Failure Modes in RC Beams Strengthened with FRP Plate
(Varastwhpour and Hamelin, 1996)

In 1984 to 1989, CFRPs were successfully employed for the first time in Switzerland for post-strengthening purposes (Meier et al, 1992). The research work showed the validity of the strain-compatibility method in the analysis of cross sections. The calculation of flexure in reinforced concrete elements post-strengthened with CFRP sheets was performed analogous to conventional reinforced concrete.

The work showed that the possible occurrence of shear cracks may lead to a peel-off of the strengthening sheet. Thus, the shear crack development represents a dimensional criterion.

Flexural cracks are typically spanned by the FRP sheets and do not influence the load capacity of the repaired structure. Compared to un-strengthened beams, FRP-retrofitted beams usually develop much finer cracks.

The following failure modes were common:

- Tensile failure of the CFRP sheet. Although the sheets failed suddenly, the failure was always announced in advanced by cracking sounds.
- Concrete failure in the compression zone (punch failure) and shearing of the concrete in the tensile zone.
- Continuous peeling-off of the FRP sheets due to uneven concrete surface. The study found that for thin sheets (less than 1 mm), applied by vacuum bagging, an extremely even concrete surface is required.
- Inter-laminar shear within the CFRP sheets.

The following modes are not likely, but theoretically possible (*Meier et al, 1992*):

- Cohesive failure within the adhesive;
- Adhesive failure at the CFRP sheet/adhesive interface;
- Adhesive failure at the CFRP/concrete interface.

These findings are related to the specific materials employed in this study and cannot be generalized.

Laboratory and field tests show that FRP composites used for strengthening RC beams exhibit greater moment bearing capacity and smaller deflections. By adding external reinforcement to a RC structure, the stiffness of the structure changes. The governing equations of RC beams must be modified to consider the effect of FRP sheet on the nominal moment capacity of the structure. The main equation of the superposition model is (*Bhutta and Al-Qadi, 1995*):

$$M_n = M_{rc} + M_{frp} \quad (4-1)$$

The following assumptions are made: the bond between FRP and concrete beam is perfect, and the RC behavior is elasto-plastic in nature.

A typical stress-strain diagram of a hybrid concrete beam externally reinforced with FRP plate is in Figure 4.11.

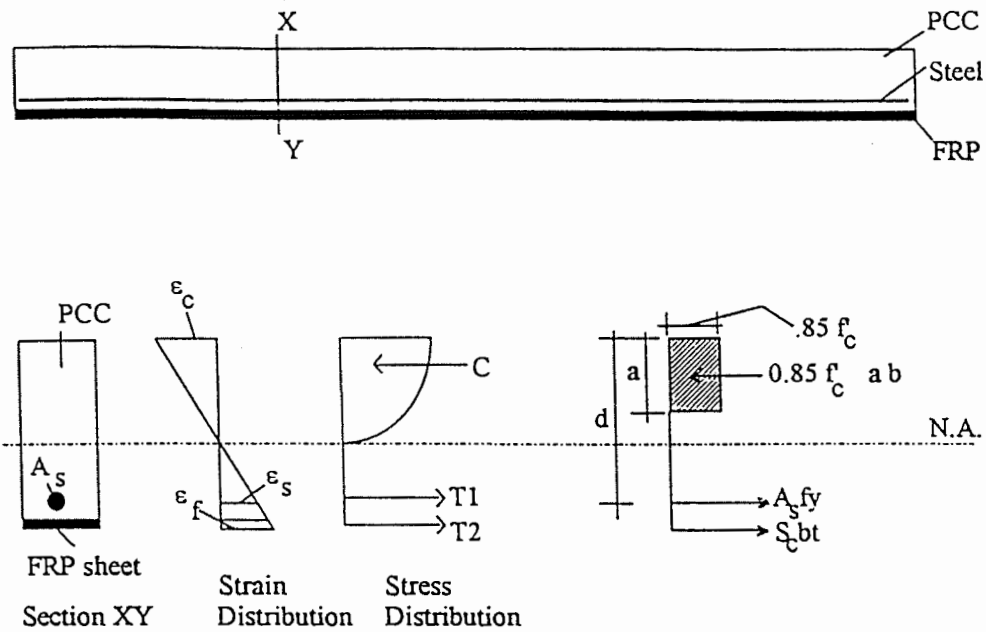


Figure 4.11: Stress-Strain Distribution of Hybrid Beam
(Bhutta and Al-Qadi, 1995)

The “generalized stiffness” is a function of the dimensions and constituent properties of the individual materials in the hybrid section. Composite laminate theory can be used for analysis of orthotropic materials (Jones, 1975). This theory can address complex structures with multiple material configuration, such as reinforced concrete structures externally reinforced with FRP composites. Using this approach Bhutta and Al-Qadi (1995) studied the effect of composite thickness on the improvement in moment capacity. Analytical results are presented in Figure 4.12 for Kevlar FRP (KFRP), CFRP and GFRP. All FRP plates were 0.025 mm thick.

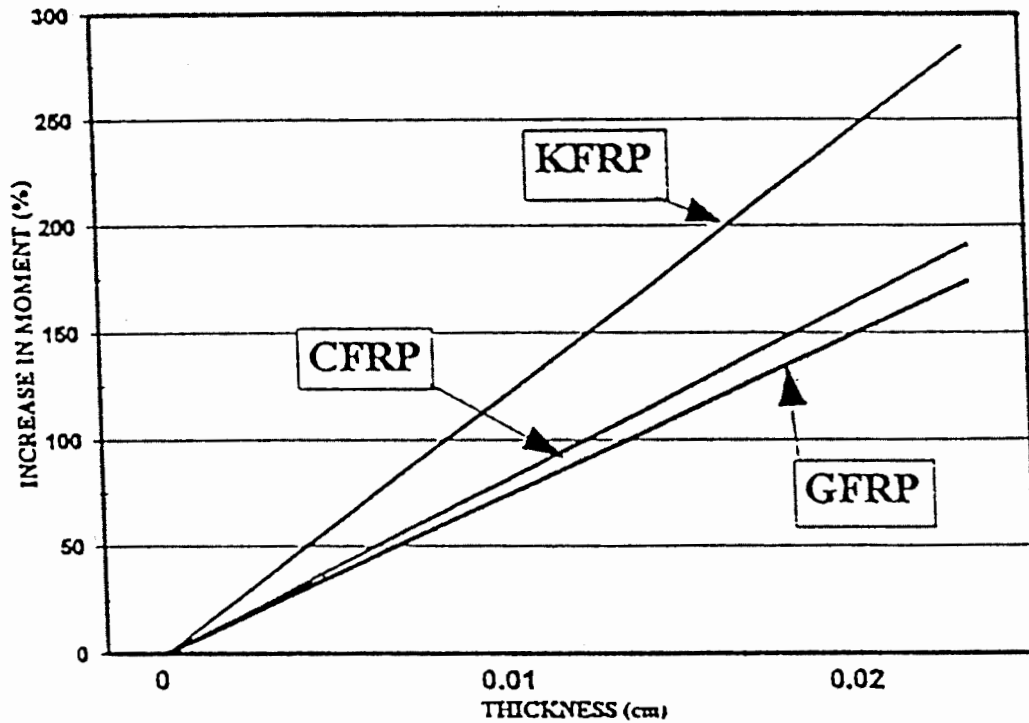


Figure 4.12: Percentage Increase in Moment Capacity
(Bhutta and Al-Qadi, 1995)

Models for stiffness and deflection of a simply supported hybrid beam were developed based on the composite laminate theory. The theory was modified to handle isotropic materials (concrete and steel reinforcing bars) and orthotropic materials (FRP). Sensitivity analysis was performed to evaluate the safety factor for hybrid beams as compared to RC beams.

KFRP showed the highest increase in moment capacity (280%), because of its high strain-to-failure value. On the other hand, CFRP has a high elastic modulus, but its strain at failure is low. The percentage increase in the moment capacity of CFRP plated beam was 190%. The smallest increase (170%) was found for GFRP. The analysis showed that the ability of the beam to handle moment is strongly dependent on the strength characteristics and the thickness of the FRP sheet. The deflection response of the hybrid beam, strengthened with 0.25 mm thick FRP provides a factor of safety of approximately 1.5 times that of a conventional RC beam.

A theoretical study of FRP beams strengthened with FRP plates was conducted at the Claude Bernard University, Lyon, France (*Varastehpour and Hamelin, 1996a*). The authors assumed that the mechanical behavior of RC beams strengthened with FRP plates strongly depends on the interaction at the plate/concrete interface. It was found that the plate/concrete bond slip depends on the surface treatment. The non-linear analysis developed in this study appears to provide a good method for predicting the flexural strength of the beam and failure modes. The two failure modes defined in this paper are interface failure due to a coupling shear and normal stresses, and rupture of the concrete layer between the reinforcing bars and the FRP plate. The analytical method provides estimation of the shear stresses distribution.

The analytical results were checked by experiment (*Varastehpour and Hamelin, 1996b*). CFRP plates with nominal thickness of 0.31 mm, elastic modulus of 117 GPa, and ultimate strength of 1350 MPa were used for strengthening. Three different geometries for FRP strengthening were used (Figure 4.13).

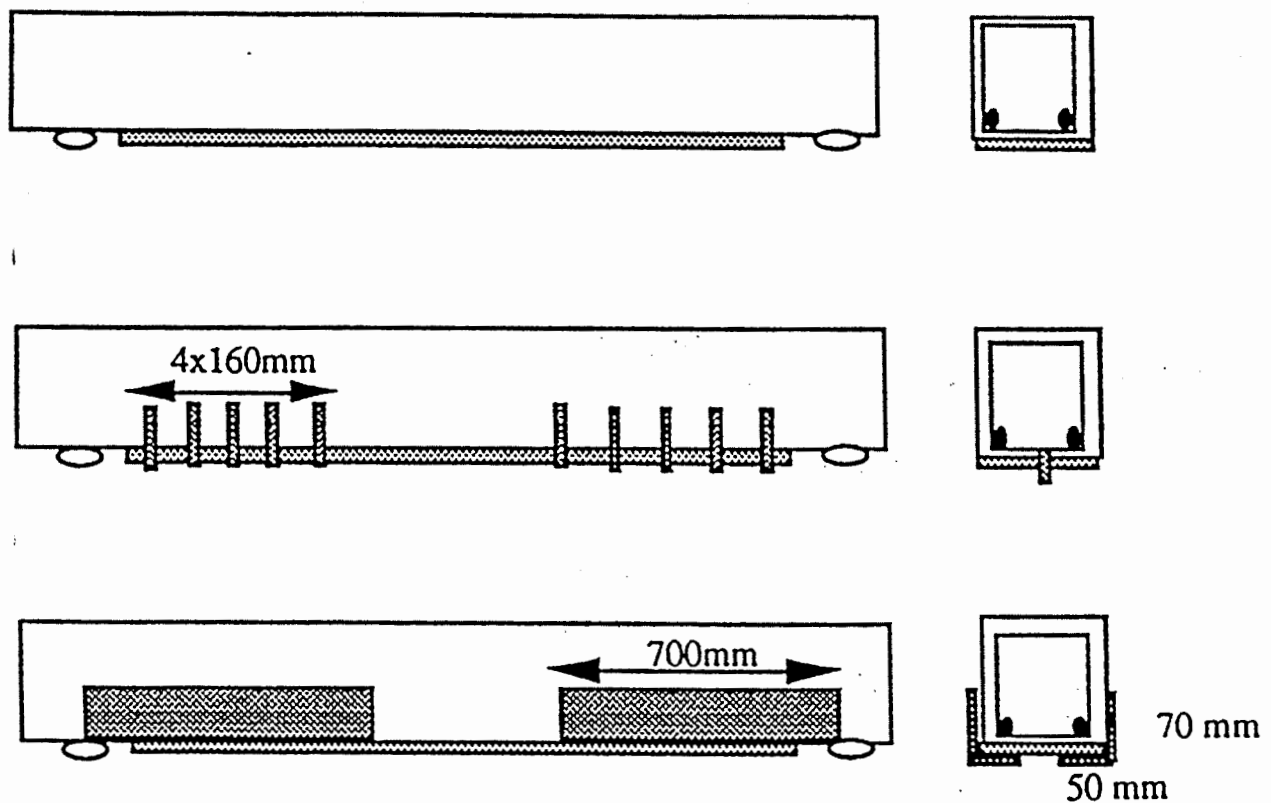


Figure 4.13: Different Methods for Strengthening RC Beams with FRP Plate
(Varastehpour and Hamelin, 1996b)

The first method used eight layers of woven textiles that were bonded by polymerization in situ, as illustrated in Figure 4.14.

A 2.5 mm thick CFRP plate was used for the second method. The plate was held in contact with the beam by vacuum bagging while the adhesive cured for one day.

The third method used mechanical anchorages made of composite materials that were 12 mm in diameter and 60 mm long. The CFRP plate was bonded to the anchorages with an adhesive (Sikadur, with elastic modulus of 8500 MPa, compressive strength of 75 MPa, and tensile strength of 25 MPa). It was placed in the shear spans, between the supports and the concentrated loads. For all beams, the ultimate measured loads were lower than the computed ones, due to premature failure on the beams. Results are presented in Table 4.10.

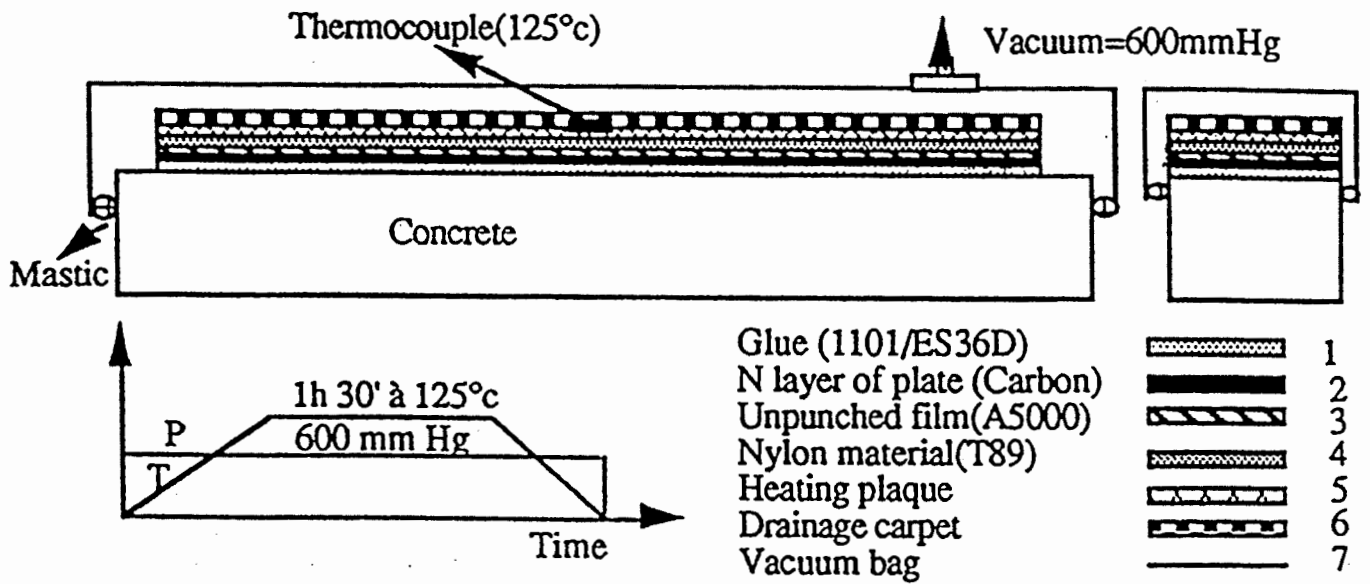


Figure 4.14: Plate Bonding by Polymerization in Situ Method and External Set Up
(Varastehpour and Hamelin, 1996b)

Table 4.10: Test Results

Beam	Ultimate Load (KN)			Ultimate Plate Strain (mm/mm x 10 ⁻³)			% over control beam	Failure Mode
	Exp	The	Exp/The	Exp	The	Exp/The		
Control	125	114	1.09	–	–	–	–	Concrete Crush
Polymerization in situ	195	238	0.82	3.53	5.5	0.64	56	Bond
Bonding by Glue	200	238	0.84	3.27	5.5	0.66	60	Bond
Glue + Mechanical Anchorage	188	238	0.79	3.31	5.5	0.31	50	Bond

(Varastehpour and Hamelin, 1996b)

The addition of the L-shape plates (Figure 4.13) bonded to the sides of the beam allowed for development of a full flexural strength of the beam.

4.7 OTHER TECHNIQUES FOR STRENGTHENING CONCRETE BEAMS USING FRP MATERIALS

The University of British Columbia investigated a novel technique for repair using a thin coat of GFRP composite applied by spraying (*Banthia et al, 1996*). Test beams were sprayed on the tension side with a 3 mm thick coat composite with randomly distributed chopped fibers. The fiber volume fraction was kept at a low 8%, which was not expected to provide a significant change in the basic properties of the matrix. The beams were notched in order to simulate structural damage. Two polymers, polyurethane and polyester, were pre-mixed. The strength and modulus of the polymer after setting were 27 MPa and 4 GPa, respectively. The properties of the E-glass fibers were: tensile strength of 2410 MPa, modulus of elasticity of 69 GPa, elongation at break of 3.5%, and a density of 2.45 g/cm³. The chopped fibers were 9.5 mm in length and about 10 µm in diameter. Typical test results are presented in Table 4.11.

Table 4.11: Results from RC Beams Strengthened with Sprayed FRP Composite

Beam Type	Load First Crack, kN	Maximum Load, kN	Fracture Energy, Nm (joules)
Un-notched, Plain	16.33	16.88	0.33
Un-notched with FRP	17.59	22.70	20.47
Notched, Plain	5.21	5.60	0.11
Notched with FRP	6.75	18.35	9.67

(*Banthia et al, 1996*)

For un-notched beams, the FRP coating led to an increase of 36% of the ultimate load. The fracture energy increased approximately 70 times. In the case of notched beams the increase in maximum load and fracture energy were 3 and 87 times, respectively. The low aspect ratio of fibers and the random distribution allowed fibers to fail by pull-out in addition to fracturing, and led to higher ductility.

This technique has a high potential for repair and retrofit. However, use of E-glass fibers in direct contact with the alkaline sub-base concrete is not recommended. The matrix has to be insensitive to UV attack. Finally, the use of higher fiber volume (up to 50%) may lead to significant improvement of the strength and modulus of the resulting composite.

4.8 FIELD APPLICATIONS

4.8.1 Canada

A study started in 1996 by the University of Alberta, and Alberta Transportation and Utilities, Canada resulted in construction and four-year durability investigations of a concrete bridge strengthened with CFRP sheets. The study emphasized the increase of shear capacity of bridge girders, construction processes and initial costs.

The bridge, located on a secondary highway, with an average annual daily traffic of 3000 vehicles, is near Edmonton, Alberta. The bridge has three 18 m spans, with 10 girders in each span. One span was selected for the project. When the monitoring is complete the span will be dismantled and the girders will be tested to failure in a laboratory. (*Alexander and Cheng, 1996*)

Two approaches to concrete surface preparation were used. Six beams were prepared according to specifications that called for grinding and patching, while the surface preparation for the other four was left to the discretion of the contractor.

Two CFRP sheets layouts were used. The sheets were placed on the inside girder surface so that the carbon fibers were perpendicular to the girder length. Six of the girders were reinforced continuously from one end to the other, while the other four had 25 cm sheets with 5 cm spacing between them.

One advantage of the FRP strengthening method is that the repair work can be done from below the deck, with very little disturbance to the traffic. However, vibrations during construction, especially from large trucks, may cause sheets to slip and not develop adequate bond to the concrete. To examine this effect, five girders were reinforced while the entire bridge was open to traffic, while the other five were strengthened while the lane above was closed to traffic. Since the girders were only covered with asphalt pavement, the traffic had very little effect on the girders beneath the closed lane.

Table 4.12 gives the costs to rehabilitate the span. The unit area costs were \$428/m² or \$39/ft².

Table 4.12: Construction Cost (Canadian Dollars) Using CFRP Sheets

Item	Span Cost, \$	Bridge Cost, \$
Man Power	7,500	22,750
CFRP Materials	11,000	33,000
Traffic Control	3,500	7,000
Miscellaneous	4,000	8,000
Total Cost	26,000	70,500

If the whole bridge had been strengthened, a reduction in CFRP material cost may have been realized. Further, if traffic control had been eliminated and the CFRP reinforcement reduced to a minimum, the total cost for this bridge could have been around \$50,000. In comparison, an alternative method using external steel stirrups would put the cost at about \$100,000 (*Alexander and Cheng, 1996*). That method would require closing the bridge for one month, removing the bridge deck, coring through the girder flanges, placing the stirrups, and replacing the bridge deck.

The study concluded that for issues such as simplicity of construction, convenience to users, and total cost of rehabilitation, the CFRP method is superior to the steel rehabilitation method.

4.8.2 United States

Rehabilitation of the T-beams of a concrete bridge using externally bonded FRP laminates was performed in rural Alabama (*Tedesco et al, 1996*). The structure consisted of thirteen 10.34 m, simple spans. Each span had four reinforced concrete T-beams, all of which exhibited significant flexural cracking due to truck load traffic over 30 years.

The concrete surfaces were prepared by leveling with power grinders, roughening by sandblasting and pressure washing to remove any remaining dust and dirt which might adversely

affect bonding. The surfaces of the concrete and the FRP laminates were cleaned with methyl ethyl ketone immediately before application.

Three CFRP laminates 3.4 m long, 266 mm wide, and 1 mm thick were installed on the bottom of each beam. The CFRP laminates had an elastic modulus of 125 GPa and a tensile strength of 1200 MPa. GFRP laminates 3.4 m long, 356 mm wide and 1 mm thick were installed on the sides of the beam stems. The laminates had an elastic modulus of 21 GPa and a tensile strength of 450 MPa. Splice plates of 0.9 m were used to maintain structural continuity in the CFRP and GFRP laminates.

The bridge response was quantified by measuring the vertical deflections and strains in the primary flexural reinforcement, concrete, and on the surface of the FRP laminates before and after strengthening. Measurements were made under static and dynamic loading conditions using a three-axle truck with a gross vehicle weight of 381 kN (85,000 # on three axles). The length between the front and rear axles was 7.1 m.

The girders had a 10% reduction in midspan deflection and similar decreases in rebar stress. Periodic monitoring has shown continued integrity of the bond between the concrete and FRP laminates, as well as improved overall serviceability.

4.8.3 Japan

Of all countries, Japan has the largest number of field applications in strengthening concrete beams with FRP materials (*Nanni, 1995*). Two petrochemical companies, Tonen and Mitsubishi Chemical, have literature describing design guidelines, construction, and field applications (Tonen, 1994; Mitsubishi Chemical, 1994).

Research in Japan has centered on the strength and ductility enhancement capabilities of FRP strengthened systems. Nanni (*1995*) describes several field applications of externally bonded FRP reinforcement. These projects used commercially available products, such as Forca Tow Sheet supplied by Tonen Corporation and Replark by Mitsubishi. Forca Tow Sheet uses dry type carbon fibers and is available in three grades, 3.9 to 5.9 kN/cm (2.2 to 3.4 kip/in.) tensile strength, and 259 to 627 kN/cm (148 to 358 kip/in.) tensile modulus. Mitsubishi's Replark is a prepreg offered in two grades, 3.4 to 5.8 kN/cm (1.9 to 3.3 kip/in.) tensile strength and 240 kN/cm (137 kip/in.) tensile modulus. The thicknesses of both products are in the 1 to 3 mm (0.04 to 0.12 in.) range.

The retrofit projects included strengthening to increase the load rating of the structure (Hiyoshikura Bridge, Tokando Highway), arresting steel reinforcement corrosion with rehabilitation (Wakayama, Central Japan) and strengthening to accommodate larger windbreak walls (Hata Bridge, Southern Japan). In all cases a 30 to 40 percent reduction of tensile strains in the steel reinforcement was confirmed.

The basic steps used in most of the retrofitting projects in Japan were concrete surface preparation such as cleaning and crack sealing, rust proofing existing steel reinforcement, smoothing (grouting), application of prime coat, application of resin undercoat; attachment of the FRP sheets, curing, and application of finish coats (*Nanni, 1995*).

4.8.4 Europe

Numerous projects involving FRP bridge strengthening were successfully completed in Europe. A commercial project took place in Italy during the second half of 1997 to strengthen highway bridge girders near Terracina, Rome (*Nanni, 1997*). The objective of the project was to compensate for the loss of prestressing caused by corrosion of the strand. Replark, Mitsubishi Chemical's CFRP material system, was adopted for the project. The repair sequence included removal of the deteriorated materials, restoration of the original cross section of the concrete with no-shrinkage mortar, protection of the steel reinforcement with a passivating coat, surface preparation, application of the FRP sheets, and a finish coat. Three sheets with 0 degree fiber orientation, 0.33 m wide and 3 m long, were bonded to the bottom of the beams. Additionally, four strips with 90 degree fiber orientation, 0.16 m wide and 3.0 m long, were wrapped around the sides and bottom of the beams.

The 228-meter long Ibach bridge, located in Lucerne, Switzerland was the first structure in the world strengthened with CFRP. The structure's prestressing tendons were accidentally damaged during installation of new traffic signals (*Meier et al, 1992*). Repair using CFRP plates was completed in three nights and the bridge remained open to traffic during the entire work.

The bridge was repaired with three CFRP sheets per beam. Each sheet was 5 m x 150 mm x 1.75 mm, with a fiber content of 55 percent, axial Young's modulus of 129 GPa, and a axial tensile strength of 1900 MPa (*Meier and Deuring, 1991*). A loading test with a 840 kN vehicle demonstrated that rehabilitation was very satisfactory. The repair work of the Ibach Bridge is an excellent demonstration of the simplicity and cost effectiveness of advanced composite materials for bridge repair.

Although the CFRP materials used in this project were approximately fifty times more expensive per kilogram, and nine times more expensive by volume than steel, the unquestionably superior properties of the CFRP plates justify their higher price (*Meier and Deuring, 1991*). The repair would have required 175 kg of steel and only 6.2 kg of CFRP was used. Additionally, the repair work was carried out from a mobile platform, thus eliminating the need for scaffolding and closing traffic. Furthermore, material cost was only 20% of the total. Ease of handling strongly reduced the labor price as well. Thus, the high price of the CRFP does not seem outrageous.

The Technical University of Braunschweig, Germany, directed the strengthening of the Kattenbusch Bridge (*Rostasy, et al, 1992*). The bridge is a continuous post-tensioned double box girder structure with eleven 36.5 m spans that had wide cracks at the joints. The cracks had broken through the bottom of the box and reached the webs of the girders. The main cause of the cracks was the temperature restraint in the summer, which was not considered in the design. As a result, an abrupt increase of the dynamic steel stresses with increased temperature was observed. Hence, additional reinforcement to control the crack width and to reduce the dynamic steel stresses was necessary. The work was performed in 1987.

Composite strengthening was selected as the means to increase the stiffness of the bottom slab. Ten mm thick GFRP plates were glued to the concrete members with adhesives commonly used for bonding of steel plates to concrete (see Table 6.1). Ninety-five percent of the fibers in the laminate were unidirectionally oriented, and the fiber content was 51 percent. The laminate had

a Young's modulus of 39 GPa, and a tensile strength of 700 MPa. In addition to laboratory tests, load tests of the bridge before and after strengthening were performed with 22-ton trucks. Figure 4.15 shows the measured reduction of stress by external strengthening in the lowest tendons. The maximum stress change was between 20 and 30 MPa. The bridge functions perfectly today (Rostasy et al, 1992).

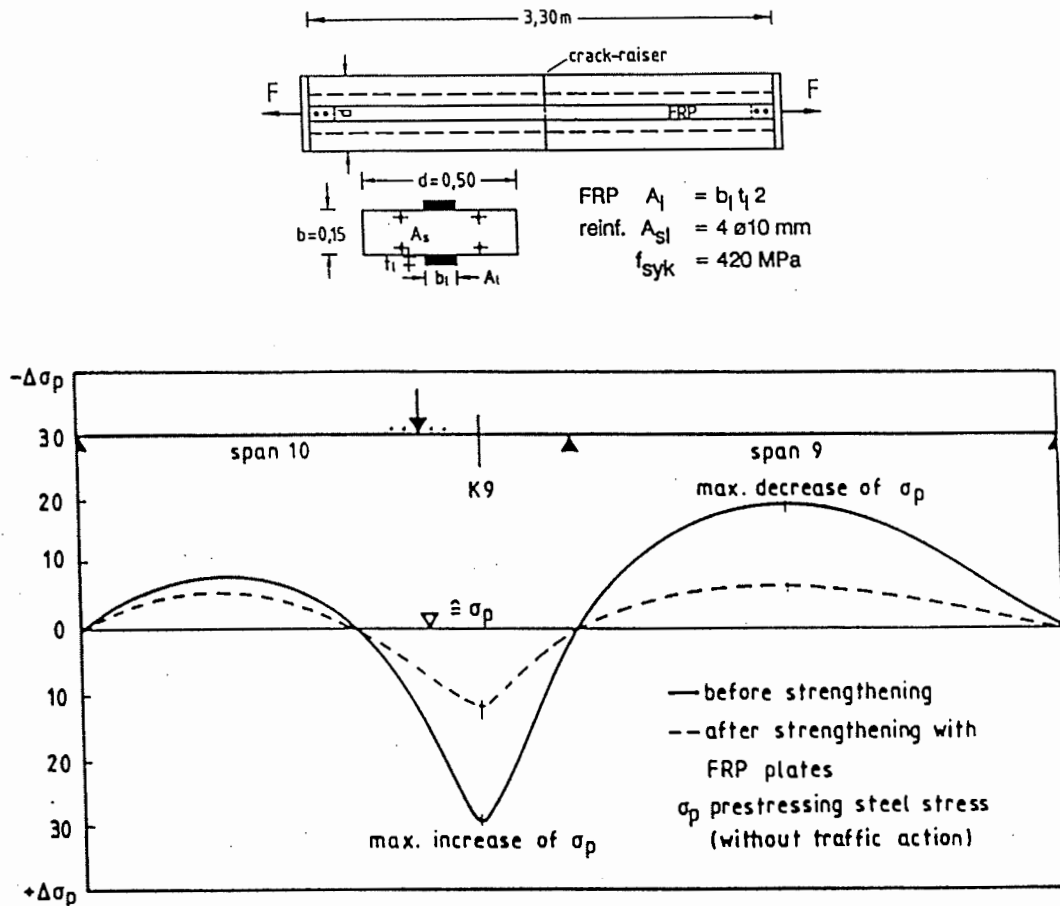


Figure 4.15: Measured Stress Reduction Due to GFRP Lamination (Rostasy et al, 1992)

4.9 SUMMARY

Much of the material in this chapter relates to taking composite strengthened reinforced concrete elements to failure. This information is very important to researchers who will be studying the failure mechanisms of composite reinforced structural elements. It will have less relevance for designers in the bridge strengthening community. Their primary concern will be how well the composite strengthened elements perform when loads on the elements are significantly below ultimate. Thus, the key advantages of FRP composites, for future designers, will be:

- advanced composite materials to reinforce concrete beams offer strength and shear enhancement significantly beyond that of traditional materials;
- they are lighter and easier to handle;
- composites have excellent corrosion resistance;
- their very low chemical reactivity;
- ability to custom design the composite's properties by varying the type, orientation and volume concentration of fibers;
- ability to easily control the number and orientation of layers for each individual application.

A perceived disadvantage in using these materials is their cost. Costs will decrease as the industrial demand increases. Even today, if costs are based on the total project rather than on materials cost, composites can be very competitive.

Other concerns, not directly covered in the preceding sections are resistance to UV and microbial degradation.

The following variables influence the response of FRP laminate bonded beams:

- size of the beam;
- thickness and area of the FRP composite;
- type of adhesive;
- type of composite;
- type of loading (static or dynamic);
- under- or over-reinforced beam;
- crack or non-cracked beams before plate bonding;
- prestressed or non-stressed main reinforcement;
- action of corrosion;
- weather;
- age.

The following sequence can be assumed to occur during static loading of FRP reinforced beams:

- 1) Elastic response predominates until tensile cracking of the beam occurs. At this point the neutral axis shifts upward and is accompanied by a change of the load-displacement curve.
- 2) After tensile cracking occurs, the beam remains elastic, the load is shifted to the concrete compression area, and the FRP holds the cracked concrete in place.
- 3) At maximum load bond failure usually occurs and the beam collapses.

Beams strengthened with very stiff FRP plates (6 mm and greater) exhibit a brittle failure mechanism, usually observed at the end of the linear elastic range. A large increase in stiffness is obtained by using thick plates. However, the fibers are underutilized and are subjected to very low stress, 1/7 to 1/4 of ultimate.

For beams strengthened to intermediate stiffness, the cracks localize at the end of the plates. In these cases, shear failure is typically observed.

Beams that are reinforced with thin glass plates exhibit ductile behavior. The first stiffness reduction typically occurs due concrete cracking in the tensile zone followed by shear cracking at the plate ends.

Adhesive selection is critical to good performance because it is responsible for the stress transfer from the concrete to the reinforcing materials. Some properties of good adhesives are:

- Proper viscosity – entrained and entrapped air must be minimized during the mixing and bonding phase;
- Rapid polymerization time to minimize the repair time and reduce the chance of being weakened by vibration or flexure during cure;
- Good adhesion to both the concrete and FRP plates.

4.10 DESIGN EXAMPLES

4.10.1 Flexural Design – Calculation of FRP Strengthened Beam Bending Resistance

Currently there are no design procedures for external reinforcement with FRP composites. In the near future ACI Committee 440 will provide engineers with guidelines for strengthening concrete structures with FRP composites. Until then, each designer must conduct his or her own review of the design concepts.

The design examples provided herein follow a logical step-by-step process based on conventional reinforced concrete design. Appropriate assumptions regarding FRP allowable strains and stresses are an integral part of the design process. Although the design follows the ACI fundamentals and European experience, additional knowledge is needed for success. These topics include, but are not limited to, the following:

- Composite behavior near ultimate loads;
- Brittle versus ductile failure modes;
- Strength loss due to elevated or low temperatures of the adhesive;
- Creep of GFRP laminates; and
- Thermal compatibility between FRP composites and concrete.

The procedures are provided only for illustration of the material presented in this chapter and cannot be regarded as a working guideline for the strengthening of concrete members with FRP laminates.

Typically, conventionally reinforced beams are designed so that concrete failure occurs when the yield point of steel is reached. The failure is normally preceded by crack formations and large deflections. By controlling the reinforcing ratio, undesired brittle modes of failure can be prevented.

The ultimate strength of a beam strengthened with FRP laminates cannot be calculated the same way, because the behavior of the composite materials is linear-elastic to failure and they do not have a plastic deformation reserve. Thus, the maximum bending resistance of the hybrid concrete-steel-FRP section is typically reached when the laminate failure occurs and before the concrete failure.

The calculation of bending resistance is based on the following assumptions, which also apply to conventionally reinforced concrete sections:

- Idealized stress-strain diagram for concrete, steel and FRP laminate;
- The tensile resistance of concrete is neglected;
- The strains are distributed across the section height proportionally to the distance from the neutral axis;
- The position of the forces and the neutral axis remains constant;
- Due to external influences, the ratios of maximum to medium strains are described by the composite factors K_L and K_S , for the FRP and steel reinforcement, respectively.

Figure 4.16 shows the forces used for calculation of the ultimate moment M_R on the rectangular cross-section.

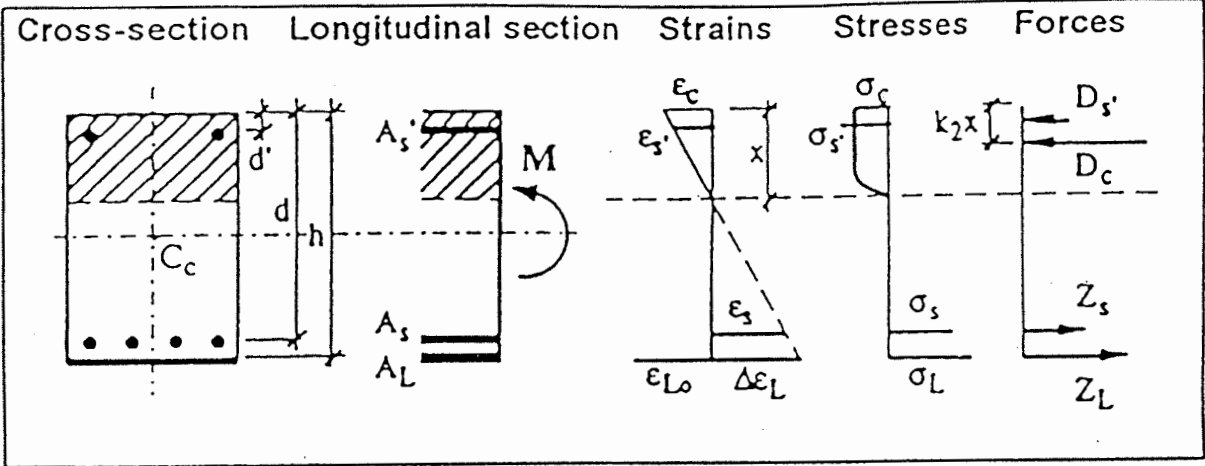


Figure 4.16: Rectangular Beam Cross-Section: Calculation of the Ultimate Moment of Resistance

4.10.1.1 Design Based on the European Experience and Design Codes

4.10.1.1.1 Assumptions

- The governing failure mode is rupture of the laminate;
- The steel reinforcement has yielded before FRP rupture.

4.10.1.1.2 Equilibrium Conditions

$$\Sigma Z = 0 \Rightarrow Z_L + Z_S - D_C = 0 \quad \text{and} \quad (4-1)$$

$$\Sigma M = 0 \Rightarrow M_R - Z_L(h - k_2c) - Z_S(d - k_2c) = 0 \quad (4-2)$$

where: $D_C = k_1bcf'_c$

4.10.1.1.3 Determination of k_1 and k_2 Coefficients

For extreme fiber concrete strain $\varepsilon_c < 0.2\%$, k_1 and k_2 are determined as follows:

$$k_1 = \frac{1000(-500\varepsilon_c^2 + 3\varepsilon_c^2)}{6} \quad (4-3)$$

$$k_2 = \frac{1 - (4 - 750\varepsilon_c)}{(6 - 1000\varepsilon_c)} \quad (4-4)$$

For extreme fiber concrete strain $0.2\% < \varepsilon_c < 0.3\%$, k_1 and k_2 are determined as follows:

$$k_1 = 1 - \frac{1}{1500\varepsilon_c} \quad (4-5)$$

$$k_2 = 1 - \frac{0.5 - (3 * 10^6 \varepsilon_c)^{-1}}{1 + (-1500\varepsilon_c)^{-1}} \quad (4-6)$$

4.10.1.1.4 Location of the Neutral Axis of the Cross Section

$$\varepsilon_c = \frac{k_L(\varepsilon_{LU})c}{h - c} \quad (4-7)$$

$$c = \frac{f_{LU}A_L + f_YA_S}{k_1bf'_c} \quad (4-8)$$

Note that the concrete strain is expressed as a function of the laminate strain and the distance to the neutral axis.

4.10.1.1.5 Calculate M_R

Since the magnitude of the concrete strain is not known, use both expressions for k_1 . Then, the concrete strains based on both models are found, and the appropriate mathematical model is identified and used to calculate k_2 and the ultimate moment capacity.

$$M_R = Z_S(d-k_2c) + Z_L(h-k_2c), \text{ or} \quad (4-9)$$

$$M_R = f_{LU} A_L(h-k_2c) + f_Y A_S(d-k_2c) \quad (4-10)$$

4.10.1.1.6 Check the Average Strains at Failure

Once the ultimate moment capacity is determined, all the underlying assumptions need to be checked. This includes a check to confirm that the concrete is not stressed beyond its crushing limits (ϵ_c is less than 0.003), and verify that steel has yielded, but did not fracture.

4.10.1.1.6.1 Bond Coefficients k_L and k_S

$$0.65 \leq k_L \leq 0.80 \quad (\text{typically } 0.70)$$

$$0.90 \leq k_S \leq 1.00 \quad (\text{typically } 0.90)$$

4.10.1.1.6.2 Strains in the FRP Laminate

$$\Delta\epsilon_{Lm} = k_L \Delta\epsilon_{Lmax} = k_L \epsilon_{LU} \Rightarrow \sigma_{max}^L = \sigma_{ult}^L \quad (4-11)$$

4.10.1.1.6.3 Strains in the Steel reinforcement

$$\Delta\epsilon_{Sm} = k_S \Delta\epsilon_{Smax} \Rightarrow \sigma_{max}^S > \sigma_y^S \quad (4-12)$$

$$\epsilon_{Sy} < \epsilon_{Smax} = \frac{\epsilon_S}{k_s} \Rightarrow \epsilon_S = \frac{\Delta\epsilon_{Lm}(d-c)}{h-c} \quad (4-13)$$

4.10.1.1.6.4 Strain in Concrete

$$\epsilon_c = \frac{\Delta\epsilon_{Lm}c}{h-c} \quad (4-14)$$

where $\epsilon_c < 0.003$

4.10.1.2 Numerical Example

The figure below illustrates the geometry of the beam and the position of the reinforcement.

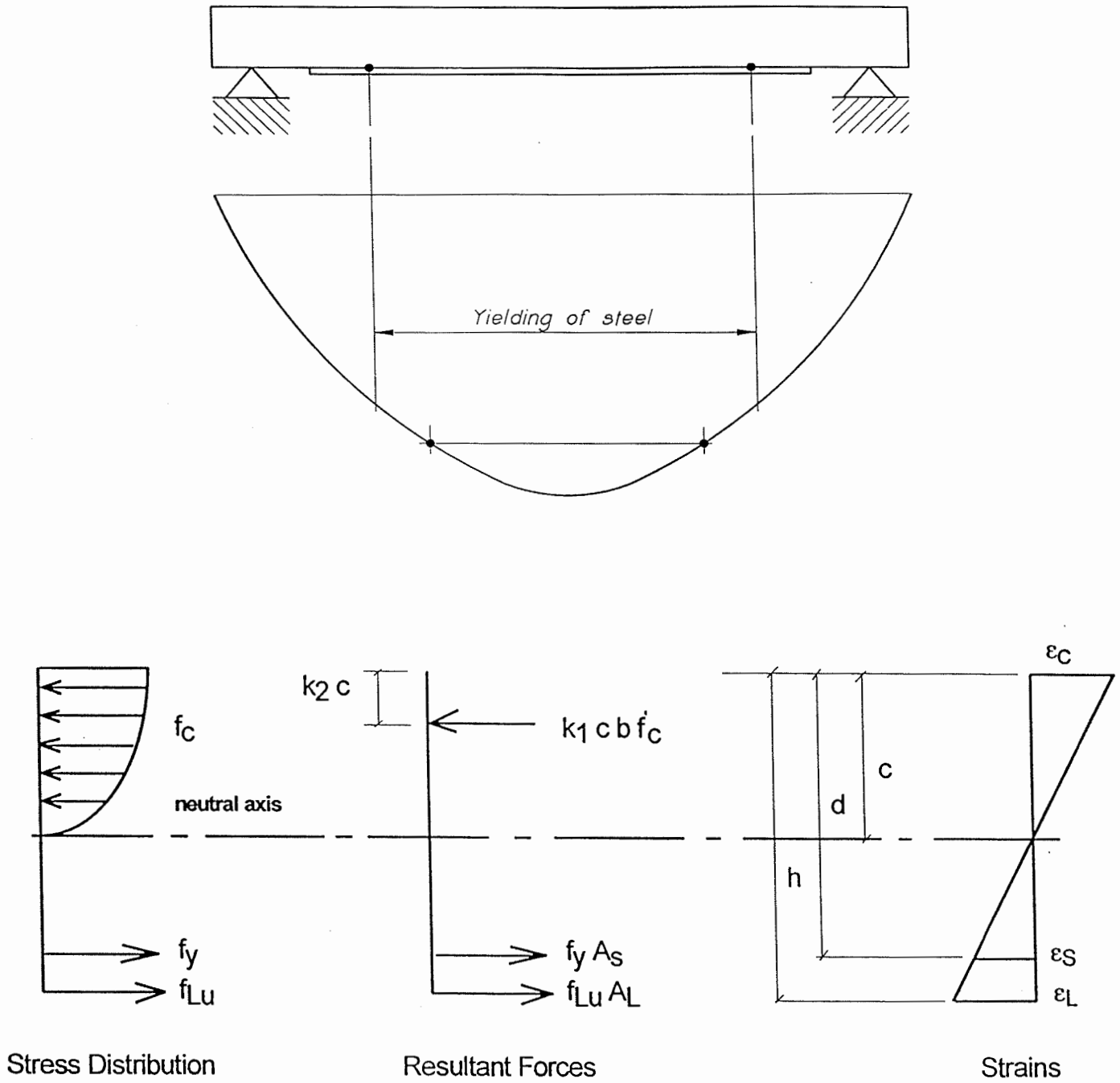


Figure 4.17: Beam Cross Section, Numerical Example

4.10.1.2.1 Design Goal

Provide additional moment capacity and stiffness on the existing reinforced concrete beam.

4.10.1.2.2 Reinforcement Details and Assumptions

4.10.1.2.2.1 Concrete Section

$$f'_c = 4,000 \text{ psi}$$

$$b = 6 \text{ in.}$$

$$h = 6 \text{ in.}$$

$$d = 3.81 \text{ in.}$$

4.10.1.2.2.2 Steel Reinforcement

$$A_s = 0.11 \text{ in}^2 \text{ (one No.3 steel rebar A60)}$$

$$d_s = 0.375 \text{ in.}$$

$$f_y = 36 \text{ ksi}$$

$$\varepsilon_s^{\max} = 0.12\%$$

4.10.1.2.2.3 FRP Reinforcement

$$f_{Lult} = 348 \text{ ksi}$$

$$\varepsilon_{L}^{ult} = 1.4\%$$

$$f_{Lmax} = 240 \text{ ksi (design value)}$$

$$\varepsilon_{L}^{\max} = 0.98\%$$

$$b_L = 5 \text{ in.}$$

$$t_L = 0.004 \text{ in.}$$

$$A_L = 0.02 \text{ in}^2$$

4.10.1.2.2.4 Determination of the Concrete Strain

Solve the following system of equations:

$$\varepsilon_c = \frac{\varepsilon_{Lult} c}{h - c}, \text{ and}$$

$$c = \frac{f_{LU} A_L + f_Y A_S}{k_1 b f'_c}$$

- Case One: $\epsilon_c < 0.002$

$$\epsilon_c = \frac{\frac{\epsilon_{Lult}(f_{Lult}A_L + f_yA_S)}{\frac{1000}{6}(-500\epsilon_c^2 + 3\epsilon_c^2)bf'_c}}{h - \frac{(f_{Lult}A_L + f_yA_S)}{\frac{1000}{6}(-500\epsilon_c^2 + 3\epsilon_c^2)bf'_c}}$$

Based on the initial assumptions for all variables included in the above equation,

$$\epsilon_c = -1.146 \times 10^{-3} \text{ in/in. Use } \epsilon_c = 0.0012 \text{ in/in.}$$

After substitution, $k_2 = 0.354$ and $k_1 = 0.48$.

Position of the neutral axis: $c = 0.76$ in.

Check Strains: Check to confirm that the concrete has not been stressed beyond its crushing point, and steel yielded, but did not fracture.

$$\epsilon_c = \frac{\epsilon_{Lult}c}{h-c} = \frac{(0.014)(0.76 \text{ in})}{6 \text{ in} - 0.76 \text{ in}} = 0.002 \text{ in/in. } < 0.003 \Rightarrow \text{O.K.}$$

$$\epsilon_s = \frac{\epsilon_{Lm}(d-c)}{h-c} = \frac{(0.014)(3.81 \text{ in} - 0.76 \text{ in})}{6 \text{ in} - 0.76 \text{ in}} = 0.008 \text{ in/in. } \Rightarrow \text{O.K.}$$

- Case Two: $0.002 < \epsilon_c < 0.003$

$$\epsilon_c = 0$$

This case is not applicable for the selected beam geometry, reinforcement quantity, FRP thickness, and material properties of concrete, steel and FRP.

4.10.1.2.2.5 Maximum Bending Resistance

$$M_R = f_{LU} A_L(h-k_2c) + f_Y A_S(d-k_2c) = \\ [6-(0.354)(0.76 \text{ in.})](0.02 \text{ in}^2)(240 \text{ ksi}) + \\ [(3.81 \text{ in.})-(0.354)(0.76 \text{ in.})](0.11 \text{ in}^2)(36 \text{ ksi})$$

$$M_R = 27.5 + 14 = 41.53 \text{ kips-in} = 3.5 \text{ kips-ft}$$

4.10.1.2.2.6 Strengthening Ratio

$$M_R^{\text{str}} / M_R^{\text{unstr}} = 1.7$$

4.10.1.3 *The ACI Based Design of FRP Strengthened RC Beam*

4.10.1.3.1 *Assumptions*

The assumptions are the same as in the European code-based design plus the following:

4.10.1.3.1.1 Concrete and Steel Reinforcement

$$\begin{aligned} E_S &= 29,000 \text{ ksi} \\ \epsilon_{S_y} &= 0.002 \text{ in/in.} \\ f_{S_y}^{\text{ult}} &= 60 \text{ ksi} \end{aligned}$$

4.10.1.3.1.2 FRP Laminate

$$E_L = 22,500 \text{ ksi}$$

The retrofit is based on 80% of the bottom face (5 in.) covered with one layer of CFRP.

$$A_L = 0.8bt_L = (0.8)(6 \text{ in.})(0.004 \text{ in.}) = 0.0192 \text{ in}^2$$

4.10.1.3.1.3 FRP Position Below the Bottom of the Beam

$$y_L = -0.004 \text{ in}$$

4.10.1.3.1.4 Equilibrium Conditions

$$T=C \Rightarrow f_{S_y}^{\text{ult}} A_S + f_L A_L = (0.85)(f_c')(a)(b)$$

where a = compression zone depth (in.)

$$\begin{aligned} (0.11 \text{ in}^2)(36 \text{ ksi}) + (0.0192 \text{ in}^2)(22,500 \text{ ksi})(0.014) \\ = (0.85)(4 \text{ ksi})(a)(6 \text{ in.}) \end{aligned}$$

$$a = 0.62 \text{ in.}$$

$$c = a / \beta = 0.73 \text{ in.} \quad (\beta = 0.85 \text{ for } f_c' < 4000 \text{ psi})$$

4.10.1.3.1.5 Calculate the Concrete Strain Based on the Ultimate Fiber Strain

$$\varepsilon_c^{ult} = \frac{\varepsilon_{Lult} c}{h - c} = \frac{(0.014)(0.73 \text{ in.})}{(6 \text{ in.} - 0.73 \text{ in.})} = 0.0194 \text{ in./in.} < 0.003 \Rightarrow \text{O.K.}$$

4.10.1.3.1.6 Moment Capacity Provided by the CFRP Laminate

$$M_R = \phi M_n = \phi [A_L f_L (d_L - a/2)]$$

$$\text{Where } d_L = h + t_L = 6 + 0.004 = 6.004 \text{ in.}$$

$$\phi M_n = (0.9)(0.0192 \text{ in.})(22,500 \text{ ksi})(0.014)(6.004 \text{ in.} - 0.31 \text{ in.})$$

$$\phi M_n = 31 \text{ kips-in} = 2.6 \text{ kips-ft}$$

4.10.1.3.1.7 Serviceability and Deflections

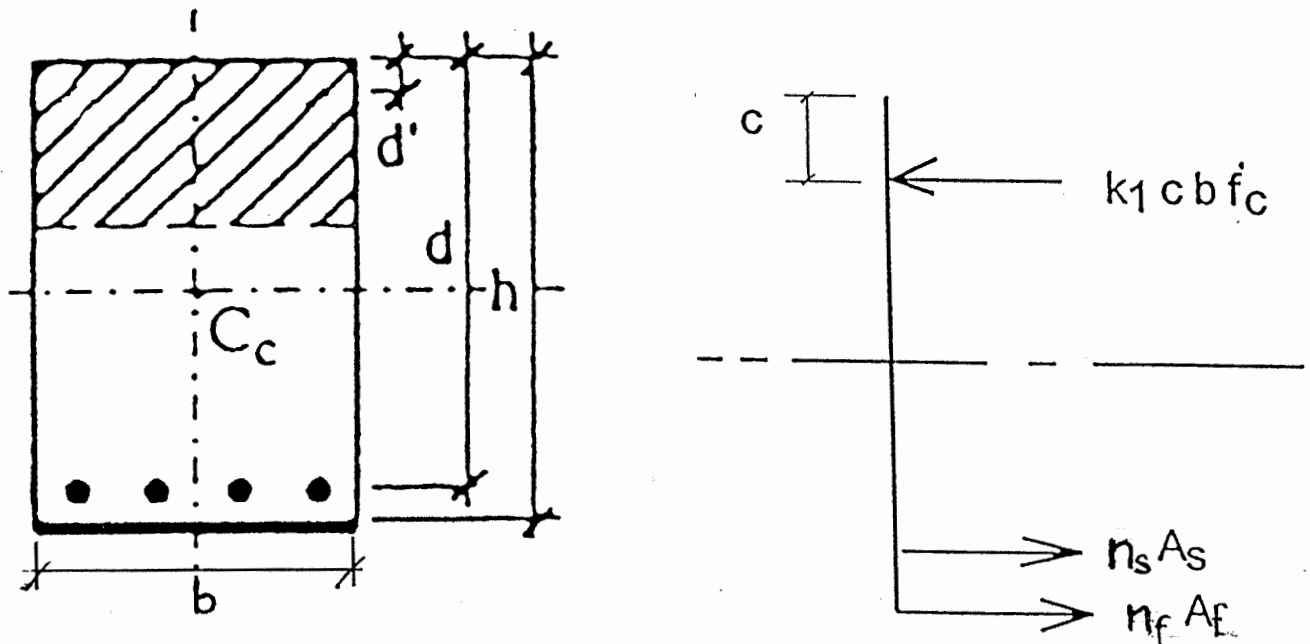


Figure 4.18: Beam Cross Section, Serviceability and Deflections

Calculations of the transformed moments of inertia are based on the modular ratios with respect to the concrete modulus.

$$E_c = 57,000 \sqrt{f'_c} = 57,000 \sqrt{4000} = 3605 \text{ ksi}$$

$$n_s = \frac{E_s}{E_c} = \frac{29000}{3605} = 8.04$$

$$n_L = \frac{E_L}{E_c} = \frac{22500}{3605} = 6.24$$

Table 4.13: Transformed Moments of Inertia Calculations

	$n_i A_i \text{ (in}^2\text{)}$	$y_i \text{ (in)}$	$n_i A_i y_i$	$y_i \text{ (in)-}$ calc.	$I = bc^3/12 \text{ (in}^4\text{)}$	$n_i A_i^2 \text{ (in}^4\text{)}$
Concrete	$6(c)$	$c/2$	$3c^2$	0.506	0.518	1.555
Steel	$(8.04)(0.11)$	$c-d = c-3.81$	$0.8844c-3.37$	-2.80	–	6.934
CFRP	$(6.24)(0.0192)$	$c-h=c-6.004$	$0.12c-0.72$	-4.992	–	2.986

$$\Sigma I + A y^2 = 11.993 \cong \underline{12 \text{ in}^4}$$

4.10.1.3.1.8 Determine the Position of the Neutral Axis

By definition, the position of the neutral axis is the distance to the centroid when $\Sigma A_i y_i = 0$

$$3c^2 + 0.8844c - 3.37 + 0.12c - 0.72 = 0$$

$$3c^2 + 1.0044c - 4.09 = 0$$

$$c = 1.012 \text{ in.}$$

4.10.1.3.1.9 Calculate the Midspan Deflection

Calculations are based on the moment of inertia (ΣI), and the maximum moment capacity of the beam ($M_R = \phi M_n$).

$$\Delta_{CL} = \frac{5}{48} \frac{\sum M_R L_{CLR}^2}{E_c I}$$

where:

L_{CLR} – beam length, (in.)

For this example: $L_{CLR} = 21 \text{ in.}$

$$\Delta_{CL} = \frac{5}{48} \frac{(31.3 \text{ kips} - \text{in})(21 \text{ in})^2}{(3605 \text{ ksi})(12 \text{ in}^4)}$$

$$\Delta_{CL} = 0.0332 \text{ in.}$$

4.10.2 Shear Strength Enhancement of RC Beams Using FRP Laminates

The most important feature for proper shear design using FRP materials, whether glass or carbon, is the strain compatibility between the composite laminate and the concrete. Rational shear strengthening designs are limited to 0.4% due to strain issues. This strain limitation is due to concrete limitations and it is independent of FRP material type.

The design example outlined in this chapter is strain based design. There are other possible approaches, based on ultimate strength and strain values which will result in different and sometimes uncertain failure modes. The strain based design approach is conservative compared to the other approaches, but it can be performed easily and does not require advanced knowledge in composite materials mechanics and behavior.

The shear strengthening design procedure is provided only for illustration and cannot be regarded as a working guideline for strengthening of concrete members with FRP laminates.

4.10.2.1 Necessary Assumptions

- f_{Lj} – Allowable jacket stress, (ksi)
- E_j – Elastic modulus of FRP jacket (ksi)
- ϵ_{uj} – Allowable jacket strain for shear (ksi)
- t_j – FRP jacket thickness (in.)
- f_{ty} – Transverse steel tensile strength (ksi)
- L_{clr} – Beam clear length (in.)

4.10.2.2 Check Existing Shear Capacity

If steel shear reinforcement is provided:

$$V_{cap} = \frac{A_v f_{ty} d}{s} \tag{4-15}$$

If no shear reinforcement is provided

$$V_{cap} = 2\sqrt{f'_c} b d \tag{4-16}$$

4.10.2.3 Calculate Needed Shear Capacity

$$V_{cap} = \frac{A_v f_{ly} d}{s'} \quad (4-17)$$

where:

s' – new shear reinforcement spacing (in.)

4.10.2.4 Calculate Shear Capacity Shortfall

$$V_{Sj} = V_S - V_{cap} \quad (4-18)$$

4.10.2.5 Calculate the Required FRP Jacket Thickness

$$t_j > \frac{V_{Sj}}{2 f_{lj} d (\cot 45)} \quad (4-19)$$

45 degree shear crack inclination has been assumed.

4.10.2.6 Required Bond Length Development

The development length is needed to prevent shear rupture of concrete. The concrete bond stress is limited to 200 psi. Development length must be provided beyond the point determined to carry the tensile force.

$$\sigma_b = \frac{T_L}{A_b} \quad (4-20)$$

$$A_b = (b_L)(l_d) \quad (4-21)$$

$$E_w = E_L(t_j) \quad (4-22)$$

$$T_L = E_w(b_L)(0.004) = E_L t_L(b_j)(0.004) \quad (4-23)$$

where 0.004 is the concrete strain limit

4.10.2.7 Numerical Example

4.10.2.7.1 Assumptions

6in. x 6in. concrete beam with no shear reinforcement provided
 $d = 3.81$ in.

$$\epsilon_{uj} = 0.004 \text{ in/in.}$$

$$E_{uj} = 22,500 \text{ ksi}$$

$$f_L^{\text{ult}} = 240 \text{ ksi}$$

$$t_L = 0.004 \text{ in.}$$

$$L_{\text{clr}} = 21 \text{ in.}$$

4.10.2.7.2 Calculate the Allowable FRP Jacket Stress

$$f_{Lj} = \frac{f_L^{\text{ult}} \epsilon_{uj}}{\epsilon_L^{\text{ult}}} = \frac{(240 \text{ ksi})(0.004 \text{ in/in})}{0.014 \text{ in/in}} = 68 \text{ ksi}$$

4.10.2.7.3 Check Shear Capacity

$$V_{\text{cap}} = V_c = 2\sqrt{f'_c}bd = 2\sqrt{4000 \text{ psi}}(6 \text{ in.})(3.81 \text{ in.}) = 2.89 \text{ kips}$$

Since no shear reinforcement is provided, ACI Code Section 11.5.5.1 requires that the maximum allowable shear force is:

$$\text{Max. } V_U = 0.5 \phi V_c = (0.5)(0.85)(2.89 \text{ kips}) = 1.23 \text{ kips}$$

4.10.2.7.4 Calculate the Needed Shear Capacity

Since the required shear force is not known in this example, it will be calculated based on the tensile resistance (capacity) of the beam. According to the theory:

$$0.707 V + 0.707 V = T$$

where:

V – shear force in the beam (kips)

T – tensile force in the beam (kips)

$$\begin{aligned} T &= f_{\text{SY}}^{\text{ult}} A_S + f_L^{\text{ult}} A_L \\ &= (0.11 \text{ in}^2)(60 \text{ ksi}) + (0.02 \text{ in}^2)(240 \text{ ksi}) = 11.4 \text{ kips} \end{aligned}$$

$$\text{Thus: } V_S = 11.4 / 1.414 = 8.06 \text{ kips (use 8.1 kips)}$$

4.10.2.7.5 Calculate Shear Capacity Shortfall

$$V_{\text{sj}} = V_S - V_{\text{cap}} = 8.1 - 2.89 = 5.21 \text{ kips}$$

4.10.2.7.6 Calculate the Required FRP Jacket Thickness

$$t_j > \frac{V_{\text{sj}}}{2f_{Lj}d(\cot 45)} = \frac{5.21}{2(68 \text{ ksi})(3.81 \text{ in.})(1.0)}$$

$$t_j > 0.01 \text{ in}$$

Individual layer thickness $t_L = 0.004 \text{ in}$. The required number of layers is 2.5. Use three layers.

Note: The beam was first strengthened for flexure and then for shear. The calculation of the maximum tensile force included the flexure capacity of CFRP laminate 0.004 in. thick applied to the tensile face of the beam. This explains the large quantity of shear reinforcement needed in this example.

4.10.2.7.7 Required Bond Length Development

$$\sigma_b = \frac{T_L}{A_b}$$

$$E_w = E_L t_j$$

$$T_L = E_w b_L (0.004) = E_L t_j b_L (0.004)$$

where 0.004 is the concrete strain limit

$$\sigma_b = 200 \text{ psi}$$

$$0.2 \text{ ksi} = \frac{(22500 \text{ ksi})(0.01 \text{ in.})(5 \text{ in.})(0.004)}{(5 \text{ in.})(l_d)}$$

$$l_d = 4.5 \text{ in.}$$

4.10.3 List of Variables

a	compression zone depth (in.)
A_b	bond area of FRP laminate (in ²)
A_L	cross-section area of FRP laminate (in ²)
A_S	cross-section area of tension steel reinforcement (in ²)
b	width of the concrete section (in.)
b_L	width of the FRP laminate (in.)
c	distance from the top of the section to the neutral axis (in.)
C	resultant compressive force in the cross section (kips)
d	effective depth of the concrete section (in.)
D_c	compressive force in concrete (kips)
d_s	steel rebar diameter (in.)
E_c	elastic modulus of concrete (ksi)
E_L	elastic modulus of FRP laminate (ksi)
E_S	elastic modulus of steel (ksi)
E_w	FRP elastic modulus per unit width (kips/in. width)
f'_c	concrete compressive strength (ksi)
f_{Lj}	allocable jacket stress, (ksi)
f_{LU} (f_{Lult})	ultimate strength of FRP laminate (ksi)
f_{ty}	transverse steel tensile strength (ksi)
f^{ult}_{Sy}	steel ultimate strength (ksi)
f_y	steel yield strength (ksi)
h	height of the concrete section (in.)
k_1	variable used to determine the magnitude of concrete compressive force
k_2	variable used to determine the location of concrete compressive force
k_L	FRP bond coefficient
k_S	steel bond coefficient
L_{CLR}	beam length (in.)
l_d	bond development length (in.)
M_n	nominal moment capacity of the beam (kips-ft)
M_R	maximum moment capacity of the beam (kips-ft)
s	center-to-center spacing of the shear reinforcement (in.)
T	resultant tensile force in the cross section (kips)
t_j	FRP jacket thickness (in.)
t_L	FRP laminate thickness (in.)
T_L	tensile force provided at strain of 0.4% , limit for shear (kips/in.)
V_c	shear resistance provided by the concrete (kips)
V_{cap}	existing shear capacity of the beam (kips)
V_S	needed (design) shear capacity of the beam (kips)
V_{Sj}	shear reinforcement shortfall (kips)
Z_c	compressive force in concrete (kips)
Z_L	tensile force in FRP laminate (kips)
Z_S	tensile force in steel (kips)

β	reduction coefficient used to determine the position of the neutral axis
ϕ	reduction factor
Δ_{CL}	midspan deflection (in.)
σ_b	bond stress of concrete (psi)
σ_{ult}^L	ultimate stress of FRP laminate (psi)
σ_{max}^S	ultimate stress of steel (psi)
ϵ_c	strain in concrete (in/in.)
ϵ_L	strain in FRP laminate (in/in.)
ϵ_{LU} ($\epsilon_L^{max} = \epsilon_L^{ult}$)	strain in FRP laminate at ultimate stress (in/in.)
ϵ_{max}^S (ϵ_S^{ult})	ultimate strain in steel (in/in.)
ϵ_S	strain in steel (in/in.)
ϵ_{uj}	allowable jacket stress for shear (ksi)
ϵ_c^{ult}	maximum allowable strain in concrete (in/in.)

5.0 EXTERNAL REINFORCEMENT OF CONCRETE COLUMNS USING FRP COMPOSITE MATERIALS

5.1 INTRODUCTION

Many concrete bridge columns designed before the new seismic design provisions were adopted in 1970 have low shear strength and low flexural strength and ductility. These problems, combined with environmental deterioration, have contributed to catastrophic bridge failures in recent earthquakes (*Cercione and Korff, 1997*). Post earthquake analysis of the seven freeway bridges that collapsed during the Northridge earthquake revealed that they could have survived if they had been retrofitted to withstand seismic forces.

The work of some researchers has indicated that increasing the confinement in the potential plastic hinge regions of the column will increase the apparent concrete compressive strength and ductility (*Saadatmanesh and Ehsani, 1994*). Therefore, strengthening techniques typically involve methods for increasing the confining forces either in the potential plastic hinge regions or over the entire column.

An unwrapped concrete column loaded in compression will fail by developing a crack network and shear cones in the column. In order to visualize the failure mechanism associated with confined concrete columns, it is important to think of the wrapped column as a system of concrete cores loaded in compression and concentrically wrapped with a tensile-loaded jacket. The existence of the jacket, which provides a high degree of confinement, can prevent or delay the initiation and propagation of the internal cracking mechanism.

Until recently, the steel jacketing of bridge columns was the only retrofitting method widely approved. This technique is effective in preventing columns from collapsing due to shear or flexural failure. However, installation is labor intensive, time consuming, and requires heavy equipment to handle the steel. Another problem is that the installation requirements rather than the confinement requirements determine the thickness and weight of the steel jackets. In order to prevent buckling under its own weight during lifting, the steel jacket has to be extremely heavy and strong. Thus, the resulting retrofit projects are typically expensive and use an excessive amount of material (*Cercione and Korff, 1997*).

Advanced composite materials have unique mechanical and durability characteristics that complement column strengthening. Research by the Advanced Composites Technology Transfer Consortium (ACTT) at the University of California, San Diego (UCSD) has shown that seismically deficient bridge columns can be wrapped with FRP materials in an automated fashion, further reducing the time requirements as compared to equivalent steel jacket installations. Recent developments in automated manufacturing and application processes for FRP column wrapping has shown that this type of structural enhancement is cost effective (*Seible, et al, 1995*).

5.2 COLUMNAR CONFINEMENT OF CONCRETE WITH ADVANCED COMPOSITE MATERIALS

Existing concrete column failure theories show that a small amount of columnar confinement will dramatically increase a column's strength and ductility (*Harmon and Slattery, 1992*). This approach could be related to the use of spiral reinforcement in steel reinforced columns. The spiral reinforcement provides no additional strength to the concrete, but greatly increases the column's ductility. Since the concrete that covers the spiral reinforcement will spall before failure is reached, its contribution to the strength increase is insignificant.

FRP materials properties are best exploited when the application requires directional, tensional restraints. Together with the FRP's ability to conform to existing substrates, this makes them a very viable material for post columnar strengthening. Further, FRP reinforcement on the outside of a column requires no cover and is corrosion resistant.

Harmon and Slattery (*1992*) demonstrated the effectiveness of using CFRP on high strength concrete cylinders to create compression members with both high strength and high ductility. The CFRP wraps had a tensile strength and elastic modulus of 3500 MPa and 235 GPa, respectively, and were applied at various thicknesses to achieve different volumetric reinforcing ratios. Figure 5.1 shows the axial strain versus stress results from the study. The stress-strain curves were bilinear with a pseudo-yield stress higher than the failure stress of the unreinforced cylinders. As the reinforcing ratio increases, the ultimate failure stress increases significantly but has only a minor effect on the yield stress.

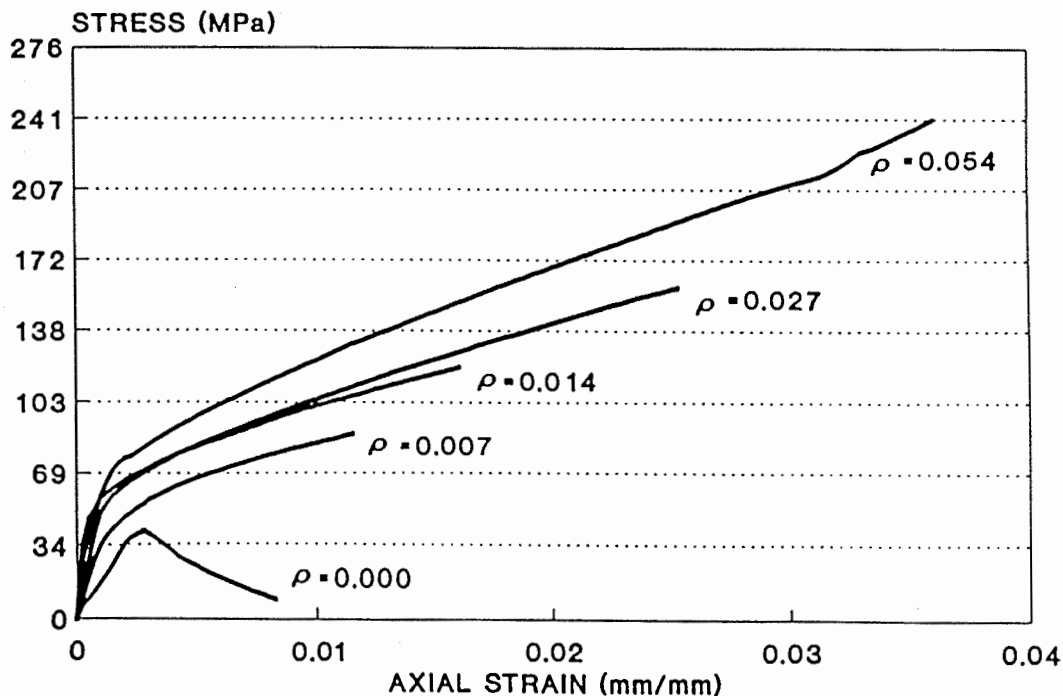


Figure 5.1: Stress vs. Axial Strain
(*Harmon and Slattery, 1992*)

This report was too large to link the entire report in one link. If you wish to continue [click here](#).